UNIVERSIDADE DO ALGARVE

Faculdade de Ciências e Tecnologia

Estudos voltamétricos na peroxidase do citocromo *c* e respetivos parceiros redox – reações intermoleculares e catálise.

David António Andrade Rodrigues
Licenciado Pré-Bolonha em Bioquímica

Relatório de Atividade Profissional para a obtenção
do grau de Mestre em Biotecnologia

Trabalho efetuado sob a orientação da Professora Deborah Power

2013

UNIVERSIDADE DO ALGARVE

Faculdade de Ciências e Tecnologia

Estudos voltamétricos na peroxidase do citocromo *c* e respetivos parceiros redox – reações intermoleculares e catálise.

David António Andrade Rodrigues
Licenciado Pré-Bolonha em Bioquímica

Relatório de Atividade Profissional para a obtenção
do grau de Mestre em Biotecnologia

Relatório nos Termos do Despacho RT.033/2011 para obtenção
do grau de Mestre pelos licenciados Pré-Bolonha

Trabalho efetuado sob a orientação da Professora Deborah Power

2013

Declaro ser o autor deste trabalho, que é original e inédito. Autores e trabalhos consultados estão devidamente citados no texto e constam da listagem de referências incluída.

David António Andrade Rodrigues

Agradecimentos

Em primeiro lugar, gostaria de agradecer à Professora Deborah Power por se ter disponibilizado para ser a orientadora do relatório de atividade profissional, para a obtenção do grau de Mestre em Biotecnologia.

Gostaria de agradecer a todos os Professores que me aceitaram para trabalhar no seu grupo de investigação: Professor Paulo Martel, Professora Margarida dos Santos, Professora Leonora Cancela, Professora Maria João Romão e Professor Guilherme Ferreira.

À Patrícia, Catarina, Teresa, Filipe e Rogério por todo o acompanhamento e companheirismo.

A todos os colegas que tive o privilégio de conhecer durante este percurso.

Por fim, à minha grande família, que são as pessoas mais importantes da minha vida.

Resumo

O meu percurso profissional apresenta uma competência laboratorial bastante diferenciada, mas com complementaridade, realizado em diferentes grupos de investigação com resultados positivos e promissores. Sendo principalmente, o objeto em estudo, as proteínas.

Este percurso iniciou-se com o estágio da licenciatura em Bioquímica, realizado na Universidade do Algarve, sob orientação do Professor Paulo Martel, durante um ano na área de Bioinformática e modelação, sendo o objetivo principal o estudo da melhor interação entre os citocromos P450 e os respetivos ligandos. Posteriormente, trabalhei como bolseiro de Investigação, no grupo da Professora Margarida dos Santos, no Instituto Superior Técnico durante 21 meses na área de Bioelectroquímica. No projeto, a minha principal tarefa, era estudar a eletroquímica catalítica das peroxidases de citocromos *c*. Após o término da bolsa anterior, trabalhei três meses como voluntário no grupo da Professora Leonor Cancela, da Universidade do Algarve. O objetivo foi ajudar na realização de tarefas de um projeto de doutoramento em curso, permitindo-me solidificar os meus conhecimentos teóricos e práticos em técnicas básicas na área da biologia molecular. De seguida, fui trabalhar como bolseiro de investigação no grupo da Professora Maria João Romão durante 2 anos na área da Cristalografia, da Universidade Nova de Lisboa. A tarefa principal do meu trabalho experimental era determinar as condições de cristalização para posteriormente, resolver a estrutura tridimensional das proteínas da família das xantinas oxidases. Por fim, fui bolseiro de investigação no grupo do Professor Guilherme Ferreira durante 1 ano, na área da Bioquímica das proteínas da Universidade do Algarve, cuja função principal foi de produzir e purificar proteínas expressas em *E. coli*.

Deste percurso profissional resultou a publicação como co-autor de quatro artigos em revistas internacionais, de várias comunicações (em forma de painel ou oral) em congressos internacionais e nacionais, uma estrutura de uma proteína depositada no *Protein Data Bank* e uma tese de Licenciatura em Bioquímica.

No presente relatório, vou apresentar um dos projetos científicos em que a minha participação foi significativa, nomeadamente na realização de todo o trabalho experimental, assim como, na participação na análise dos resultados e discussão do conteúdo do campo de investigação. O estudo é na área dos Biossensores que caracteriza a utilização de elétrodos de membrana para o estudo de metaloproteínas. Este estudo descreve o benefício do uso de elétrodos de membrana na eletroquímica das metaloproteínas. A enzima em estudo é a peroxidase do citocromo c, que é responsável pela redução do H_2O_2 a H_2O, sendo portanto de

extrema importância para a célula, pois impede a formação de radicais livres. Este estudo permite compreender aspetos importantes da química, como por exemplo, a termodinâmica, a cinética e os mecanismos de transferências de eletrões biológicos da enzima em estudo.

Sabendo que a Biotecnologia engloba várias áreas, desde a Química à Biologia, considero que o meu percurso profissional se enquadra no mestrado em Biotecnologia.

Abstract

My professional carrier is comprised of a diverse, but complementary laboratorial experience with various research groups. My work has been particularly centered on proteins from which positive and promising results have been produced.

I initiated my career with work for my undergraduate dissertation project in the area of bioinformatics and modulation, for my degree in Biochemistry at the University of Algarve. Under the guidance of Professor Paulo Martel, and during a year, I performed a study with the objective to determine the best interaction between cytochromes P450 and their respective ligands. I later was awarded a research grant to work in bioelectrochemistry at Professor Margarida dos Santos' group at the *Instituto Superior Técnico* for 21 months. The project focused on the study of the catalytic electrochemistry of cytochromes *c* peroxidases. I then worked three months as a volunteer for the group of Professor Leonor Cancela, at the University of Algarve. The main objective of which was to assist in tasks of an ongoing PhD project, in order to solidify my knowledge and skills in basic techniques in molecular biology. Soon after, and with a research grant, I worked for two years with Professor Maria João Romão at the *Universidade Nova de Lisboa* in the field of Crystallography. The project's objective was to determine protein crystallization conditions in order to ascertain the three dimensional structure of the xanthine oxidase protein family. Finally, I worked as a research fellow in the field of protein biochemistry with Professor Guilherme Ferreira's group at the University of Algarve, for one year. My main task was to produce and purify proteins expressed in *E. coli*.

My considerable work experience has resulted in the completion of a degree thesis in Biochemistry and the publication, as co-author, of four papers in international peer-reviewed journals, several communications (poster and oral) in national and international conferences, as well as a protein structure deposited in the *Protein Data Bank.*

In the present report I discuss one of the scientific projects of which I played a central role. I carried out the experimental work, analyzed results and discussed them in the context of the field of Biosensors. The work was specifically focused on the use of membrane electrodes for studying metalloproteins and describes the advantages of using these electrodes in the electrochemistry of metalloproteins. The study was centered on the Cytochrome c peroxidase enzyme which is responsible for the reduction of H_2O_2 to H_2O, a mechanism fundamental for the cell in the prevention of the formation of free radicals. This work elaborates important aspects of chemistry such as, the thermodynamics, kinetics and mechanisms of biological electron transfer of the Cytochrome c peroxidase enzyme.

In light of the fact that biotechnology covers areas ranging from chemistry to biology, I believe that my work experience and professional career coincide with the masters' degree in Biotechnology.

Abreviaturas

Ag/AgCl – Prata/Cloreto de prata

AOH1 – "Aldehyde Oxidase Homolog 1"

AUME – "Gold membrane electrode"

BCCP – "Bacterial cytochrome *c* peroxidase"

$CaCl_2$ – Cloreto de Cálcio

CPP – "cytochrome c peroxidase"

CYPs – "Cytochrome P450"

D – "Diffusion coefficient"

E.coli – *Escherichia coli*

$E^{0'}$ – "Formal reduction potential"

$E_{1/2}$ – "Half-wave potential"

EC – "Electron transfer reaction followed by a chemical reaction"

$E_{lp}^{0'}$ – "Reduction potential at low pH"

$E_{p/2}$ – "Peak potential at half height"

$E_p^{a/c}$ – "Anodic/Cathodic peak potential"

H_2O_2 – Peróxido de Hidrogénio

i_{cat} – "Catalytic current"

i_{max} – "catalytic current observed at the maximum rate"

$i_p^{a/c}$ – "Anodic/Cathodic peak current"

k – "Rate constant"

kDa – "Kilodalton"

K_M – Michaelis-Menten constant

$K_{O/R}$ – "Proton dissociation constant of the oxidised/reduced form"

ME – "Membrane Electrode"

Mo – Molibdénio

NaCl – Cloreto de Sódio

Ne – *Nitrosomonas europaea*

O_2 – Oxigénio

P.p. – *Paracoccus pantotrophus*

PAz – "Pseudoazurin"

PG – "Pyrolytic graphite"

p*K* – “proton dissociation constant”

PLL – “poly-L-lysine”

SHE – “Standard hydrogen electrode”

V – “Entrapped solution volume”

v – “Scan rate”

VLP – “Virus like particule”

XO – “Xanthine Oxidase”

ε – “Extinction coefficient”

τ - “Time required to scan from $E_{1/2}$ to switching potential”

Índice

Índice das figuras

Capítulo I

Introdução

Peroxidase do citocromo *c Paracoccus pantotrophus*

A redução incompleta do oxigénio molecular para água resulta na formação do peróxido de hidrogénio (H_2O_2). O peróxido de hidrogénio é uma molécula que pode induzir danos ou morte celular devido à sua capacidade de produzir radicais livres. Em processos biológicos, o peróxido de hidrogénio pode ser eliminado em forma de água, através da catalase numa reação de dismutação ou de redução pela peroxidase [Halliwell and Gutteridge 1989].

A peroxidase do citocromo *c* periplásmico (CPP - "cytochrome *c* peroxidase") *Paracoccus pantotrophus* (*P.p.*) é uma enzima dimérica e di-hémica que catalisa a redução de H_2O_2 a H_2O, utilizando pequenos citocromos mono-hémicos como dador fisiológico, através do processo de oxidação [Goodhew *et al*. 1990, Pettigrew 1991]. Cada monómero apresenta um peso molecular de 37,5 kDa, constituído por dois grupos prostético (hemo), denominados como hemo E (hemo de transferência de electrões) e o hemo P (hemo peroxidático). Para a formação do dímero e respetiva ativação, a presença do átomo de cálcio é essencial.

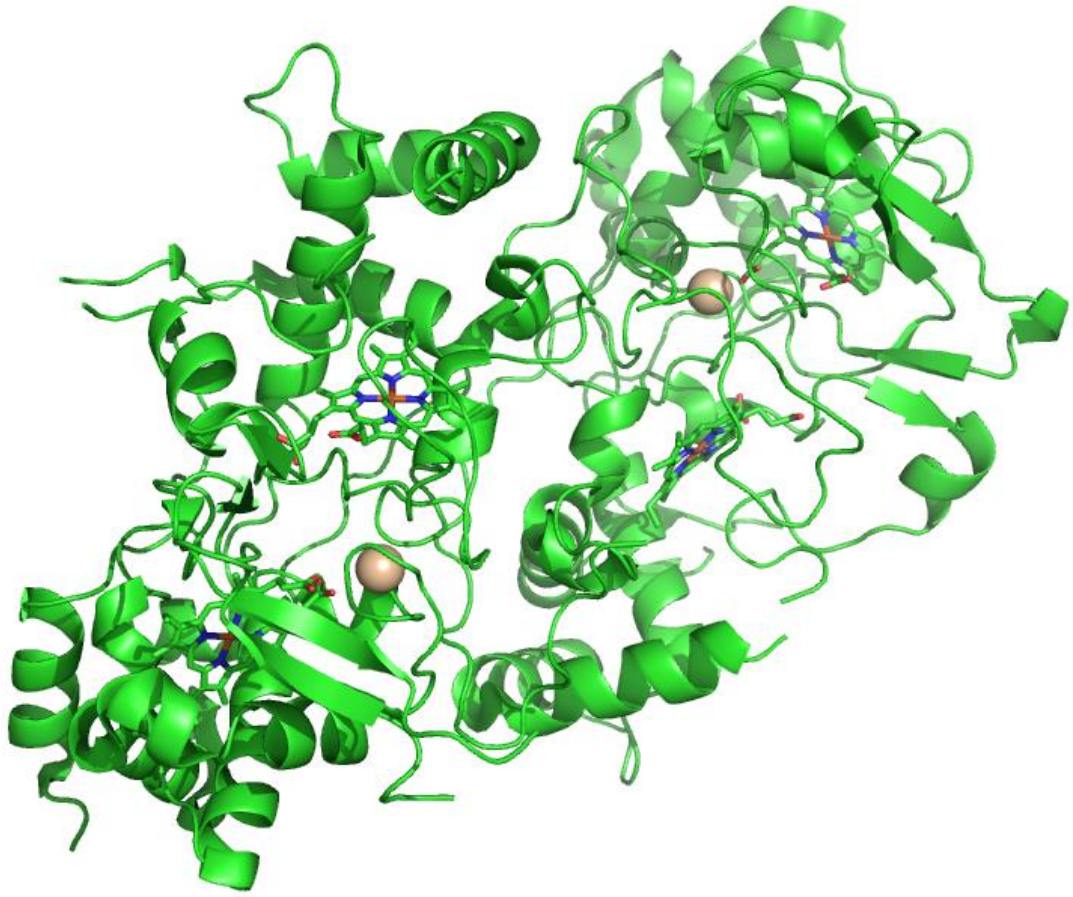

Figura 1 – Estrutura cristalográfica dimérica da Peroxidase do citocromo c *Paracoccus pantotrophus* (código pdb 2C1U) [Echalier *et al*. 2006]. Em cada monómero visualiza-se o átomo de cálcio (em formato *spheres*) no meio dos dois hemos (em formato *stick*).

Mecanismo catalítico – estado redox

A enzima é isolada num estado totalmente oxidado (inativo), em que o hemo E (centro I, potencial alto) encontra-se num equilíbrio de *spin* alto e *spin* baixo, enquanto o hemo P (centro II, potencial baixo) é de *spin* baixo. Durante o mecanismo catalítico, o centro I atua como um centro de transferência de eletrões, aceitando e transferindo eletrões para o hemo P (centro II). A entrada de um eletrão para o hemo de potencial alto leva a uma mudança complexa de estados de *spin* e potenciais redox de ambos os hemos, num mecanismo que envolve fortes interações entre os dois hemos, produzindo uma enzima *mixed valence* em que o hemo P se torna penta-coordenado de *spin* alto, proporcionando o acesso ao substrato, a fim de atingir um "*ready state*" para reagir com o peróxido [Pettigrew *et al*. 2006, Gilmour *et al*. 1993, Gilmour *et al*. 1994].

As transições conformacionais induzidas pela mudança de estado redox de centro I e associada com a formação do hemo P ativo (*mixed valence*) são dependentes da presença do cálcio ligado [Prazeres *et al*. 1993, Prazeres *et al*. 1995a, Prazeres *et al*. 1995b, Gilmour *et al*. 1995]. Esta ativação resulta da reação na transição do hemo de potencial baixo para um estado de *spin* alto com a perda de um ligando de histidina, permitindo a ligação do substrato (suportada por EPR e RMN) [Prazeres *et al*. 1993, Prazeres *et al*. 1995a, Prazeres *et al*. 1995b, Gilmour *et al*. 1995, Gilmour *et al*. 1993]. A estrutura cristalográfica do *P.p.* CCP apoia essas observações [Echalier *et al*. 2006].

Dadores Fisiológicos

Apesar dos citocromos tipo *c* e as proteínas de cobre azul serem estruturalmente muito diferentes, compartilham características de uma superfície de transferência de eletrões que confere "pseudo-especificidade" nas suas interações com uma série de parceiros redox [Williams *et al*. 1995]. É proposto a Pseudoazurina (PAz) ser um dos transportadores de eletrões no periplasma das bactérias, transportando os eletrões entre o complexo de citocromo *bc1* e várias enzimas periplasmáticas envolvidas na desnitrificação [Berks *et al*. 1993, Richter *et al*. 2002]. Outra proteína redox, citocromo *c*550, foi também identificada como dador de eletrões para estas enzimas [Berks *et al*. 1993, Richter *et al*. 2002]. O citocromo *c* mitocondrial é um parente próximo do citocromo *c*550 e, devido à sua disponibilidade, é frequentemente usado como um dador de eletrões alternativo não fisiológico. Contudo, anteriormente, o citocromo *c* de coração

de cavalo (uma proteína comercialmente disponível – hemo do tipo *C*) foi também utilizado, como dador de eletrões para *P.p.* CCP em estudos cinéticos de *Steady-State*, realizados espectrofotometricamente [Prazeres *et al*. 1993]. Embora não seja um parceiro fisiológico da *P.p.* CCP, foi demonstrado que esta pequena proteína é cineticamente competente como dador de eletrões para a enzima *Paracoccus*. No entanto, o citocromo *c* de cavalo exibe um comportamento cinético e de ligação distinto em relação aos outros dadores de eletrões mencionados anteriormente.

Eletroquímica de metaloproteínas

Atualmente está provado que técnicas de voltametria permitem estudar aspetos importantes da química de metaloproteínas e metaloenzimas. A eletroquímica direta destas moléculas atrai grande interesse, uma vez que o processo de reconhecimento de superfície da proteína pelo elétrodo, pode proporcionar um modelo para a transferência de eletrões entre proteínas e enzimas em sistemas biológicos. Informação sobre a termodinâmica, cinética e mecanismos de transferências de eletrões biológicos e, reações acopladas a transferência de eletrões, é acessível com técnicas eletroquímicas [Armstrong 2002]. Uma ampla diversidade de elétrodos de trabalho e estratégias podem ser utilizados com fim a caracterizar e compreender as funções fisiológicas de proteínas e enzimas redox [Correia dos Santos *et al*. 2001, Correia dos Santos *et al*. 2004].

Uma possibilidade é a utilização de elétrodos de membrana, onde a proteína em estudo está presa entre uma membrana de diálise e a superfície do elétrodo [Correia dos Santos *et al*. 2003]. Esta estratégia apresenta várias vantagens importantes, nomeadamente a utilização de volumes muito pequenos de proteína (aproximadamente, 2-4 μl), a facilidade de preparação do elétrodo e o baixo custo, assim como, a capacidade para rapidamente investigar parâmetros experimentais com a mesma amostra de proteína. Além disso, as membranas de diálise são carregadas negativamente, oferecendo uma forma de modular o ambiente elétrico perto da superfície do elétrodo.

Num trabalho anterior, foi demonstrada a competência da *P.p.* PAz como um dador de eletrões para a *P.p.* CCP e, a cinética de transferência de eletrões intermolecular foi analisada [Paes de Sousa *et al*. 2006]. Os estudos foram realizados por voltametria cíclica, usando um

elétrodo de ouro de membrana, e os resultados foram analisados segundo a teoria de *thin-layer* [Bard and Faulker 2001]. Neste caso, a reação de transferência de eletrões é um processo sem difusão, contrariamente à situação em que as espécies em estudo estão em solução e o processo é controlado por difusão.

Importância do desenvolvimento de biossensores para a Biotecnologia

Nas últimas décadas tem havido um enorme interesse nos elétrodos enzimáticos e no desenvolvimento de uma variedade de novas estratégias, em que a transferência de eletrões de ou para enzimas redox é acoplada mais próxima ao elétrodo, tendo sidos explorados vários métodos, especialmente o uso de "elétrodos modificados" [Murray *et al*. 1987]. O rápido crescimento na área da biotecnologia exige novas e melhores técnicas analíticas, incluindo biossensores melhorados [Bianco 2002]. Nos últimos anos, o método de imobilização de proteína com SWNTs (*single-walled carbon nanotubes*) tem sido muito usado, tornando-se num método bastante promissor na bioelectroquímica [Azamian *et al*. 2002] e, por sua vez, na nanotecnologia. Entre todas as tecnologias eletroquímicas, a bioelectroquímica tem sido a mais bem-sucedida no desenvolvimento de biossensores. O uso de biossensores tem tido uma enorme relevância no campo clínico e da saúde, assim como, na deteção e controlo em fins ambientais. Portanto, o desenho de biossensores está destinado a ser um ramo promissor e excitante no campo da biotecnologia analítica [Bianco 2002].

Objetivo

O objetivo do trabalho foi estudar a interação da *P.p.* CCP com o parceiro não fisiológico, citocromo *c* de coração de cavalo, usando diferentes métodos voltamétricos, assim como, configurações de elétrodos diferentes. Os estudos foram realizados: (1) com ambas as proteínas em solução por voltametria cíclica. O elétrodo de trabalho usado foi um elétrodo de ouro, com o auxílio de um promotor, funcionando como intermediário entre o elétrodo e a proteína. Estas experiências foram realizadas na ausência e na presença do substrato, H_2O_2, e os resultados foram analisados em termos de processo de controlo por difusão; (2) com as proteínas aprisionadas numa membrana, usando as mesmas técnicas e o comportamento analisado em termos de um processo sem difusão. O elétrodo anterior foi utilizado e analisada a necessidade

de utilização de um promotor. Foi ainda analisada a influência das condições de solução, tais como, o pH e a força iónica. Os resultados obtidos em (1) e (2), nomeadamente, as cinéticas de transferência eletrónica intermolecular, foram comparados, assim como, a influência da membrana carregada.

Capítulo II

"Benefits of membrane electrodes in the electrochemistry of metalloproteins: mediated catalysis of *paracoccus pantotrophus* cytochrome *c* peroxidase by horse cytochrome *c*: a case study"

Autores: P. M. Paes de Sousa, S. R. Pauleta, **D. Rodrigues**, M. L. Simões Gonçalves, G. W. Pettigrew, I. Moura, J. J. G. Moura, M. M. Correia dos Santos

Contribuição dos autores:

Planeamento do projeto da investigação: P. M. Paes de Sousa, **D. Rodrigues** e M. M. Correia dos Santos.

Realização das experiências: **D. Rodrigues**.

Realização da análise de dados: P. M. Paes de Sousa, **D. Rodrigues** e M. M. Correia dos Santos.

Contribuição para a escrita do manuscrito: P. M. Paes de Sousa, S. R. Pauleta, **D. Rodrigues** M. L. Simões Gonçalves, G. W. Pettigrew, I. Moura, J. J. G. Moura, M. M. Correia dos Santos

Abstract

A comparative study of direct and mediated electrochemistry of metalloproteins in bulk and membrane-entrapped solutions is presented. This work reports the first electrochemical study of the electron transfer between a bacterial cytochrome *c* peroxidase and horse heart cytochrome *c*. The mediated catalysis of the peroxidase was analysed both using the membrane electrode configuration and with all proteins in solution. An apparent Michaelis constant of 66 ± 4 and 42 ± 5 μM was determined at pH 7.0 and 0 M NaCl for membrane and bulk solutions, respectively. The data revealed that maximum activity occurs at 50 mM NaCl, pH 7.0, with intermolecular rate constants of $(4.4 \pm 0.5) \times 10^6$ and $(1.0 \pm 0.5) \times 10^6$ M^{-1} s^{-1} for membrane-entrapped and bulk solutions, respectively. The influence of parameters such as pH or ionic strength on the mediated catalytic activity was analysed using this approach, drawing attention to the fact that careful analysis of the results is needed to ensure that no artefacts are introduced by the use of the membrane configuration and/or promoters, and therefore the dependence truly reflects the influence of these parameters on the (mediated) catalysis. From the pH dependence, a pK of 7.5 was estimated for the mediated enzymatic catalysis.

Introduction

The use of membrane electrodes (ME), with the protein imprisoned between a dialysis membrane and the electrode surface, has some important advantages. These are (1) the use of very small volumes of protein - 2 µl (to overcome the limitation of sample availability), (2) the ease of electrode preparation and low cost, (3) the rapid investigation of various experimental parameters, such as pH and ionic strength and (4) the thin layer configuration, which easily allows quantitative information about the redox processes to be obtained [Haladjian *et al*. 1994, Haladjian *et al*. 1996].

Moreover, the membranes used in this type of electrode configuration are charged, offering a convenient way to modulate the electric environment close to the electrode surface, and thus ascertain the role of electrostatic interactions in the efficiency of the electron transfer. It is also important to point out that this configuration is an interesting strategy when adsorption of a protein or an enzyme to the electrode surface is not successfully achieved, hindering the use of protein film voltammetry [Armstrong 2002]. Additionally, the entrapment of proteins between the membrane and the electrode surface enables the achievement of thin-layer conditions and avoids diffusional problems [Laviron 1979].

Studies reporting the benefits of the ME in protein electrochemistry and its role in modulating the redox behaviour focused on the direct electrochemistry of small electron transfer proteins. In these works, a critical comparison was made with data obtained with non-ME [Lojou and Bianco 2000, Correia dos Santos *et al*. 2003, Santos *et al*. 2006]. More recently ME were used to study multiredox cofactor-containing enzymes and their interaction with both physiological and non-physiological redox partners [Lojou *et al*. 2003, Ferapontova *et al*. 2003]. In both studies, although the direct electrochemistry and the mediated catalysis of the proteins were analysed using that strategy, with the proteins in solution or adsorbed on a modified electrode, no comparison was made among the different strategies.

The mediated catalysis of the bacterial cytochrome *c* peroxidase (BCCP) from *Paracoccus pantotrophus* by *P. pantotrophus* pseudoazurin examined at a gold ME (AUME) was recently reported by us [Paes de Sousa *et al*. 2007]. Cyclic voltammetry was used to analyse the direct transfer to pseudoazurin and to probe its interaction with BCCP. The results obtained showed that this small copper protein is a competent electron donor to BCCP, in agreement with

solution steady-state kinetics performed spectrophotometrically [Pauleta *et al*. 2004a]. The pH and ionic strength effect on the voltammetric signal of pseudoazurin as well as on the intermolecular rate constant were also easily studied at the ME. Horse heart cytochrome *c*, a commercially available small *c*-type haem protein, has been previously used as an electron donor to *Paracoccus* BCCP in solution steady-state kinetic studies performed spectrophotometrically [Gilmour *et al*. 1994]. Although it is not a physiological partner of BCCP, this small protein was shown to be kinetically competent as an electron donor to the *Paracoccus* enzyme. However, horse cytochrome *c* exhibits a distinct kinetic and binding behaviour from the physiological partners pseudoazurin, a type I copper protein, and cytochrome *c*550, which is also a small *c*-type haem protein. The physiological partners bind at the same site on the surface of BCCP near the electron-transferring haem of the enzyme [Pauleta *et al*. 2004b], while horse cytochrome c has been proposed to have two binding sites, a looser binding site near the electron-transferring haem and an additional tight one in-between the two haems of the enzyme [Pettigrew *et al*. 1999]. Below 50 mM NaCl, there is little change in the activity when the electron donor is either cytochrome *c*550 or pseudoazurin. In contrast, when horse cytochrome *c* is used as an electron donor there is a threefold decrease in activity as the ionic strength is lowered, and this correlates with an increased binding affinity [Pettigrew *et al*. 2003a, Pettigrew *et al*. 2003b]. It was concluded that the higher-affinity binding was, in fact, non-productive and that only when that attachment was loosened by raised ionic strength could the horse cytochrome *c* migrate to the true electron transfer site.

This work reports the first electrochemical study of the electron transfer between BCCP and horse cytochrome *c*. The mediated catalysis of BCCP was analysed using the ME configuration and with all proteins in solution. Our aim is to compare the results obtained with these two strategies in order to gain a better insight into the interactions that occur at the ME surface and to highlight the effects of this strategy on the direct and mediated electrochemistry of metalloproteins.

Materials and Methods

Proteins and chemicals

Horse heart cytochrome *c* was obtained from Sigma and used without further purification. Pseudoazurin and BCCP were isolated and purified as described before [Goodhew *et al*. 1990]. The concentration of the proteins was determined spectrophotometrically using the extinction coefficient at 409 nm, $\varepsilon = 250\ mM^{-1}\ cm^{-1}$, and at 550 nm, $\varepsilon = 29.5\ mM^{-1}\ cm^{-1}$, for fully oxidized BCCP and reduced horse cytochrome *c*, respectively [Goodhew *et al*. 1990, Bowden *et al*. 1982].

4,4´-Dithiodipyridine and $CaCl_2$ were obtained from Sigma and all other chemicals were pro analysis grade. All solutions were prepared with deionised water from a Milli-Q water purification system.

Apparatus and procedures

The cyclic voltammograms were obtained using an EG&G-PAR model 273A potentiostat/galvanostat controlled via the 270 software. The scan rate varied between 5 and 200 $mV\ s^{-1}$. Throughout this article, all potential values are referred to the standard hydrogen electrode.

A conventional three-electrode configuration cell was used, with a platinum auxiliary electrode and an Ag/AgCl reference electrode (BAS MF-2052; 205 mV vs. the standard hydrogen electrode). The working electrode was a gold disk electrode from BAS (MF-2014) with a nominal radius of 0.8 mm. The effective surface area of the electrode was determined from its response in a known concentration of the ferrocyanide/ferricyanide couple ($D = 7.84 \times 10^{-6}\ cm^2\ s^{-1}$ [Kakihana *et al*. 1980]) and was found to be $0.0195\ cm^2$.

Before each experiment the electrode was polished by hand on a polishing cloth (Buehler 40-7212) using a water/alumina (0.05 μm) slurry (Buehler 40-6365-006), sonicated for 5 min, rinsed well with Milli-Q water and finally dipped into 1 mM 4,4´-dithiodipyridine solution for 5 min. The membrane configuration was prepared as previously described [Correia dos Santos *et al*. 2003] using a negatively charged Spectra/Por MWCO 3500 membrane.

In typical experiments, the supporting electrolyte, as well as the working solution, contained 10 mM phosphate buffer pH 7.0 ± 0.1, 0.5 mM 4,4´-dithiodipyridine and 1 mM $CaCl_2$. Horse cytochrome *c* was present in a concentration of 100 μM and the concentration of BCCP

varied between 0.25 and 1 µM. In the experiments with a saturating concentration of substrate, 100 - 350 µM H_2O_2 was present in the electrolyte solution. The effect of substrate concentration was determined by varying the H_2O_2 concentration between 10 and 200 µM. The pH of the electrolyte was varied from 5.4 to 10.5 by adding 5 M HCl or 2 M NaOH to a mixed-buffer system containing 10 mM 2-morpholinoethanesulfonic acid, sodium phosphate, *N*-(2-hydroxyethyl) piperazine-*N´*-ethanesulfonic acid, tris(hydroxymethyl) aminomethane and 3-cyclohexylamino-1-propanesulfonic acid. The effect of the ionic strength was studied by adding increasing amounts of NaCl (up to 500 mM).

It should be pointed out that in order to have reproducible results for some BCCP concentrations more than one ME had to be prepared, to cover the whole range of experimental variables. This is due to the fact that the enzyme exists in a monomer-dimer equilibrium in which only the dimer is active. Dilution of the enzyme shifts the equilibrium towards the monomer and therefore the activity is lost with time [Pettigrew *et al*. 1999], which corresponds to a decrease of the catalytic current.

All solutions were deaerated for 10 min with high-purity nitrogen, and all measurements were performed at least in duplicate in a temperature-controlled room at 20 ± 1 ºC.

Results and Discussion

Catalytic activity of *P. pantotrophus* BCCP with horse heart cytochrome *c* as an electron donor.

ME cyclic voltammetry

The electrochemical behaviour of horse cytochrome *c* is well known either in bulk or entrapped on a ME. Indeed, Eddowes and Hill [Eddowes and Hill 1977] found that essentially reversible voltammetry of cytochrome *c* in solution could be observed at a 4,4´-dipyridyl-modified gold electrode. Latter, Lojou and Bianco [Lojou and Bianco 2000] showed that fast electrochemical response was observed when a thin layer of protein solution was entrapped between a negatively charged dialysis membrane and a non-modified gold electrode surface. In both cases favourable conditions for electron transfer to occur were achieved, which accounts for the similarity of the values determined for the formal potentials.

In this work, the direct electrochemistry of cytochrome *c* was revisited at a AUME, but this time in the presence of 4,4´-dithiodipyridine (data not shown). The promoter was used in order to have similar experimental conditions for the studies both in solution and with the membrane-con- figuration electrode (further reasons will be explained below).

Thin-layer behaviour will be observed as long as the entrapped layer thickness l is smaller than the diffusion- layer thickness for a given experimental time scale, t:

$$l < (2Dt)^{1/2} \qquad (1)$$

where D is the diffusion coefficient of the species [Bard and Faulkner 2001]. Under our experimental conditions (cyclic voltammetry with scan rates between 5 and 200 mV s^{-1}), this condition was verified for the lowest scan rates (v < 100 mV s^{-1}), with i_p varying linearly with v in this range. From this variation [Bard and Faulkner 2001], an entrapped-solution volume, V, of 1.2×10^{-5} cm^3 was estimated, which corresponds to an entrapped-layer thickness $l = V/A = 6.2 \times 10^{-4}$ cm. Since the diffusion coefficient of cytochrome *c* is $D = 1.2 \times 10^{-6}$ cm^2 s^{-1} (see below), thin-layer conditions occur for v < 160 mV s^{-1}, as verified.

The ratio of the cathodic (i_{pc}) and anodic (i_{pa}) peak currents was close to 1 and the peak-to-peak separation, $\Delta E_p = E_{pa} - E_{pc}$, was close to 20 mV for the lowest scan rates. In the same

range, the width at half height ($\Delta E_{p,1/2}$) was also constant for the cathodic and anodic peaks, with a value close to 90 mV. Although ΔE_p increased with *v*, the average of the reduction and oxidation peak potentials remained almost constant for all scan rates and a formal reduction potential $E^{o\prime} = (E_{pc} + E_{pa})/2 = 250 \pm 5$mV was estimated at pH 7.0, in agreement with other reported values (e.g. 280 mV, ME at pH 7.6 [Lojou and Bianco 2000], and 255 mV, bulk solution at pH 7.0 [Eddowes and Hill 1977]). The catalytic activity of *P. pantotrophus* BCCP towards horse cytochrome *c* was then investigated at the AUME, with working solutions of 100 µM cytochrome *c* and different BCCP concentrations (0.25 - 1 µM) in the presence of a saturating substrate concentration (125 - 350 µM, depending on the enzyme concentration) or with a working solution of 100 µM cytochrome *c* and 0.25 µM BCCP in the presence of increasing H_2O_2 concentrations. These solutions and the electrolyte contained 1 mM $CaCl_2$ (for enzyme activation [Gilmour *et al*. 1994, Gilmour *et al*. 1993]).

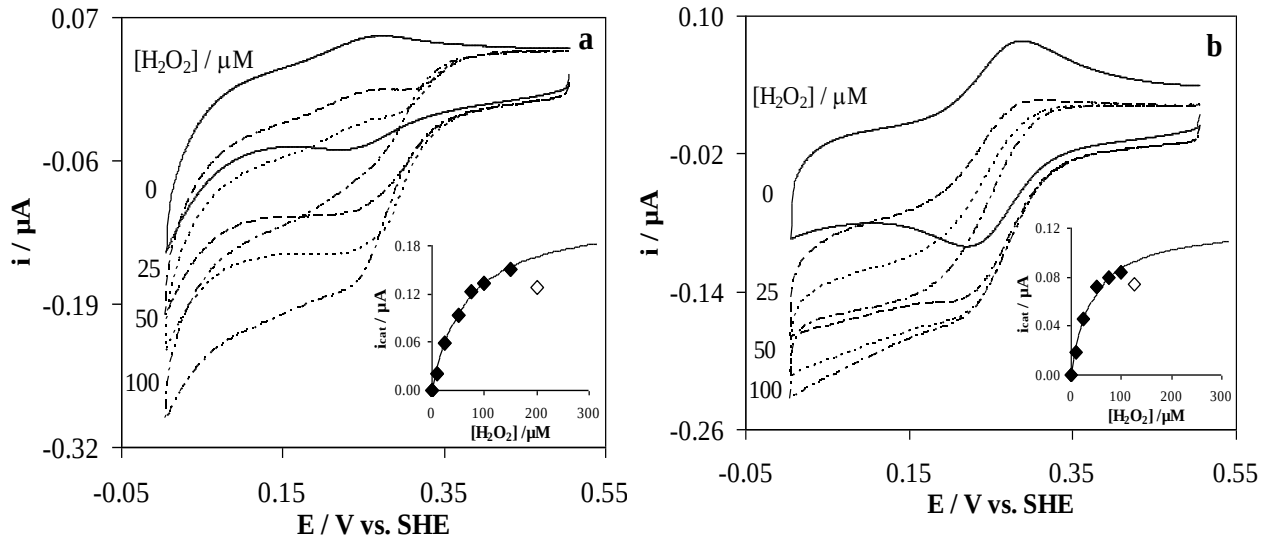

Figure 2 – Cyclic voltammograms (v = 20 mV s^{-1}) at the gold membrane electrode (a) or bulk solution (b) of 100 µM horse heart cytochrome *c* and 0.5 µM bacterial cytochrome *c* peroxidase (BCCP) in the presence of increasing concentrations of H_2O_2. The medium consisted of 10 mM phosphate buffer pH 7.0, 0.5 mM 4,4´-dithiodipyridine and 1 mM $CaCl_2$. *SHE* – standard hydrogen electrode

The cytochrome *c* response is unchanged in the presence of BCCP. Moreover, although cytochrome *c* is known to feature a small peroxidase activity [Vandewalle and Petersen 1987, LoÈtzbeyer *et al*. 1996], its response also remained unchanged upon addition of H_2O_2 in the absence of enzyme. However, it is clear from **Figure 2a** that in the presence of BCCP the cytochrome *c* peak current increases with H_2O_2 concentration in the electrolyte, and a sigmoidal

wave develops when a saturating concentration of substrate is reached. Voltammograms from solutions containing only BCCP either in the presence or in the absence of H_2O_2 were indistinguishable from the background current (data not shown).

The half-wave potential of the sigmoidal waves ($E_{1/2}$ = 275±10 mV = $E^{o\prime}$) shows that the actual transfer process is the catalysed reduction of cytochrome *c*. The catalytic current is scan rate independent up to 50 mV s^{-1} and increases for increasing BCCP concentrations. This behaviour is consistent with a reaction mechanism involving an initial heterogeneous electron transfer reaction at the electrode (**Figure 3, step 1**), followed by homogeneous chemical reactions: the oxidized form of cytochrome *c* is regenerated by BCCP (**Figure 3, step 2**) which, in turn, is recycled by H_2O_2 (**Figure 3, step 3**). This mechanism can be simplified to

$$\mathbf{Ox + e^- \rightleftharpoons Red} \qquad \mathbf{(2)}$$

$$\mathbf{Red + Z \rightarrow Ox}$$

provided that the following conditions are obeyed: (1) the heterogeneous electron transfer (**Figure 3, step 1**) is a reversible reaction; (2) the homogeneous chemical reaction (**Figure 3, step 2**) is irreversible; (3) the reaction between cytochrome c and BCCP is pseudo first order with a reaction rate constant given by $k' = k\ C_{BCCP}$, where k is the second-order rate constant [Paes de Sousa *et al.* 2007, Lopes *et al.* 2001].

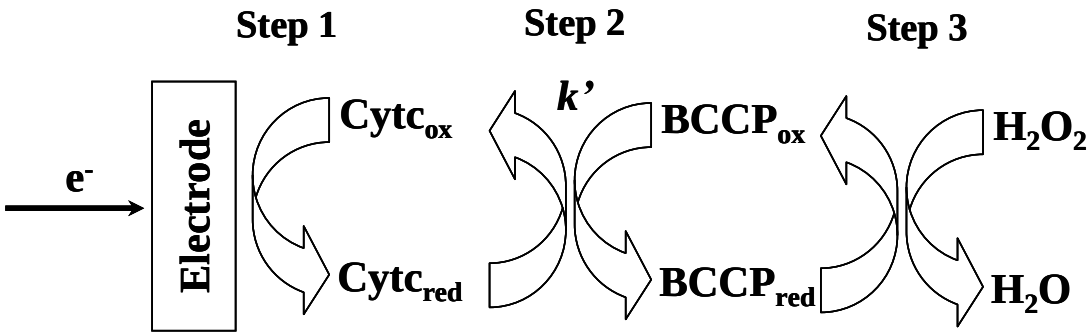

Figure 3 – Mediation scheme for BCCP: the electrode reduces horse heart cytochrome *c*, which is immediately reoxidized by BCCP; the level of oxidized BCCP is then restored by conversion of hydrogen peroxide to water.

The first condition is well obeyed, as previously demonstrated. The second condition is fulfilled because BCCP is being reoxidized in the catalytic cycle owing to the excess of H_2O_2 in solution (**Figure 3, step 3**), and not by transferring electrons back to horse cytochrome *c*. As to

requisite 3, it would imply that BCCP is present in large excess, which is not the case. However, under saturating concentrations of H_2O_2, this requisite is obeyed when the rate of recycling the oxidised BCCP by H_2O_2 is not rate limiting. If this is the case, BCCP will always be available to react with cytochrome *c* and pseudo-first-order conditions are met.

Cyclic voltammograms at 20 mV s^{-1} were obtained for 100 µM cytochrome *c* and increasing BCCP concentrations (0.25 - 1 µM), in the absence and in the presence of a saturating concentration of H_2O_2 (125 - 350 µM, depending on the enzyme concentration), and are shown in **Figure 4**.

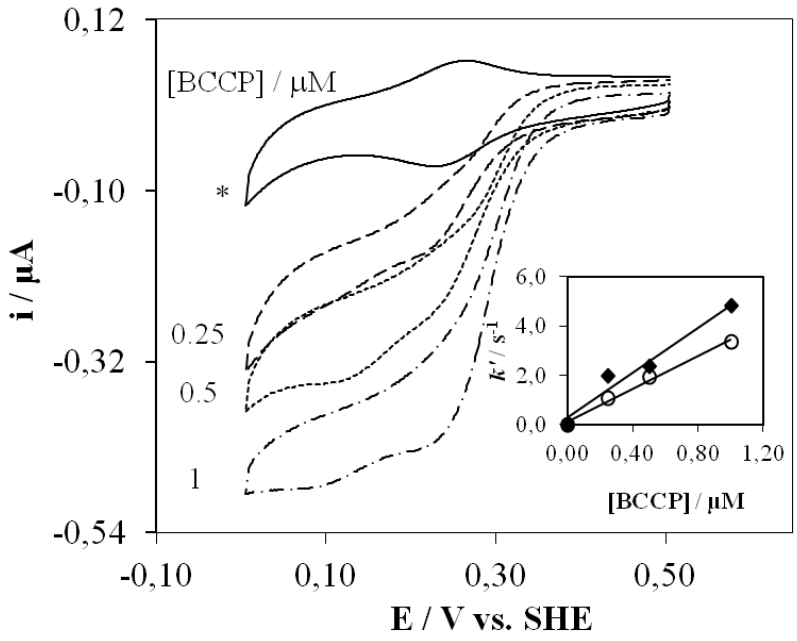

Figure 4 – Cyclic voltammograms (v = 20 mV s^{-1}) obtained at the gold membrane electrode for 100 µM cytochrome *c* and increasing BCCP concentrations (0.25 - 1 µM), in the absence (*asterisk*) and in the presence of a saturating H_2O_2 concentration (125 - 350 µM, depending on the enzyme concentration). *Insert*: Variation of the pseudo-first-order rate constant with BCCP concentration for 0 mM (*circles*) and 50 mM (*diamonds*) NaCl. The medium consisted of 10 mM phosphate buffer pH 7.0, 0.5 mM 4,4´-dithiodipyridine and 1 mM $CaCl_2$.

From these recordings the catalytic current (i_{cat}) was determined as the difference between the current in the presence and in the absence of substrate, both measured at the same potential. The data was treated according to Laviron's theory for diffusionless electrochemical systems [Laviron 1979, Paes de Sousa *et al*. 2007], where the catalytic current is given by

$$\mathbf{i_{cat} = n\,F\,k'\,V\,C_{Cyt\,c}} \qquad \mathbf{(3)}$$

In this equation, V is the entrapped-solution volume, C is the concentration and the other terms have the usual meaning.

From the variation of the pseudo-first-order rate constant, k´, with BCCP concentration, an intermolecular rate constant $k = (3.2 \pm 0.5) \times 10^6$ M^{-1} s^{-1} was estimated (**Figure 4**, insert, circles).

For assays where the H_2O_2 concentration was varied, for a constant cytochrome *c* and BCCP mixture, the catalytic current was plotted as a function of the substrate concentration (**Figure 2a**, insert). It is clear that the catalytic current decreases after 150 µM H_2O_2 and so the data were fitted to the Michaelis–Menten kinetics for concentrations up to that value. Since thin-layer conditions are verified, the Michaelis-Menten equation has the form

$$i_{cat} = \frac{i_{max} C_{H_2O_2}}{C_{H_2O_2} + K_M} = \frac{nFk'VC_{Cytc}C_{H_2O_2}}{C_{H_2O_2} + K_M} \qquad \mathbf{(4)}$$

Using the CERN library Fortran program MINUIT algorithm, we estimated an apparent Michaelis–Menten constant $K_M = 66 \pm 4$ µM and an intermolecular electron transfer rate constant $k = (3.4 \pm 0.3) \times 10^6$ M^{-1} s^{-1}.

This electron transfer rate constant is higher than the value determined for a physiological donor, pseudoazurin ($(1.4 \pm 0.2) \times 10^5$ M^{-1} s^{-1} [Paes de Sousa *et al.* 2007]). The more likely explanation for the difference between the rate constants would be a difference in the redox potential of these two electron donors, but the values determined at pH 7.0 are very similar.

Therefore, this behaviour must be related to another factor that influences the donor-enzyme interaction. In the case of these small electron donors the global charge surface is high and asymmetrically distributed, creating a significant dipole moment. Actually, the dipole moment of pseudoazurin is 651 D, and that of horse cytochrome *c* is 299 D [Pauleta *et al.* 2004a]. This twofold difference in the dipole moment probably results in a stronger association of pseudoazurin with BCCP, and consequently the dissociation of the complex is disfavoured, explaining the lower rate constants observed.

Solution cyclic voltammetry

The mediated catalysis of BCCP by horse cytochrome *c* was also analysed at the gold electrode from solutions containing 100 µM horse heart cytochrome *c*, 0.5 µM BCCP and 1 mM $CaCl_2$. Again, the peak current increases with H_2O_2 concentration in the electrolyte, and a sigmoidal wave develops when a saturating concentration of substrate (100 µM) is present in the electrolyte, which is scan rate independent up to 50 mV s^{-1} (**Figure 2b**).

The theory describing such a mechanism for diffusion-controlled processes was developed by Nicholson and Shain [Nicholson and Shain 1964] and applied to several kinetic studies of reactions between mediators and redox proteins [Lopes *et al*. 2001]. The intermolecular rate constant can also be calculated from the value of the H_2O_2 saturated limiting current using Equation 5 [Coury *et al*. 1990, Savéant and vianello 1965]:

$$\mathbf{i_{cat} = n\ F\ A\ D^{1/2}\ C_{Cyt\ c}\ (k')^{1/2}} \qquad \mathbf{(5)}$$

In this equation, *D* is the diffusion coefficient of cytochrome *c*. The valid value for our experimental conditions, $D = (1.2 \pm 0.1) \times 10^{-6}$ cm^2 s^{-1}, was computed from the dependence on the scan rate of either the cathodic or the anodic peak currents of the cyclic voltammograms for solutions containing both cytochrome *c* and BCCP in the absence of H_2O_2, using the Randles-Ševčík equation [Bard and Faulkner 2001]. Calculations using Equation 5 gave an intermolecular rate constant of $k = (4.0 \pm 0.5) \times 10^5$ M^{-1} s^{-1}.

The catalytic current for the different H_2O_2 concentrations (**Figure 2b**, insert) was also fitted to Michaelis-Menten kinetics for concentrations up to 100 µM, and $K_M = 42 \pm 5$ lM and k $= (3.9 \pm 0.3) \times 10^5$ M^{-1} s^{-1} were obtained.

Similar apparent Michaelis-Menten constants were estimated for the proteins in bulk and entrapped solution, indicating that the membrane does not hamper the substrate diffusion. A higher value for the intermolecular rate constant was obtained for the proteins using the membrane configuration, reflecting a more favourable domain for the molecular interactions that must be established for electron transfer to occur between BCCP and cytochrome *c*. In both situations an inhibition effect by the substrate is observed for higher H_2O_2 concentrations, as verified in the case of the catalysis mediated by pseudoazurin [Paes de Sousa *et al*. 2007]. A

similar inhibitory effect was observed in the study of other peroxidases [Kim *et al*. 1990, Scott and Bowden 1994, Dequaire *et al*. 2002].

Ionic strength and pH effects

One of the advantages of the ME approach is the ability to rapidly investigate effects on the redox behaviour of various experimental conditions, such as the pH or the supporting electrolyte composition. Another advantage of the approach is the small amount of protein needed for a series of measurements. This is so because once the ME has been mounted in the cell, it does not need to be removed or exchanged while changing any of those variables.

The same approach can also be applied to study the effect of such experimental variables on the kinetic activity of a more complex system, such as in mediated catalysis. Changes in the pH and/or the ionic strength of the medium may influence the rate of association, pre-orientation within the encounter complex, stability of the reactive complex or/and rate of dissociation of the products. However, the interpretation of ionic strength (or pH) dependences of the kinetic activity is complex and the behaviour observed should not be masked by the influence of those variables on the direct electrochemistry of the redox partners.

The effect of the ionic strength on the intermolecular rate constant for BCCP and horse cytochrome *c* was analysed with the proteins entrapped at the AUME and in bulk solution with a working solution containing 100 µM horse cytochrome *c*, 0.5 µM BCCP and 1 mM $CaCl_2$, in the presence of increasing amounts of NaCl (in the range 0 - 500 mM) and a saturated H_2O_2 concentration.

In both situations, the ionic strength dependence of the mediated catalysis has a bell-shaped curve, with a maximum activity at 50 mM NaCl (**Figure 5**). The decrease of activity with increasing NaCl concentrations is consistent with the electrostatic character of the interaction between BCCP and the electron donor, cytochrome *c*. Indeed, cytochrome *c* has an asymmetric charge distribution with a positive surface that surrounds the exposed haem edge, which is the region proposed to interact with the negative surface around the exposed electron-transferring haem of the peroxidase [Gilmour *et al*. 1994, Pettigrew *et al*. 1999]. The increase of activity at low NaCl concentrations can be explained considering that for the lowest ionic strength the

encounter complex formed has an orientation that is not so favourable for electron transfer. Therefore, the increase in NaCl concentration enables the lateral search at the peroxidase surface for the competent electron transfer orientation [Pauleta *et al*. 2004, Pettigrew 2006]. Another explanation for this effect is that at low ionic strength cytochrome *c* reduction at the electrode might be affected by the lower k_{off} rate constant of the complex with BCCP.

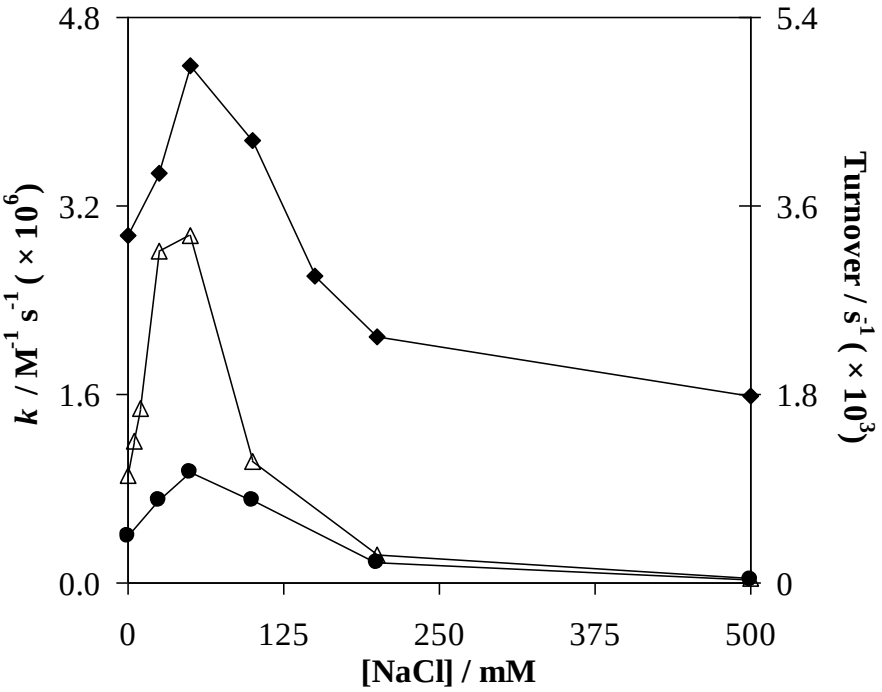

Figure 5 – Effect of ionic strength on the intermolecular rate constant for 100 µM horse heart cytochrome *c*, 0.5 µM BCCP and saturating H_2O_2 (150 µM diamonds or 100 µM circles) at the gold membrane electrode (diamonds) or in bulk solution (circles) and on the activity of BCCP with horse cytochrome *c* as an electron donor from solution steady-state kinetics performed spectrophotometrically (triangles) [Pauleta *et al*. 2004]. The medium consisted of 10 mM phosphate buffer pH 7.0 and 1 mM $CaCl_2$.

Using the approach described above (Equation 3), one can use the analysis of the catalytic current variation as a function of BCCP concentration (**Figure 4**, insert, diamonds) to estimate an intermolecular rate constant for maximum activity $k = (4.4 \pm 0.5) \times 10^6$ M^{-1} s^{-1} for the membrane configuration. In the case of the bulk solution, a rate constant for maximum activity $k = (1.0 \pm 0.5) \times 10^6$ M^{-1} s^{-1} was determined using Equation 5.

Similar behaviour was observed by solution steady-state kinetics performed spectrophotometrically, when this small cytochrome is used as an electron donor, with a

maximum turnover also occurring at 50 mM NaCl [Pauleta *et al*. 2004], as can be observed in **Figure 5**. However, in the voltammetric experiments with the membrane the variation in activity with ionic strength is less pronounced than that found with the proteins in bulk solution (either in the voltammetric assays or in solution steady-state kinetics performed spectrophotometrically). In fact, from 50 to 500 mM NaCl the activity decreases by 64% at the ME, while in the other two cases the decrease is 98%.

A similar effect was observed for the mediated catalysis of *P. pantotrophus* BCCP by *P. pantotrophus* pseudoazurin, where similar profiles were obtained with the membrane configuration and solution steady-state kinetics performed spectrophotometrically, though the maximum activity was observed for higher NaCl concentration in the former case. The differences may be due to the charge of the membrane, which somehow favours the formation of the encounter complex, making it less dependent on the ionic strength, in spite of the electrostatic forces that govern the interaction. This may be also the reason why higher rate constants were determined for horse cytochrome *c* using the membrane configuration, although values of the same order of magnitude were obtained for maximum activity [$k = (4.4 \pm 0.5) \times 10^6$ M^{-1} s^{-1} for the membrane configuration and $k = (1.0 \pm 0.5) \times 10^6$ M^{-1} s^{-1} for bulk solution] as illustrated in **Figure 5**.

The behaviour observed in the voltammetric experments truly reflects the effect of ionic strength on the interaction between the enzyme and the electron donor rather than on the direct electrochemistry of horse cytochrome *c* due to the presence of the promoter. The horse cytochrome *c* peak current was shown to be NaCl-independent when 4,4´-dithiodipyridine is present in the medium (data not shown). Behaviour different from that observed at a bare gold electrode in the membrane configuration was evidenced, where a sharp decrease in current was observed at increasing NaCl concentrations [Lojou and Bianco 2000]. Similar behaviour was also observed for the direct electrochemistry of pseudoazurin at a dithiodipyridine gold modified electrode [Paes de Sousa *et al*. 2007].

The pH behaviour of horse cytochrome *c* is well known to present a p*K* close to 9.5 associated with the disappearance of the 695 nm absorption band, which is believed to be due to the replacement of the iron-coordinated methionine residue by a nitrogenous ligand, assigned as Lys73 [Moore and Pettigrew 1991, Assfalg *et al*. 2003].

Previous bulk voltammetric studies of horse cytochrome *c* at a 4,4´-bipyridyl-modified gold electrode in the pH range 4.5 - 10.5 showed that while the peak potential remains essentially constant until pH 9, the peak current profile has a bell shape [Eddowes and Hill 1979]. The maximum current was observed at pH 7 and two p*K* values around 9 and 5 were computed from that variation. The former is in agreement with the value obtained by other techniques, as well as with the observed E_p variation. The latter was attributed by the authors to the protonation of the promoter that disrupts the interaction between the gold surface and the protein, leading to a decrease of the electrochemical current [Eddowes and Hill 1979].

For the reasons presented above, the pH dependence of the intermolecular rate constant for BCCP and horse cytochrome *c* was analysed at the bare AUME, i.e. in the absence of 4,4´-dithiodipyridine.

In order to accurately interpret the results of this pH dependence, the effect of this parameter on the electrochemical signal of horse cytochrome *c* alone was studied between pH 5 and 10 in the same conditions. As expected, the redox potential remained constant for pH < 9 and a pronounced decrease was observed for higher pH values (data not shown). A p*K* of 9.1 ± 0.1 was determined, in accordance with reported values [Moore and Pettigrew 1991, Assfalf *et al.* 2003, Eddowes and Hill 1979]. For the peak current, a bell-shaped profile was obtained (**Figure 6**, circles), behaviour similar to that observed for bulk solution in the presence of the promoter [Eddowes and Hill 1979]. The peak current pH dependence was fitted to the following equation [Cornish-Bowden 2001]

$$\mathbf{i_{cat} = (i_{opt})/(1+10^{(pKa1-pH)} + 10^{(pH-pKa2)})} \qquad \mathbf{(6)}$$

and p*K* values of 5.3 ± 0.3 and 9.5 ± 0.3 were estimated. The latter is in clear agreement with the characteristic alkaline p*K* of this protein.

Several electrochemical studies using different approaches have observed a similar behaviour for the dependence on the pH of the horse cytochrome *c* current, and in some cases an acidic p*K* with an identical value, within the experimental errors, has been determined. However, depending on the authors and the conditions employed in the studies, the p*K* was assigned differently, namely to the proton-dissociation constant of the promoter [Eddowes and Hill 1979], the Coulombic properties of the electrode surface [Harmer and Hill 1984, Armstrong *et al.*

1987], the competitive adsorption of protons on the clay-modified electrodes [Sallez *et al*. 2000] or the protein denaturation induced by the applied electric field at the electrode–solution interface [Fedurco *et al*. 2005]. In the present work a ME was employed, and so another possible cause for the profile observed at low pH is the degradation of the membrane–protein–electrode interaction, given that in the absence of a promoter charge effects stand out as being most important, as previously mentioned.

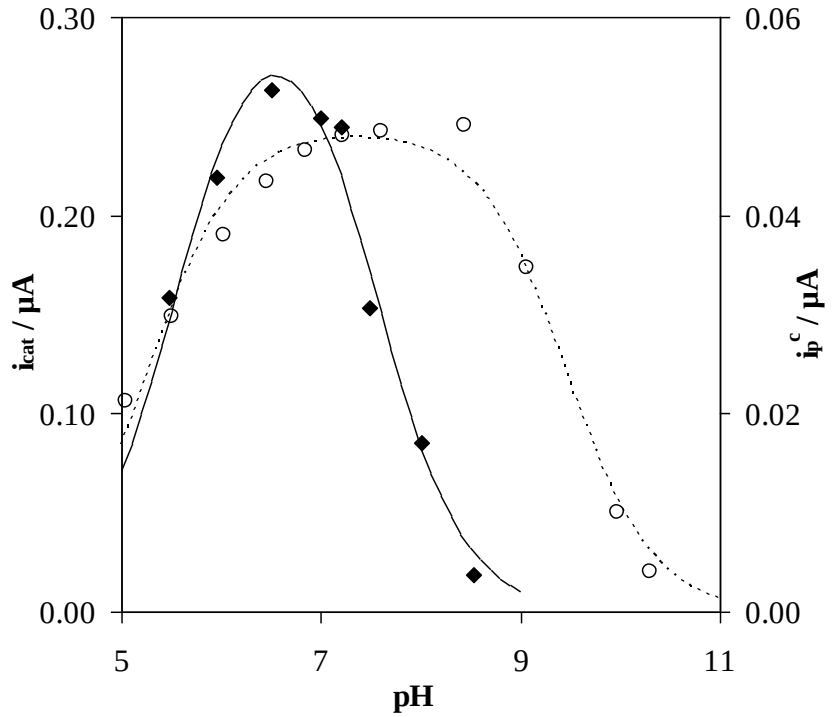

Figure 6 – pH dependence of 100 µM horse heart cytochrome *c* at the gold membrane electrode (circles) and catalytic current for 100 µM horse heart cytochrome *c*, 1.0 µM BCCP and saturating H_2O_2 (350 µM) at the gold membrane electrode (diamonds). The medium consisted of a mixed-buffer system (10 mM each) and 1 mM $CaCl_2$. The curves were fitted with Equation 6.

In the present study the same behaviour was observed either in the presence (data not shown) or in the absence of 4,4´-dithiodipyridine, eliminating the promoter protonation as the possible cause. Moreover, considering the fact that the profile obtained at the bare ME is similar to that observed for the several bulk conditions, it seems that the acidic p*K* is not due to an artefact of the membrane.

In fact, this acidic p*K* may be the result of an acidic residue or a group of residues involved in the interaction with the electrode, but not affecting the haem environment and consequently not changing the redox potential. Denaturation of the protein would also lower the concentration of horse cytochrome *c* responding at low pH, and must be considered. Indeed, the analysis of the voltammograms of horse cytochrome *c* at decreasing electrolyte pH shows that the redox signal is at the same potential, but with a decreasing current which does not return to the initial value when the pH is raised back to 7.0 (data not shown).

The pH effect in the mediated catalysis at the AUME was studied in the range 5 - 10, using solutions containing 100 µM horse cytochrome *c*, 1 µM BCCP, 1 mM $CaCl_2$ and a saturated H_2O_2 concentration (350 µM). The catalytic current presents a bell-shape profiled (**Figure 6**, diamonds) with no activity being observed above pH 9, which can be attributed to the inactivation of the enzyme at high pH [Paes de Sousa *et al.* 2007]. This curve can be fitted to Equation 6 with i_{opt} at pH 6.5 and two p*K* values, 5.6 ± 0.1 and 7.5 ± 0.1.

Taking into account the above results, we cannot conclude if the acidic p*K* estimated for the mediated catalysis is also related to the protein–protein interaction or only due to horse cytochrome *c* alone. However, preliminary solution steady-state kinetics performed spectrophotometrically of *Paracoccus* BCCP using horse cytochrome *c* as an electron donor (Pauleta *et al*., unpublished results) revealed an acidic p*K* at the same value, and similar values were observed for the enzymatic activity of *Pseudomonas aeruginosa* (5.2) [Soininen and Ellfolk 1972] and *Rhodobacter capsulatus* (6.1) [Koh *et al.* 2003] BCCP.

Moreover, binding studies using microcalorimetry showed that the formation of this electron transfer complex involves the release of 0.46 protons at pH 6.0, which also suggests the existence of an acidic p*K*, at around pH 6.0 [Pettigrew *et al*. 2003]. Therefore, this p*K* reflects a proton-dissociation process associated both with the horse cytochrome *c* and with the interaction/activity of this protein with BCCP.

A more basic p*K* was also observed for the solution steady-state kinetics determined spectrophotometrically of *P. aeruginosa* (6.8) and *R. capsulatus* (7.9) BCCP [Soininen and Ellfolk 1972, Koh *et al*. 2003], as now estimated for the *Paracoccu*s enzyme. This p*K* can be clearly attributed to the mediated enzymatic catalysis, since the current profile of the horse cytochrome *c* itself is invariable in this pH region (**Figure 6**). As several authors have suggested,

these p*K* values can be assigned to the propionates of the BCCP haems, histidine ligands or proposed residues involved in the catalysis such as Glu128 [Pettigrew *et al*. 2006, Koh *et al*. 2003, Echalier *et al*. 2006]. However, the identity of the residue(s) responsible for this proton dissociation can only be disentangled through site-directed mutagenesis.

Conclusions

This work highlights the use of ME in the study of direct and mediated electrochemistry of metalloproteins. The results reported in the present work show that ME are very attractive for the study of complex metalloproteins systems, particularly with regard to the very small amounts of protein needed and the ease with which experimental variables can be changed.

Mediated catalysis of BCCP by horse cytochrome *c* was easily analysed, with minimum consumption of proteins, just varying the H_2O_2 concentration in the electrolyte solution. While the proteins stay entrapped in close vicinity to the electrode surface, small ions can diffuse through the membrane. For the same reasons, the effect on the catalytic activity of experimental conditions, such as pH and ionic strength, can be rapidly analysed.

The fitting to Michaelis–Menten kinetics of the experimental data, from studies with the proteins either entrapped in the membrane or freely diffusing in solution, led to similar K_M values, showing that no artefacts are introduced in the study by the use of a ME. Higher values for the intermolecular rate constants for horse cytochrome *c* and BCCP were obtained with the membrane configuration, which shows that the membrane does not disrupts the formation of the encounter complex and can even favour it. Since electrostatic interactions are fundamental for the formation of the complexes between *P. pantotrophus* BCCP and its electron donors, this configuration seems to be an adequate option for the electrochemical study of the mediated catalysis in biological systems, where electro- static forces play an important role.

To draw conclusions about the influence of variables, such as pH or ionic strength, on the mediated catalytic activity, one must first pay attention to the behaviour of the mediator, i.e. the protein that actually exchanges the electrons with the electrode. For this reason, the ionic strength effect was analysed using a promoter to render the cytochrome *c*-electrode-membrane interaction more hydrophobic in nature, so the variation observed for the catalytic activity could only be due to changes in the binding between BCCP and the redox partner. On the other hand, the use of promoters might mask the pH effect depending on their acid-base behaviour and a possible interference must be verified.

Acknowledgments: This work was within the research project POCI/QUI/55743/2004, from Fundacão para a Ciência e Tecnologia (FCT). D.R. thanks FCT for financial support.

Capítulo III

Curriculum Vitae

Percurso Académico	
Data	**Janeiro de 2004 – Dezembro de 2005**
Instituição	Faculdade de Ciências e Tecnologia, Universidade do Algarve
Cargo ocupado	Estagiário no Laboratório de Bioinformática, sob a orientação do Professor Paulo Martel.
Resumo e descrição das tarefas	Os citocromos P450 (CYPs) são uma larga e ubíqua família de enzimas oxidantes envolvidas na destoxificação de compostos estranhos ao organismo (xenobióticos), assim como, numa variedade de vias metabólicas. Dada a função dos P450 como enzimas metabolizadoras de xenobióticos, a eficácia de muitos fármacos está dependente da rapidez com que os mesmos são metabolizados por determinados citocromos P450 humanos. O conhecimento da capacidade de ligação de determinados fármacos aos citocromos P450 e o impacto da variabilidade, destes últimos, na actividade, são pois aspectos fundamentais da moderna farmacologia. A previsão teórica da afinidade e geometrias de ligação de ligandos aos citocromos P450 reverte-se, pois, de grande importância. <u>Tarefas:</u> • Testar a eficiência do *software* de docking AUTODOCK na determinação da correcta orientação proteína-ligando para um conjunto de complexos cristalográficos P450-ligando; • Optimizar as geometrias das águas cristalográficas de vários complexos utilizando simulações de dinâmica molecular (GROMACS); • Incorporar a flexibilidade da proteína nas simulações de docking, utilizando conformações sucessivas extraídas de uma trajectória de dinâmica molecular (GROMACS).
Classificação	**18/20**

Data	**Outubro de 1999 – Dezembro de 2005**
Designação do Grau	Licenciatura em Bioquímica
Instituição	Universidade do Algarve, Faro, Portugal
Classificação	**14/20**

Data	**Outubro de 1999 – Dezembro de 2005**
Designação do Grau	Agrupamento 1, Científico-natural, Curso de Carácter Geral.
Instituição	Externato Liceal de Torre de Dona Chama
Classificação	**16/20**

Atividade profissional	
Data	**Junho de 2011 – Junho 2012**
Nome do empregador	Laboratório de Biossensores e Biosseparações da FCT - Universidade do Algarve (Prof. Guilherme Ferreira).
Cargo ocupado	Bolsa de investigação no âmbito do Projeto PTDC/BIO/69682/2006 "Engenharia de Biomoléculas para Produção de Nanopartículas Virais *in vitro*".
Resumo do projeto e descrição das tarefas	O transporte de proteínas terapêuticas e material genético irá ter no futuro uma importância estratégica face ao desenvolvimento de novos sistemas terapêuticos. O transporte viral para terapia molecular pode ser conseguido utilizando sistemas deficientes de replicação, como os vectores adenovirais e retrovirais, e alternativamente pode recorrer -se à produção de partículas tipo virais (VLP) não infeciosas. Estas partículas virais podem ser produzidas pela expressão heteróloga de proteínas estruturais de vírus, o que as torna semelhante às capsides virais nativas, tanto a nível estrutural, como imunológico. As VLPs geram-se espontaneamente dentro da célula, através da auto-montagem das proteínas estruturais do vírus. Neste projeto combinam-se abordagens de engenharia de biomoléculas com engenharia de bioprocessos para estabelecer uma nova metodologia para produção de nanopartículas virais. Estes são clonados e expressos em sistemas bacterianos e, após purificadas, as proteínas são combinadas *in vitro* em condições ótimas para promover a sua associação espontânea em nanoparticulas. <u>Tarefas:</u> • Transformar estirpes adequadas de *E. coli* para a expressão e produção das proteínas acima referidas; • Efetuar estudos de produção e otimização das condições da expressão proteica, tanto a nível de meios como condições de cultura, condições de

	indução, tempos ótimos de expressão, entre outros; • Proceder à purificação das proteínas expressas, por processos cromatográficos (afinidade, exclusão molecular, troca iónica, entre outros);
Data	**Novembro de 2008 – Novembro de 2010**
Nome do empregador	Grupo de Cristalografia de Proteínas da FCT – Universidade Nova de Lisboa (Prof. Maria Romão).
Cargo ocupado	Bolsa de investigação no âmbito do Projeto PTDC/QUI/64733/2006 "Enzimas da Família da Xantina Oxidase: Estrutura, Função e Especificidade".
Resumo do projeto e descrição das tarefas	As enzimas da família da xantina oxidase (XO) são um importante subgrupo das enzimas mononucleares de molibdénio (Mo). Catalisam a hidroxilação de uma grande variedade de compostos, em particular N-heterociclos e são reconhecidas como possuindo uma enorme importância em numerosas áreas relacionadas com a saúde, ambiente e indústria. Estas enzimas possuem, como cofatores, um átomo de Mo coordenado por um cofator orgânico (molibdopterina ou piranopterina), dois centros do tipo [2Fe-2S] e por vezes flavina. Neste projeto pretendeu-se estudar uma enzima homóloga da aldeído oxidase de fígado de rato (AOH1), cuja especificidade e estrutura cristalina era ainda desconhecida. <u>Tarefas:</u> • Determinar as condições de cristalização para a AOH1 recombinante expressa em *E.coli* e extrapolar essas condições de cristalização para AOH1 de fígado de rato. • Determinar a estrutura tri-dimensional da AOH1 de fígado de rato, usando a estrutura da XO como modelo.

	• Expressar, purificar e cristalizar as proteínas (XdhC, PaoD, YqeB) que funcionam como *chaperones* das enzimas da família da XO recombinante.
Data	**Agosto de 2008 – Outubro de 2008**
Nome do empregador	Grupo EDGE da Universidade do Algarve (Prof. Leonor Cancela).
Cargo ocupado	Voluntário no Laboratório de Biologia Molecular.
Resumo do projeto e descrição das tarefas	Os fatores de transcrição RUNX são importantes reguladores da expressão genética em importantes vias de desenvolvimento. O gene runx3 codifica um membro da família de fatores de transcrição de domínio *runt*. Esta proteína (subunidade alfa) atua por heterodimerização com uma subunidade beta, formando um complexo que se liga à sequência de ADN 5'-PYGPYGGT-3', encontrada num número de potenciadores e promotores, e pode activar ou reprimir a transcrição. Pode também interagir com outros fatores de transcrição. Funciona como um supressor de tumor, estando o gene frequentemente ausente ou transcricionalmente silenciado no cancro. Até à data foram encontradas várias variantes transcricionais para este gene, que codificam diferentes isoformas. Com este estágio pretendeu-se dar apoio a um projeto de Doutoramento em curso, nomeadamente nas tarefas de clonagem, microinjecção de embriões de peixe zebra e na análise bioinformática das sequências obtidas. <u>Tarefas:</u> • Clonagem das diferentes isoformas do runx3 no plasmídeo de expressão pCMX-PL2. • Clonagem de vários fragmentos dos dois promotores (distal e proximal) do runx3 no plasmídeo pGL3-Basic. • Análise bioinformática das sequências de cDNA obtidas. • Análise *in sílico* das sequências de ambos os promotores do runx3, para

	determinação de putativos locais de ligação de fatores de transcrição.
Data	**Setembro de 2006 – Abril de 2008**
Nome do empregador	Instituto Superior Técnico da Universidade Técnica de Lisboa (Prof. Margarida Romão).
Cargo ocupado	Bolsa de investigação no âmbito do Projeto POCI/QUI/55743/2004 "Mecanismos e Energética do Transporte de Eletrões em Metaloproteínas por Voltametria Dinâmica".
Resumo do projeto e descrição das tarefas	Os métodos voltamétricos constituem uma ferramenta especialmente adequada ao estudo de metaloproteinas e metaloenzimas. Contrariamente às convencionais titulações potenciométricas, os métodos voltamétricos permitem não só uma determinação mais expedita de potenciais redox mas fornecem também informação cinética não só dos processos de elétrodo bem como de reações químicas associadas, incluindo reações catalíticas. O êxito da aplicação de métodos voltamétricos ao estudo de reações redox de metaloproteínas passa por todo o trabalho que tem sido investido na compreensão e controle da interação proteína/elétrodo. Ocorrendo uma reação direta, a informação que se pode obter supera largamente a extraída por métodos estáticos. O estudo de processos, tais como, transferência eletrónica intra e inter moleculares, o reconhecimento de parceiros redox e de correntes catalíticas são possíveis devido ao carácter dinâmico da metodologia. Este projeto teve como finalidade obter informação de carácter termodinâmico, cinético e mecanístico sobre um conjunto de metaloproteínas não anteriormente estudadas por método eletroquímicos dinâmicos e a caracterização dos caminhos de transferência de eletrões "dentro" da proteína (intra-molecular) e o reconhecimento de parceiros redox (inter-molecular). <u>Tarefas:</u> • Estudo comparativo da catálise mediada da peroxidase do citocromo *c*

Paracoccus denitrificans pelo parceiro não fisiológico citocromo *c* mitocondrial de coração de cavalo com as proteínas em solução e retidas num elétrodo de membrana. Análise do efeito do pH e da força iónica em condições de non-turnover e turnover. Avaliação dos benefícios dos elétrodos de membrana e/ou promotores em eletroquímica.

- Eletroquímica direta e catálise não mediada da peroxidase do citocromo c *Paracoccus pantotrophus*. Estudo do mecanismo de ativação da enzima.
- Estudos da atividade catalítica da peroxidase do citocromo c *Pseudomonas stutzeri* por eletroquímica direta e mediada. Análise da resposta direta em condições de non-turnover e turnover. Estudo da resposta do parceiro fisiológico, citocromo *c*551 *Pseudomonas stutzeri* e da catálise mediada.

Publicações

Tese de Licenciatura:

- **David Rodrigues**, "**Docking de ligandos no centro de activo de citocromos P450**", Dezembro de 2005, Universidade do Algarve, Faro.

Posters:

- Ana Rita Cardozo, Meina Neumman, Viola Schwuchow, **David Rodrigues,** Aldino Viegas, Eurico Cabrita, Maria João Romão, Teresa Silva, "**Stabilization and Crystallization studies on molecular chaperone, PaoD"**, 2nd Meeting of Synchrotron Radiation Users from Portugal, Lisbon, Portugal.

- Catarina Coelho, **David Rodrigues**, José Trincão, Martin Mahro, Mineko Terao, Enrico Garattini, Silke Leimkühler, Maria João Romão, "**Aldehyde Oxidase Homologue 1 (AOH1) - The Crystal Structure of a New Member of the XO family**", 6th GRC conference on Molybdenum & Tungsten Enzymes, July 5-10, 2009, Lucca (Barga), Italy.

- B. Simões, **D. Rodrigues**, N. Conceição, R. Kelsh, L. Cancela, "**Spatial-temporal expression of runx3 during early zebrafish development and in silico and in vitro analysis of its promoter regions**", XIVth Biochemistry National Congress, October 22-25, 2008, Ponta Delgada, Azores, Portugal.

- Patrícia Paes de Sousa, Sofia Pauleta, **David Rodrigues**, M. Lurdes Simões Gonçalves, Graham Pettigrew, Isabel Moura, José J. G. Moura, Margarida Correia dos Santos "**Membrane electrodes for the direct and mediated electrochemistry of enzymes**", 12th International Conference on Electroanalysis, June 16-19, 2008, Prague, Czech.

- Patrícia M. Paes de Sousa, Sofia R. Pauleta, **David Rodrigues**, M. Lurdes Simões Gonçalves, Graham W. Pettigrew, Isabel Moura, Margarida M. Correia dos Santos, José J. G. Moura, "**Rate limiting event for Paracoccus pantotrophus CCP catalysis as revealed by direct electrochemistry**", 13th Int. Conf. on Biological Inorganic Chemistry, July 15-20, 2007, Vienna, Austria.

- P Martel, **D Rodrigues**, G Ferreira, V Marques, "**Docking studies of ligands to cytochrome P450: evaluation and optimization of the Autodock automated docking procedure**", 14th Int. Conf. on Cytochromes P450, May 31- June 5, 2005, Dallas, Texas, USA.

- **David Rodrigues** and Paulo Martel, "**Docking studies of ligands to cytochrome P450**", XIV Portuguese Biochemistry Society meeting, December 2004, Vilamoura, Portugal;

- Martel, P.J., Afonso, J.P, **Rodrigues, D.A.**, Ribeiro, V., Ferreira, G.N.M., "**Modelling the effect of SNPs in Human CYP enzymes**", 15th International Symposium on Microsomes and Drug Oxidations: Chemical Biology in the Postgenomic Era New Approaches and Applications, July 2004, Mainz, Germany;

Artigos (*in per-reviewed journals*):

- Ana Rita C. O. Cardoso, Viola Schwuchow, **David Rodrigues**, Eurico J. Cabrita, Silke Leimkühler, Maria João Romão, Teresa Santos-Silva. "**Biochemical, Stabilization and Crystallization Studies on a molecular chaperone (PaoD) involved in the maturation of molybdoenzymes**". (a ser submetido)

- Catarina Coelho, Jacopo Marangon, **David Rodrigues**, José J.G. Moura, Maria João Romão, Patrícia M. Paes de Sousa, Margarida M. Correia dos Santos. "**Induced peroxidase activity of haem containing nitrate reductases revealed by protein film electrochemistry**". (J Electroanal Chem. 2013, 693:105-113)

- Mahro M, Coelho C, Trincao J, **Rodrigues D**, Terao M, Garattini E, Saggu M, Lendzian F, Hildebrandt P, Romao MJ, Leimkuehler S. "**Characterization and crystallization of mouse Aldehyde Oxidase 3 (mAOX3): from mouse liver to E. coli heterologous protein expression**". Drug Metab Dispos. 2011, 39(10):1939-1945.

- P. M. Paes de Sousa, **D. Rodrigues**, Cristina G. Timóteo, M. L. Simões Gonçalves, G. W. Pettigrew, I. Moura, J. J. G. Moura , M. M. Correia dos Santos, "**Analysis of the activation mechanism of *Pseudomonas stutzeri* cytochrome c peroxidase through an electron transfer chain**". J Biol Inorg Chem. 2011, 16(6): 881–888.

- P. M. Paes de Sousa, S. R. Pauleta, **D. Rodrigues**, M. L. Simões Gonçalves, G. W. Pettigrew, I. Moura, J. J. G. Moura, M. M. Correia dos Santos, "**Benefits of membrane electrodes in the electrochemistry of metalloproteins: mediated catalysis of *Paracoccus pantotrophus* cytochrome c peroxidase by horse cytochrome c – a case study**". J Biol Inorg Chem. 2008, 13(5): 779–787.

Comunicações Orais:

- Patrícia M. Paes de Sousa, **David Rodrigues**, Sofia R. Pauleta, Cristina G. Timóteo, M. Lurdes Simões Gonçalves, Graham W. Pettigrew, Isabel Moura, José J. G. Moura, Margarida M. Correia dos Santos, "**Activation Mechanisms of Cytochrome c Peroxidases Revealed by Direct Electrochemistry**", XV Portuguese Electrochemistry Society meeting, September 4-5, 2008, Lisbon, Portugal.

Outras publicações

- Estrutura depositada no Protein Data Bank – código do PDB **3ZYV**:
  Trincao J, Coelho C, Mahro M, **Rodrigues D**, Terao M, Garattini E, Leimkuehler S, Romao M.J. "**Crystal structure of the mouse liver Aldehyde Oxydase 3 (mAOX3)**".

Participação ou representações

- Junho 2011: "19th Biennial Meeting Affinity 2011", Tavira, Portugal.
- Julho de 2009: "6th GRC conference on Molybdenum & Tungsten Enzymes", Lucca (Barga), Italia.
- Março de 2007: "VI Analytical Chemistry Division meeting", Lisboa, Portugal. (Membro da comissão organizadora)
- Dezembro de 2006: "XX Portuguese Chemistry Society meeting", Monte da Caparica, Portugal.
- Dezembro de 2004: "XIV Portuguese Biochemistry Society meeting", Vilamoura, Portugal.

Competências Profissionais

- **Bioinformática:**
  - Autodock – Docking de uma forma automática proteína-ligando;
  - Modeller – Modelação estrutural por homologia;
  - Gromacs – Métodos de simulação de dinâmica molecular;
  - Programas para a análise de sequências de proteínas.
- **Espectroscopia UV/VIS**.
- **Bioeletroquímica:** Métodos voltamétricos.
- **Técnicas de Biologia Molecular:**
  - PCR, Eletroforese, Purificação, Preparação do Plasmídeo, Clonagem

- **Biologia Estrutural**
    - Expressão de proteínas recombinantes;
    - Purificação de proteínas – FPLC (Cromatografia de afinidade, cromatografia de troca iónica e cromatografia de exclusão)
    - Técnica de análise de Proteínas (SDS-PAGE)
- **Cristalografia de proteínas por raio X.**

Outras competências

Línguas	**Compreensão**		**Conversação**		**Escrita**
	Compreensão oral	Leitura	Interação oral	Produção oral	
Português	Língua materna		Língua materna		Língua materna
Inglês	Utilizador independente	Utilizador independente	Utilizador independente	Utilizador independente	Utilizador independente
Francês	Utilizador proficiente	Utilizador proficiente	Utilizador proficiente	Utilizador proficiente	Utilizador proficiente

Aptidões e competências informáticas:

- Competente com o sistema operativo Windows e os programas do Microsoft Office;
- Conhecimentos em Linux e Pascal;
- Utilizador experiente na internet;
- Conhecimentos em *hardware*.

Capítulo IV

Análise Crítica do Percurso Profissional e a sua Adequação ao Grau de Mestre

A essência do Mestrado em Biotecnologia é promover o pensamento teórico e prático, assim como, o desenvolvimento do conhecimento científico e fomentar um conhecimento abrangente, multidisciplinar para numerosas implicações. Por este motivo, considero que a minha evolução profissional apresenta relevância como atividade no Mestrado em Biotecnologia, por ter adquirido uma formação sólida em domínios multidisciplinares das ciências e, tecnologias biológicas e químicas.

Ao longo do meu percurso, tive o privilégio de trabalhar com conceituados profissionais de diversos domínios científicos, o que me proporcionou uma aprendizagem de interação, integração e discussão científica bastante relevante. O fato de ter estado envolvido em vários grupos de investigação, demonstra uma vontade de aprendizagem de novas técnicas, uma boa capacidade de adaptação, um bom trabalho de equipa e, essencialmente, uma enorme persistência e rigor no desenvolvimento das técnicas.

A nível profissional, fui constantemente confrontado com dificuldades experimentais que tiveram de ser superadas. Para superar essas mesmas dificuldades, a interação com colegas e professores nas reuniões de grupo e uma profunda pesquisa bibliográfica foram essenciais. De um modo geral, proporcionou-me uma perícia técnica, um espirito crítico e uma perspetiva analítica, que permitiu desenvolver atributos pessoais fundamentais na ciência.

Para além disso, exerci funções de auxílio na orientação de alunos de mestrado, assim como, na gestão do laboratório e na organização de um congresso internacional. Os conhecimentos adquiridos nessas funções são complementares aos adquiridos na investigação e essa complementaridade, aliada com estratégia e inovação, traduz a essência da Biotecnologia.

Em síntese, sabendo que a bioinformática, (bio)eletroquímica, biologia molecular, cristalografia e bioquímica das proteínas, são áreas fundamentais para a biotecnologia, considero que a minha experiência profissional me permitiu adquirir competências como técnico superior em laboratórios de equipas de investigação no desenvolvimento tecnológico multidisciplinar em instituições Públicas ou Empresas. Deste modo, de acordo com os objetivos do curso de 2º ciclo em Biotecnologia, considero-me eletivo para o grau de Mestre nesta área.

Capítulo V

Referências

Armstrong FA (2002) In: Bard AJ, Stratmann M, Wilson GS (eds) Encyclopedia of Electrochemistry, Volume 9, Bioelectrochemistry. John Wiley & Sons, New York

Armstrong FA, Cox PA, Hill HAO, Lowe VJ, Oliver BN (1987) J Electroanal Chem 217:331-366

Assfalg M, Bertini I, Dolfi A, Turano P, Mauk AG, Rosell FI, Gray HB (2003) J Am Chem Soc 125:2913-2922

Azamian BR, Davis JJ, Coleman KS, Bagshaw CB, Green ML (2002) J Am Chem Soc. 124:12664-12665

Bard AJ, Faulkner LR (eds) (2001) Electrochemical Methods, Fundamentals and Applications. John Wiley & Sons, New York

Berks BC, Baratta D, Richardson DJ, Ferguson SJ (1993) Eur J Biochem 212:467-476

Bianco P. (2002) Journal of biotechnology 82:393-409

Bowden EF, Hawkridge FM, Chlebowski JF, Bancroft EE, Thorpe C, Blount HN (1982) J Am Chem Soc 104:7641-7644

Cornish-Bowden A (ed) (2001) Fundamentals of Enzyme Kinetics. Portland Press, London

Correia dos Santos MM, Paes de Sousa PM, Simões Gonçalves ML, Ascenso C, Moura I, Moura JJG (2001) J Electroanal Chem 501:173-179

Correia dos Santos MM, Paes de Sousa PM, Simões Gonçalves ML, Krippahl L, Moura JJG, Lojou E, Bianco P (2003) J Electroanal Chem 541:153-162

Correia dos Santos MM, Paes de Sousa PM, Simões Gonçalves ML, Romão MJ, Moura I, Moura JJG (2004) Eur J Biochem 271:1329-1338

Coury LA, Oliver BN, Egekeze JO, Sosnoff CS, Brumfield JC, Buck RP, Murray RW (1990) Anal Chem 62:452-458

Dequaire M, Limoges B, Moiroux J, Savéant JM (2002) J Am Chem Soc 124:240-253

Echalier A, Goodhew CF, Pettigrew GW, Fülöp V (2006) Structure 14:107-117

Eddowes MJ, Hill HAO (1977) J Chem Soc Chem Commun 21:771-772

Eddowes MJ, Hill HAO (1979) J Am Chem Soc 101:4461-4464

Fedurco M, Augustynski J, Indiani C, Smulevich G, Antalik M, Bano M, Sedlak E, Glascock MC, Dawson JH (2005) J Am Chem Soc 127:7638-7646

Ferapontova EE, Ruzgas T, Gorton L (2003) Anal Chem 75:4841-4850

Gilmour R, Goodhew CF, Pettigrew GW, Prazeres S, Moura I, Moura JJG (1993) Biochem J 294:745-752

Gilmour R, Goodhew CF, Pettigrew GW, Prazeres S, Moura I, Moura JJG (1994) Biochem J 300:907-914

Gilmour R, Prazeres S, McGinnity DF, Goodhew CF, Moura JJG, Moura I, Pettigrew GW (1995) Eur J Biochem 234:878-886

Goodhew CF, Wilson IB, Hunter DJ, Pettigrew GW (1990) Biochem J 271:707-712

Haladjian J, Bianco P, Nunzi F, Bruschi M (1994) Anal Chim Acta 289:15-20

Haladjian J, Thierry-Chef I, Bianco P (1996) Talanta 43:1125-1130

Halliwell B, Gutteridge JMC (eds) (1989) Free Radicals in Biology and Medicine. Oxford Science Publications, Oxford

Harmer MA, Hill HAO (1984) J Electroanal Chem 170:369-375

Kakihana M, Ikeuchi H, Satô GP, Tokuda K (1980) J Electroanal Chem 108:381-383

Kim KL, Kang DS, Vitello LV, Erman JE (1990) Biochem 29:9150-9159

Koh M, Meyer TE, De Smet L, Van Beeumen JJ, Cusanovich MA (2003) Arch Biochem Biophys 410:230-237

Koppenol WH, Rush JD, Mills JD, Margoliash E (1991) Mol Biol Evol 8:545-558

Laviron E (1979) J Electroanal Chem 101:19-28

LoÈtzbeyer T, Schuhmann W, Schmidt HL (1996) Sens Actuators B 33:50-54

Lojou E, Bianco P (2000) J Electroanal Chem 485:71-80

Lojou E, Cutruzzola F, Tegoni M, Bianco P (2003) Electrochim Acta 48:1055-1064

Lopes H, Besson S, Moura I, Moura JJG (2001) J Biol Inorg Chem 6:55-62

Moore GR, Pettigrew GW (eds) (1991) Cytochromes c: Evolutionary, Structural and Physicochemical Aspects. Springer-Verlag, Berlin Heidelberg New York

Murray, R.W., Ewing, A.G., Durst, R.A. (1987) Anal. Chem. 59:379A-390A

Nicholson RS, Shain I (1964) Anal Chem 36:706-723

Paes de Sousa PM, Pauleta SR, Simões Gonçalves ML, Pettigrew GW, Moura I, Correia dos Santos MM, Moura JJG (2007) J Biol Inorg Chem 12:691-698

Pauleta SR, Cooper A, Nutley M, Errington N, Harding S, Guerlesquin F, Goodhew CF, Moura I, Moura JJG, Pettigrew GW (2004b) Biochem 43:14566-14576

Pauleta SR, Guerlesquin F, Goodhew CF, Devreese B, Van Beeumen J, Pereira AS, Moura I, Pettigrew GW (2004a) Biochemistry 43:11214-11225

Pettigrew GW (1991) Biochim Biophys Acta 1058:25-27

Pettigrew GW, Echalier A, Pauleta SR (2006) J Inorg Biochem 100:551-567

Pettigrew GW, Goodhew CF, Cooper A, Nutley M, Jumel K, Harding SE (2003b) Biochem 42:2046-2055

Pettigrew GW, Pauleta SR, Goodhew CF, Cooper A, Nutley M, Jumel K, Harding SE, Costa C, Krippahl L, Moura I, Moura J (2003a) Biochem 42:11968-11981

Pettigrew GW, Prazeres S, Costa C, Palma N, Krippahl L, Moura I, Moura JJG (1999) J Biol Chem 274:11383-11389

Prazeres S, Moura I, Gilmour R, Pettigrew GW, Ravi N, Huynh BH (1995b) In: La Mar G (ed) Nuclear magnetic resonance of paramagnetic molecules. Kluwer, Dordrecht, pp 141-163

Prazeres S, Moura I, Moura JJG, Gilmour R, Goodhew CF, Pettigrew GW (1993) Magn Reson Chem 31:S68-S72

Prazeres S, Moura JJG, Moura I, Gilmour R, Goodhew CF, Pettigrew GW, Ravi N, Huynh BH (1995a) J Biol Chem 270:24264-24269

Richter CD, Allen JWA, Higham CW, Koppenhöfer A, Zajicek RS, Watmough NJ, Ferguson SJ (2002) J Biol Chem 277:3093-3100

Sallez Y, Bianco P, Lojou E, (2000) J Electroanal Chem 493:37-49

Santos M, Correia dos Santos MM, Simões Gonçalves ML, Costa C, Romão JC, Moura JJG (2006) J Inorg Biochem 100:2009-2016

Savéant JM, Vianello E (1965) Electrochim Acta 10:905-920

Scott DL, Bowden EF (1994) Anal Chem 66:1217-1223

Soininen R, Ellfolk N (1972) Acta Chem Scand 26:861-872

Vandewalle PL, Petersen NO (1987) FEBS Lett 210:195-198

Williams PA, Fulop V, Leung YC, Chan C, Moir JW, Howlett G, Ferguson SJ, Radford SE, Hajdu J (1995) Nat Struct Biol 2:975-982

Capítulo VI

Anexos

(Artigos publicados)

J Biol Inorg Chem (2008) 13:779–787
DOI 10.1007/s00775-008-0365-8

ORIGINAL PAPER

Benefits of membrane electrodes in the electrochemistry of metalloproteins: mediated catalysis of *Paracoccus pantotrophus* cytochrome *c* peroxidase by horse cytochrome *c*: a case study

P. M. Paes de Sousa · S. R. Pauleta · D. Rodrigues · M. L. Simões Gonçalves · G. W. Pettigrew · I. Moura · J. J. G. Moura · M. M. Correia dos Santos

Received: 19 December 2007 / Accepted: 10 March 2008 / Published online: 26 March 2008

Abstract A comparative study of direct and mediated electrochemistry of metalloproteins in bulk and membrane-entrapped solutions is presented. This work reports the first electrochemical study of the electron transfer between a bacterial cytochrome *c* peroxidase and horse heart cytochrome *c*. The mediated catalysis of the peroxidase was analysed both using the membrane electrode configuration and with all proteins in solution. An apparent Michaelis constant of 66 ± 4 and 42 ± 5 μM was determined at pH 7.0 and 0 M NaCl for membrane and bulk solutions, respectively. The data revealed that maximum activity occurs at 50 mM NaCl, pH 7.0, with intermolecular rate constants of $(4.4 \pm 0.5) \times 10^6$ and $(1.0 \pm 0.5) \times 10^6$ M^{-1} s^{-1} for membrane-entrapped and bulk solutions, respectively. The influence of parameters such as pH or ionic strength on the mediated catalytic activity was analysed using this approach, drawing attention to the fact that careful analysis of the results is needed to ensure that no artefacts are introduced by the use of the membrane configuration and/or promoters, and therefore the dependence truly reflects the influence of these parameters on the (mediated) catalysis. From the pH dependence, a p*K* of 7.5 was estimated for the mediated enzymatic catalysis.

Keywords Membrane electrode · Mediated catalysis · Bacterial cytochrome *c* peroxidase · Horse cytochrome *c*

Abbreviations

AUME	Gold membrane electrode
BCCP	Bacterial cytochrome *c* peroxidase
ME	Membrane electrode

P. M. Paes de Sousa · S. R. Pauleta · I. Moura · J. J. G. Moura
ReQuimte, Centro de Química Fina e Biotecnologia,
Departamento de Química,
Faculdade de Ciências e Tecnologia,
Universidade Nova de Lisboa,
2829-516 Caparica, Portugal
e-mail: patricia.sousa@dq.fct.unl.pt

D. Rodrigues · M. L. Simões Gonçalves ·
M. M. Correia dos Santos (✉)
Centro de Química Estrutural,
Instituto Superior Técnico,
Av. Rovisco Pais,
1049-001 Lisbon, Portugal
e-mail: mcsantos@ist.utl.pt

G. W. Pettigrew
Royal (Dick) School of Veterinary Studies,
University of Edinburgh,
Summerhall,
Edinburgh EH9 1QH, UK

Introduction

The use of membrane electrodes (ME), with the protein imprisoned between a dialysis membrane and the electrode surface, has some important advantages. These are (1) the use of very small volumes of protein—2 μl (to overcome the limitation of sample availability), (2) the ease of electrode preparation and low cost, (3) the rapid investigation of various experimental parameters, such as pH and ionic strength and (4) the thin layer configuration, which easily allows quantitative information about the redox processes to be obtained [1, 2].

Moreover, the membranes used in this type of electrode configuration are charged, offering a convenient way to modulate the electric environment close to the electrode surface, and thus ascertain the role of electrostatic interactions in the efficiency of the electron transfer. It is also

important to point out that this configuration is an interesting strategy when adsorption of a protein or an enzyme to the electrode surface is not successfully achieved, hindering the use of protein film voltammetry [3]. Additionally, the entrapment of proteins between the membrane and the electrode surface enables the achievement of thin-layer conditions and avoids diffusional problems [4].

Studies reporting the benefits of the ME in protein electrochemistry and its role in modulating the redox behaviour focused on the direct electrochemistry of small electron transfer proteins. In these works, a critical comparison was made with data obtained with non-ME [5–7]. More recently ME were used to study multiredox cofactor-containing enzymes and their interaction with both physiological and non-physiological redox partners [8, 9]. In both studies, although the direct electrochemistry and the mediated catalysis of the proteins were analysed using that strategy, with the proteins in solution or adsorbed on a modified electrode, no comparison was made among the different strategies.

The mediated catalysis of the bacterial cytochrome *c* peroxidase (BCCP) from *Paracoccus pantotrophus* by *P. pantotrophus* pseudoazurin examined at a gold ME (AUME) was recently reported by us [10]. Cyclic voltammetry was used to analyse the direct transfer to pseudoazurin and to probe its interaction with BCCP. The results obtained showed that this small copper protein is a competent electron donor to BCCP, in agreement with solution steady-state kinetics performed spectrophotometrically [11]. The pH and ionic strength effect on the voltammetric signal of pseudoazurin as well as on the intermolecular rate constant were also easily studied at the ME.

Horse heart cytochrome *c*, a commercially available small *c*-type haem protein, has been previously used as an electron donor to *Paracoccus* BCCP in solution steady-state kinetic studies performed spectrophotometrically [12]. Although it is not a physiological partner of BCCP, this small protein was shown to be kinetically competent as an electron donor to the *Paracoccus* enzyme. However, horse cytochrome *c* exhibits a distinct kinetic and binding behaviour from the physiological partners pseudoazurin, a type I copper protein, and cytochrome c_{550}, which is also a small *c*-type haem protein. The physiological partners bind at the same site on the surface of BCCP near the electron-transferring haem of the enzyme [13], while horse cytochrome *c* has been proposed to have two binding sites, a looser binding site near the electron-transferring haem and an additional tight one in-between the two haems of the enzyme [14]. Below 50 mM NaCl, there is little change in the activity when the electron donor is either cytochrome c_{550} or pseudoazurin. In contrast, when horse cytochrome *c* is used as an electron donor there is a threefold decrease in activity as the ionic strength is lowered, and this correlates with an increased binding affinity [15, 16]. It was concluded that the higher-affinity binding was, in fact, non-productive and that only when that attachment was loosened by raised ionic strength could the horse cytochrome *c* migrate to the true electron transfer site.

This work reports the first electrochemical study of the electron transfer between BCCP and horse cytochrome *c*. The mediated catalysis of BCCP was analysed using the ME configuration and with all proteins in solution. Our aim is to compare the results obtained with these two strategies in order to gain a better insight into the interactions that occur at the ME surface and to highlight the effects of this strategy on the direct and mediated electrochemistry of metalloproteins.

Materials and methods

Proteins and chemicals

Horse heart cytochrome *c* was obtained from Sigma and used without further purification. Pseudoazurin and BCCP were isolated and purified as described before [17]. The concentration of the proteins was determined spectrophotometrically using the extinction coefficient at 409 nm, $\varepsilon = 250\ \text{mM}^{-1}\ \text{cm}^{-1}$, and at 550 nm, $\varepsilon = 29.5\ \text{mM}^{-1}\ \text{cm}^{-1}$, for fully oxidized BCCP and reduced horse cytochrome *c*, respectively [17, 18].

4,4′-Dithiodipyridine and $CaCl_2$ were obtained from Sigma and all other chemicals were pro analysis grade. All solutions were prepared with deionized water from a Milli-Q water purification system.

Apparatus and procedures

The cyclic voltammograms were obtained using an EG&G-PAR model 273A potentiostat/galvanostat controlled via the 270 software. The scan rate varied between 5 and 200 mV s^{-1}. Throughout this article, all potential values are referred to the standard hydrogen electrode.

A conventional three-electrode configuration cell was used, with a platinum auxiliary electrode and an Ag/AgCl reference electrode (BAS MF-2052; 205 mV vs. the standard hydrogen electrode). The working electrode was a gold disk electrode from BAS (MF-2014) with a nominal radius of 0.8 mm. The effective surface area of the electrode was determined from its response in a known concentration of the ferrocyanide/ferricyanide couple ($D = 7.84 \times 10^{-6}\ \text{cm}^2\ \text{s}^{-1}$ [19]) and was found to be 0.0195 cm^2.

Before each experiment the electrode was polished by hand on a polishing cloth (Buehler 40-7212) using a water/alumina (0.05 μm) slurry (Buehler 40-6365-006),

sonicated for 5 min, rinsed well with Milli-Q water and finally dipped into 1 mM 4,4′-dithiodipyridine solution for 5 min. The membrane configuration was prepared as previously described [6] using a negatively charged Spectra/Por MWCO 3500 membrane.

In typical experiments, the supporting electrolyte, as well as the working solution, contained 10 mM phosphate buffer pH 7.0 ± 0.1, 0.5 mM 4,4′-dithiodipyridine and 1 mM $CaCl_2$. Horse cytochrome *c* was present in a concentration of 100 μM and the concentration of BCCP varied between 0.25 and 1 μM. In the experiments with a saturating concentration of substrate, 100–350 μM H_2O_2 was present in the electrolyte solution. The effect of substrate concentration was determined by varying the H_2O_2 concentration between 10 and 200 μM. The pH of the electrolyte was varied from 5.4 to 10.5 by adding 5 M HCl or 2 M NaOH to a mixed-buffer system containing 10 mM 2-morpholinoethanesulfonic acid, sodium phosphate, *N*-(2-hydroxyethyl) piperazine-*N*′-ethanesulfonic acid, tris(hydroxymethyl) aminomethane and 3-cyclohexylamino-1-propanesulfonic acid. The effect of the ionic strength was studied by adding increasing amounts of NaCl (up to 500 mM).

It should be pointed out that in order to have reproducible results for some BCCP concentrations more than one ME had to be prepared, to cover the whole range of experimental variables. This is due to the fact that the enzyme exists in a monomer–dimer equilibrium in which only the dimer is active. Dilution of the enzyme shifts the equilibrium towards the monomer and therefore the activity is lost with time [14], which corresponds to a decrease of the catalytic current.

All solutions were deaerated for 10 min with high-purity nitrogen, and all measurements were performed at least in duplicate in a temperature-controlled room at 20 ± 1 °C.

Results and discussion

Catalytic activity of *P. pantotrophus* BCCP with horse heart cytochrome *c* as an electron donor

ME cyclic voltammetry

The electrochemical behaviour of horse cytochrome *c* is well known either in bulk or entrapped on a ME. Indeed, Eddowes and Hill [20] found that essentially reversible voltammetry of cytochrome *c* in solution could be observed at a 4,4′-dipyridyl-modified gold electrode. Latter, Lojou and Bianco [5] showed that fast electrochemical response was observed when a thin layer of protein solution was entrapped between a negatively charged dialysis membrane and a non-modified gold electrode surface. In both cases favourable conditions for electron transfer to occur were achieved, which accounts for the similarity of the values determined for the formal potentials.

In this work, the direct electrochemistry of cytochrome *c* was revisited at a AUME, but this time in the presence of 4,4′-dithiodipyridine (data not shown). The promoter was used in order to have similar experimental conditions for the studies both in solution and with the membrane-configuration electrode (further reasons will be explained below).

Thin-layer behaviour will be observed as long as the entrapped layer thickness l is smaller than the diffusion-layer thickness for a given experimental time scale, t:

$$l < (2Dt)^{1/2} \quad (1)$$

where D is the diffusion coefficient of the species [21]. Under our experimental conditions (cyclic voltammetry with scan rates between 5 and 200 mV s^{-1}), this condition was verified for the lowest scan rates ($v < 100$ mV s^{-1}), with i_p varying linearly with v in this range. From this variation [21], an entrapped-solution volume, V, of 1.2×10^{-5} cm^3 was estimated, which corresponds to an entrapped-layer thickness $l = V/A = 6.2 \times 10^{-4}$ cm. Since the diffusion coefficient of cytochrome *c* is $D = 1.2 \times 10^{-6}$ cm^2 s^{-1} (see below), thin-layer conditions occur for $v < 160$ mV s^{-1}, as verified.

The ratio of the cathodic (i_{pc}) and anodic (i_{pa}) peak currents was close to 1 and the peak-to-peak separation, $\Delta E_p = E_{pa} - E_{pc}$, was close to 20 mV for the lowest scan rates. In the same range, the width at half height ($\Delta E_{p,1/2}$) was also constant for the cathodic and anodic peaks, with a value close to 90 mV. Although ΔE_p increased with v, the average of the reduction and oxidation peak potentials remained almost constant for all scan rates and a formal reduction potential $E^{\circ\prime} = (E_{pc} + E_{pa})/2 = 250 \pm 5$ mV was estimated at pH 7.0, in agreement with other reported values (e.g. 280 mV, ME at pH 7.6 [5], and 255 mV, bulk solution at pH 7.0 [20]).

The catalytic activity of *P. pantotrophus* BCCP towards horse cytochrome *c* was then investigated at the AUME, with working solutions of 100 μM cytochrome *c* and different BCCP concentrations (0.25–1 μM) in the presence of a saturating substrate concentration (125–350 μM, depending on the enzyme concentration) or with a working solution of 100 μM cytochrome *c* and 0.25 μM BCCP in the presence of increasing H_2O_2 concentrations. These solutions and the electrolyte contained 1 mM $CaCl_2$ (for enzyme activation [12, 22]).

The cytochrome *c* response is unchanged in the presence of BCCP. Moreover, although cytochrome *c* is known to feature a small peroxidase activity [23, 24], its response also remained unchanged upon addition of H_2O_2 in the absence of enzyme. However, it is clear from Fig. 1a that in the presence of BCCP the cytochrome *c* peak current

increases with H_2O_2 concentration in the electrolyte, and a sigmoidal wave develops when a saturating concentration of substrate is reached. Voltammograms from solutions containing only BCCP either in the presence or in the absence of H_2O_2 were indistinguishable from the background current (data not shown).

The half-wave potential of the sigmoidal waves ($E_{1/2} = 275 \pm 10$ mV $= E^{o\prime}$) shows that the actual transfer process is the catalysed reduction of cytochrome *c*. The catalytic current is scan rate independent up to 50 mV s^{-1} and increases for increasing BCCP concentrations. This behaviour is consistent with a reaction mechanism involving an initial heterogeneous electron transfer reaction at the electrode (Fig. 2, step 1), followed by homogeneous chemical reactions: the oxidized form of cytochrome *c* is regenerated by BCCP (Fig. 2, step 2) which, in turn, is recycled by H_2O_2 (Fig. 2, step 3). This mechanism can be simplified to

$$\begin{aligned} &\mathrm{Ox} + e^- \rightleftharpoons \mathrm{Red} \\ &\mathrm{Red} + Z \rightarrow \mathrm{Ox} \end{aligned} \quad (2)$$

provided that the following conditions are obeyed: (1) the heterogeneous electron transfer (Fig. 2, step 1) is a reversible reaction; (2) the homogeneous chemical reaction (Fig. 2, step 2) is irreversible; (3) the reaction between cytochrome *c* and BCCP is pseudo first order with a reaction rate constant given by $k' = kC_{\mathrm{BCCP}}$, where *k* is the second-order rate constant [10, 25].

The first condition is well obeyed, as previously demonstrated. The second condition is fulfilled because BCCP is being reoxidized in the catalytic cycle owing to the excess of H_2O_2 in solution (Fig. 2, step 3), and not by transferring electrons back to horse cytochrome *c*. As to requisite 3, it would imply that BCCP is present in large excess, which is not the case. However, under saturating concentrations of H_2O_2, this requisite is obeyed when the rate of recycling the oxidised BCCP by H_2O_2 is not rate-limiting. If this is the case, BCCP will always be available to react with cytochrome *c* and pseudo-first-order conditions are met.

Cyclic voltammograms at 20 mV s^{-1} were obtained for 100 μM cytochrome *c* and increasing BCCP concentrations (0.25–1 μM), in the absence and in the presence of a saturating concentration of H_2O_2 (125–350 μM, depending on the enzyme concentration), and are shown in Fig. 3.

From these recordings the catalytic current (i_{cat}) was determined as the difference between the current in the presence and in the absence of substrate, both measured at the same potential. The data was treated according to Laviron's theory for diffusionless electrochemical systems [4, 10], where the catalytic current is given by

$$i_{\mathrm{cat}} = n F k' V C_{\mathrm{Cyt}c} \quad (3)$$

In this equation, *V* is the entrapped-solution volume, *C* is the concentration and the other terms have the usual meaning.

From the variation of the pseudo-first-order rate constant, *k*′, with BCCP concentration, an intermolecular rate

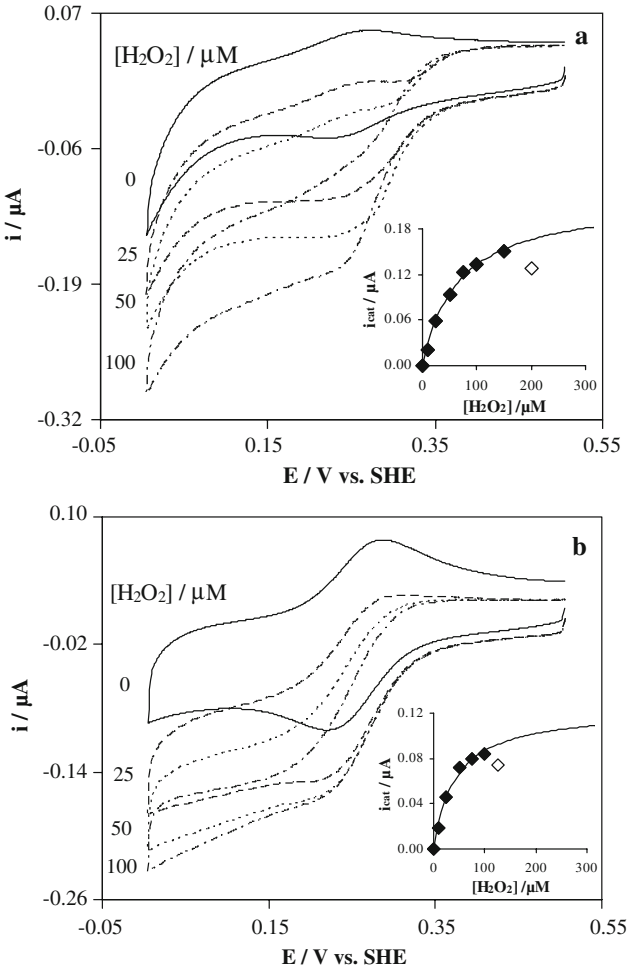

Fig. 1 Cyclic voltammograms ($v = 20$ mV s^{-1}) at the gold membrane electrode (**a**) or bulk solution (**b**) of 100 μM horse heart cytochrome *c* and 0.5 μM bacterial cytochrome *c* peroxidase (BCCP) in the presence of increasing concentrations of H_2O_2. The medium consisted of 10 mM phosphate buffer pH 7.0, 0.5 mM 4,4′-dithiodipyridine and 1 mM $CaCl_2$. *SHE* standard hydrogen electrode

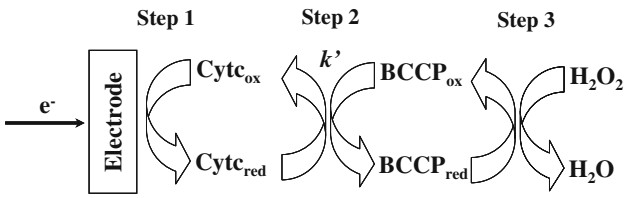

Fig. 2 Mediation scheme for BCCP: the electrode reduces horse heart cytochrome *c*, which is immediately reoxidized by BCCP; the level of oxidized BCCP is then restored by conversion of hydrogen peroxide to water

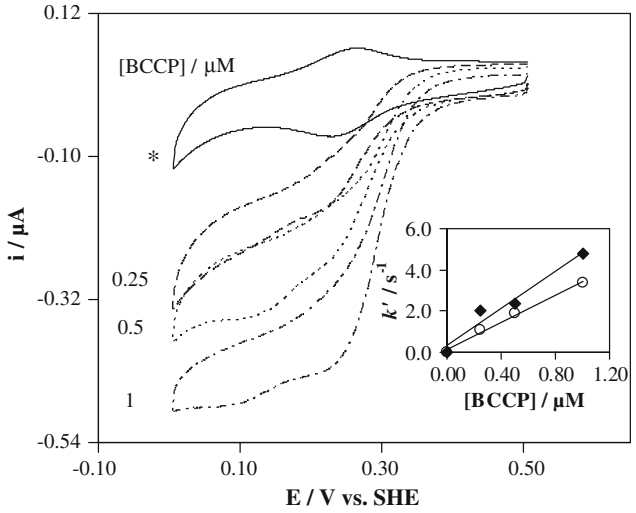

Fig. 3 Cyclic voltammograms ($v = 20$ mV s^{-1}) obtained at the gold membrane electrode for 100 μM cytochrome *c* and increasing BCCP concentrations (0.25–1 μM), in the absence (*asterisk*) and in the presence of a saturating H_2O_2 concentration (125–350 μM, depending on the enzyme concentration). *Insert*: Variation of the pseudo-first-order rate constant with BCCP concentration for 0 mM (*circles*) and 50 mM (*diamonds*) NaCl. The medium consisted of 10 mM phosphate buffer pH 7.0, 0.5 mM 4,4′-dithiodipyridine and 1 mM $CaCl_2$

constant $k = (3.2 \pm 0.5) \times 10^6$ M^{-1} s^{-1} was estimated (Fig. 3, insert, circles).

For assays where the H_2O_2 concentration was varied, for a constant cytochrome *c* and BCCP mixture, the catalytic current was plotted as a function of the substrate concentration (Fig. 1a, insert). It is clear that the catalytic current decreases after 150 μM H_2O_2 and so the data were fitted to the Michaelis–Menten kinetics for concentrations up to that value. Since thin-layer conditions are verified, the Michaelis–Menten equation has the form

$$i_{cat} = \frac{i_{max} C_{H_2O_2}}{C_{H_2O_2} + K_M} = \frac{nFk'VC_{Cytc}C_{H_2O_2}}{C_{H_2O_2} + K_M} \quad (4)$$

Using the CERN library Fortran program MINUIT algorithm, we estimated an apparent Michaelis–Menten constant $K_M = 66 \pm 4$ μM and an intermolecular electron transfer rate constant $k = (3.4 \pm 0.3) \times 10^6$ M^{-1} s^{-1}.

This electron transfer rate constant is higher than the value determined for a physiological donor, pseudoazurin ($(1.4 \pm 0.2) \times 10^5$ M^{-1} s^{-1} [10]). The more likely explanation for the difference between the rate constants would be a difference in the redox potential of these two electron donors, but the values determined at pH 7.0 are very similar.

Therefore, this behaviour must be related to another factor that influences the donor–enzyme interaction. In the case of these small electron donors the global charge surface is high and asymmetrically distributed, creating a significant dipole moment. Actually, the dipole moment of pseudoazurin is 651 D, and that of horse cytochrome *c* is 299 D [11]. This twofold difference in the dipole moment probably results in a stronger association of pseudoazurin with BCCP, and consequently the dissociation of the complex is disfavoured, explaining the lower rate constants observed.

Solution cyclic voltammetry

The mediated catalysis of BCCP by horse cytochrome *c* was also analysed at the gold electrode from solutions containing 100 μM horse heart cytochrome *c*, 0.5 μM BCCP and 1 mM $CaCl_2$. Again, the peak current increases with H_2O_2 concentration in the electrolyte, and a sigmoidal wave develops when a saturating concentration of substrate (100 μM) is present in the electrolyte, which is scan rate independent up to 50 mV s^{-1} (Fig. 1b).

The theory describing such a mechanism for diffusion-controlled processes was developed by Nicholson and Shain [26] and applied to several kinetic studies of reactions between mediators and redox proteins [25]. The intermolecular rate constant can also be calculated from the value of the H_2O_2 saturated limiting current using Eq. 5 [27, 28]:

$$i_{cat} = nFAD^{1/2}C_{Cytc}(k')^{1/2} \quad (5)$$

In this equation, *D* is the diffusion coefficient of cytochrome *c*. The valid value for our experimental conditions, $D = (1.2 \pm 0.1) \times 10^{-6}$ cm^2 s^{-1}, was computed from the dependence on the scan rate of either the cathodic or the anodic peak currents of the cyclic voltammograms for solutions containing both cytochrome *c* and BCCP in the absence of H_2O_2, using the Randles–Ševčík equation [21]. Calculations using Eq. 5 gave an intermolecular rate constant of $k = (4.0 \pm 0.5) \times 10^5$ M^{-1} s^{-1}.

The catalytic current for the different H_2O_2 concentrations (Fig. 1b, insert) was also fitted to Michaelis–Menten kinetics for concentrations up to 100 μM, and $K_M = 42 \pm 5$ μM and $k = (3.9 \pm 0.3) \times 10^5$ M^{-1} s^{-1} were obtained.

Similar apparent Michaelis–Menten constants were estimated for the proteins in bulk and entrapped solution, indicating that the membrane does not hamper the substrate diffusion. A higher value for the intermolecular rate constant was obtained for the proteins using the membrane configuration, reflecting a more favourable domain for the molecular interactions that must be established for electron transfer to occur between BCCP and cytochrome *c*. In both situations an inhibition effect by the substrate is observed for higher H_2O_2 concentrations, as verified in the case of the catalysis mediated by pseudoazurin [10]. A similar

inhibitory effect was observed in the study of other peroxidases [29–31].

Ionic strength and pH effects

One of the advantages of the ME approach is the ability to rapidly investigate effects on the redox behaviour of various experimental conditions, such as the pH or the supporting electrolyte composition. Another advantage of the approach is the small amount of protein needed for a series of measurements. This is so because once the ME has been mounted in the cell, it does not need to be removed or exchanged while changing any of those variables.

The same approach can also be applied to study the effect of such experimental variables on the kinetic activity of a more complex system, such as in mediated catalysis. Changes in the pH and/or the ionic strength of the medium may influence the rate of association, pre-orientation within the encounter complex, stability of the reactive complex or/and rate of dissociation of the products. However, the interpretation of ionic strength (or pH) dependences of the kinetic activity is complex and the behaviour observed should not be masked by the influence of those variables on the direct electrochemistry of the redox partners.

The effect of the ionic strength on the intermolecular rate constant for BCCP and horse cytochrome *c* was analysed with the proteins entrapped at the AUME and in bulk solution with a working solution containing 100 μM horse cytochrome *c*, 0.5 μM BCCP and 1 mM $CaCl_2$, in the presence of increasing amounts of NaCl (in the range 0–500 mM) and a saturated H_2O_2 concentration.

In both situations, the ionic strength dependence of the mediated catalysis has a bell-shaped curve, with a maximum activity at 50 mM NaCl (Fig. 4). The decrease of activity with increasing NaCl concentrations is consistent with the electrostatic character of the interaction between BCCP and the electron donor, cytochrome *c*. Indeed, cytochrome *c* has an asymmetric charge distribution with a positive surface that surrounds the exposed haem edge, which is the region proposed to interact with the negative surface around the exposed electron-transferring haem of the peroxidase [12, 14]. The increase of activity at low NaCl concentrations can be explained considering that for the lowest ionic strength the encounter complex formed has an orientation that is not so favourable for electron transfer. Therefore, the increase in NaCl concentration enables the lateral search at the peroxidase surface for the competent electron transfer orientation [11, 32]. Another explanation for this effect is that at low ionic strength cytochrome *c* reduction at the electrode might be affected by the lower k_{off} rate constant of the complex with BCCP.

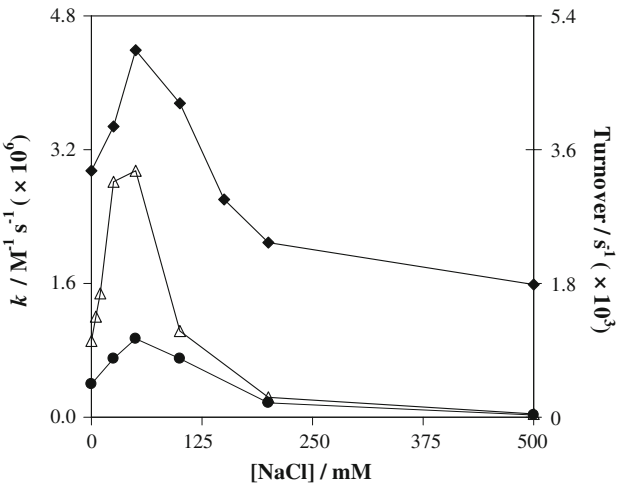

Fig. 4 Effect of ionic strength on the intermolecular rate constant for 100 μM horse heart cytochrome *c*, 0.5 μM BCCP and saturating H_2O_2 (150 μM *diamonds* or 100 μM *circles*) at the gold membrane electrode (*diamonds*) or in bulk solution (*circles*) and on the activity of BCCP with horse cytochrome *c* as an electron donor from solution steady-state kinetics performed spectrophotometrically (*triangles*) [11]. The medium consisted of 10 mM phosphate buffer pH 7.0 and 1 mM $CaCl_2$

Using the approach described above (Eq. 3), one can use the analysis of the catalytic current variation as a function of BCCP concentration (Fig. 3, insert, diamonds) to estimate an intermolecular rate constant for maximum activity $k = (4.4 \pm 0.5) \times 10^6\ M^{-1}\ s^{-1}$ for the membrane configuration. In the case of the bulk solution, a rate constant for maximum activity $k = (1.0 \pm 0.5) \times 10^6\ M^{-1}\ s^{-1}$ was determined using Eq. 5.

Similar behaviour was observed by solution steady-state kinetics performed spectrophotometrically, when this small cytochrome is used as an electron donor, with a maximum turnover also occurring at 50 mM NaCl [11], as can be observed in Fig. 4. However, in the voltammetric experiments with the membrane the variation in activity with ionic strength is less pronounced than that found with the proteins in bulk solution (either in the voltammetric assays or in solution steady-state kinetics performed spectrophotometrically). In fact, from 50 to 500 mM NaCl the activity decreases by 64% at the ME, while in the other two cases the decrease is 98%.

A similar effect was observed for the mediated catalysis of *P. pantotrophus* BCCP by *P. pantotrophus* pseudoazurin, where similar profiles were obtained with the membrane configuration and solution steady-state kinetics performed spectrophotometrically, though the maximum activity was observed for higher NaCl concentration in the former case. The differences may be due to the charge of the membrane, which somehow favours the formation of the encounter complex, making it less dependent on the ionic strength, in spite of the electrostatic forces that govern the interaction.

This may be also the reason why higher rate constants were determined for horse cytochrome *c* using the membrane configuration, although values of the same order of magnitude were obtained for maximum activity [$k = (4.4 \pm 0.5) \times 10^6\ M^{-1}\ s^{-1}$ for the membrane configuration and $k = (1.0 \pm 0.5) \times 10^6\ M^{-1}\ s^{-1}$ for bulk solution] as illustrated in Fig. 4.

The behaviour observed in the voltammetric experiments truly reflects the effect of ionic strength on the interaction between the enzyme and the electron donor rather than on the direct electrochemistry of horse cytochrome *c* due to the presence of the promoter. The horse cytochrome *c* peak current was shown to be NaCl-independent when 4,4′-dithiodipyridine is present in the medium (data not shown). Behaviour different from that observed at a bare gold electrode in the membrane configuration was evidenced, where a sharp decrease in current was observed at increasing NaCl concentrations [5]. Similar behaviour was also observed for the direct electrochemistry of pseudoazurin at a dithiodipyridine gold modified electrode [10].

The pH behaviour of horse cytochrome *c* is well known to present a p*K* close to 9.5 associated with the disappearance of the 695 nm absorption band, which is believed to be due to the replacement of the iron-coordinated methionine residue by a nitrogenous ligand, assigned as Lys73 [33, 34].

Previous bulk voltammetric studies of horse cytochrome *c* at a 4,4′-bipyridyl-modified gold electrode in the pH range 4.5–10.5 showed that while the peak potential remains essentially constant until pH 9, the peak current profile has a bell shape [35]. The maximum current was observed at pH 7 and two p*K* values around 9 and 5 were computed from that variation. The former is in agreement with the value obtained by other techniques, as well as with the observed E_p variation. The latter was attributed by the authors to the protonation of the promoter that disrupts the interaction between the gold surface and the protein, leading to a decrease of the electrochemical current [35].

For the reasons presented above, the pH dependence of the intermolecular rate constant for BCCP and horse cytochrome *c* was analysed at the bare AUME, i.e. in the absence of 4,4′-dithiodipyridine.

In order to accurately interpret the results of this pH dependence, the effect of this parameter on the electrochemical signal of horse cytochrome *c* alone was studied between pH 5 and 10 in the same conditions. As expected, the redox potential remained constant for pH < 9 and a pronounced decrease was observed for higher pH values (data not shown). A p*K* of 9.1 ± 0.1 was determined, in accordance with reported values [33–35]. For the peak current, a bell-shaped profile was obtained (Fig. 5, circles), behaviour similar to that observed for bulk solution in the

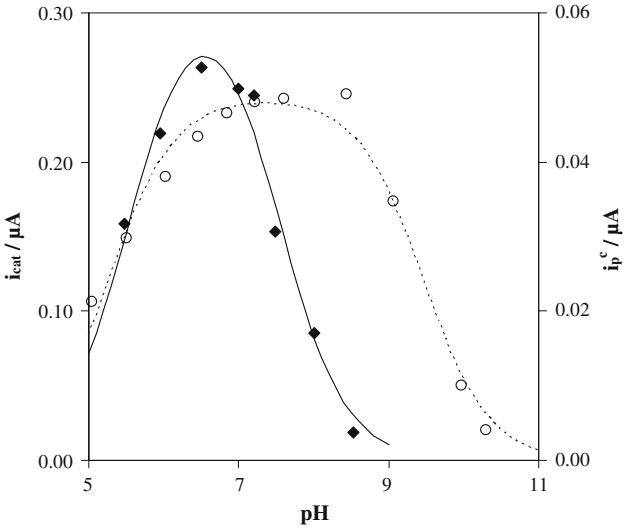

Fig. 5 pH dependence of 100 μM horse heart cytochrome *c* at the gold membrane electrode (*circles*) and catalytic current for 100 μM horse heart cytochrome *c*, 1.0 μM BCCP and saturating H_2O_2 (350 μM) at the gold membrane electrode (*diamonds*). The medium consisted of a mixed-buffer system (10 mM each) and 1 mM $CaCl_2$. The curves were fitted with Eq. 6

presence of the promoter [35]. The peak current pH dependence was fitted to the following equation [36]

$$i_{cat} = \left(i_{opt}\right) \Big/ \left(1 + 10^{(pKa_1 - pH)} + 10^{(pH - pKa_2)}\right) \quad (6)$$

and p*K* values of 5.3 ± 0.3 and 9.5 ± 0.3 were estimated. The latter is in clear agreement with the characteristic alkaline p*K* of this protein.

Several electrochemical studies using different approaches have observed a similar behaviour for the dependence on the pH of the horse cytochrome *c* current, and in some cases an acidic p*K* with an identical value, within the experimental errors, has been determined. However, depending on the authors and the conditions employed in the studies, the p*K* was assigned differently, namely to the proton-dissociation constant of the promoter [35], the Coulombic properties of the electrode surface [37, 38], the competitive adsorption of protons on the clay-modified electrodes [39] or the protein denaturation induced by the applied electric field at the electrode–solution interface [40]. In the present work a ME was employed, and so another possible cause for the profile observed at low pH is the degradation of the membrane–protein–electrode interaction, given that in the absence of a promoter charge effects stand out as being most important, as previously mentioned.

In the present study the same behaviour was observed either in the presence (data not shown) or in the absence of 4,4′-dithiodipyridine, eliminating the promoter protonation as the possible cause. Moreover, considering the fact that

the profile obtained at the bare ME is similar to that observed for the several bulk conditions, it seems that the acidic p*K* is not due to an artefact of the membrane.

In fact, this acidic p*K* may be the result of an acidic residue or a group of residues involved in the interaction with the electrode, but not affecting the haem environment and consequently not changing the redox potential. Denaturation of the protein would also lower the concentration of horse cytochrome *c* responding at low pH, and must be considered. Indeed, the analysis of the voltammograms of horse cytochrome *c* at decreasing electrolyte pH shows that the redox signal is at the same potential, but with a decreasing current which does not return to the initial value when the pH is raised back to 7.0 (data not shown).

The pH effect in the mediated catalysis at the AUME was studied in the range 5–10, using solutions containing 100 μM horse cytochrome *c*, 1 μM BCCP, 1 mM $CaCl_2$ and a saturated H_2O_2 concentration (350 μM). The catalytic current presents a bell-shape profiled (Fig. 5, diamonds) with no activity being observed above pH 9, which can be attributed to the inactivation of the enzyme at high pH [10]. This curve can be fitted to Eq. 6 with i_{opt} at pH 6.5 and two p*K* values, 5.6 ± 0.1 and 7.5 ± 0.1.

Taking into account the above results, we cannot conclude if the acidic p*K* estimated for the mediated catalysis is also related to the protein–protein interaction or only due to horse cytochrome *c* alone. However, preliminary solution steady-state kinetics performed spectrophotometrically of *Paracoccus* BCCP using horse cytochrome *c* as an electron donor (Pauleta et al., unpublished results) revealed an acidic p*K* at the same value, and similar values were observed for the enzymatic activity of *Pseudomonas aeruginosa* (5.2) [41] and *Rhodobacter capsulatus* (6.1) [42] BCCP.

Moreover, binding studies using microcalorimetry showed that the formation of this electron transfer complex involves the release of 0.46 protons at pH 6.0, which also suggests the existence of an acidic p*K*, at around pH 6.0 [16]. Therefore, this p*K* reflects a proton-dissociation process associated both with the horse cytochrome *c* and with the interaction/activity of this protein with BCCP.

A more basic p*K* was also observed for the solution steady-state kinetics determined spectrophotometrically of *P. aeruginosa* (6.8) and *R. capsulatus* (7.9) BCCP [41, 42], as now estimated for the *Paracoccus* enzyme. This p*K* can be clearly attributed to the mediated enzymatic catalysis, since the current profile of the horse cytochrome *c* itself is invariable in this pH region (Fig. 5). As several authors have suggested, these p*K* values can be assigned to the propionates of the BCCP haems, histidine ligands or proposed residues involved in the catalysis such as Glu128 [32, 42, 43]. However, the identity of the residue(s) responsible for this proton dissociation can only be disentangled through site-directed mutagenesis.

Conclusions

This work highlights the use of ME in the study of direct and mediated electrochemistry of metalloproteins. The results reported in the present work show that ME are very attractive for the study of complex metalloproteins systems, particularly with regard to the very small amounts of protein needed and the ease with which experimental variables can be changed.

Mediated catalysis of BCCP by horse cytochrome *c* was easily analysed, with minimum consumption of proteins, just varying the H_2O_2 concentration in the electrolyte solution. While the proteins stay entrapped in close vicinity to the electrode surface, small ions can diffuse through the membrane. For the same reasons, the effect on the catalytic activity of experimental conditions, such as pH and ionic strength, can be rapidly analysed.

The fitting to Michaelis–Menten kinetics of the experimental data, from studies with the proteins either entrapped in the membrane or freely diffusing in solution, led to similar K_M values, showing that no artefacts are introduced in the study by the use of a ME. Higher values for the intermolecular rate constants for horse cytochrome *c* and BCCP were obtained with the membrane configuration, which shows that the membrane does not disrupts the formation of the encounter complex and can even favour it. Since electrostatic interactions are fundamental for the formation of the complexes between *P. pantotrophus* BCCP and its electron donors, this configuration seems to be an adequate option for the electrochemical study of the mediated catalysis in biological systems, where electrostatic forces play an important role.

To draw conclusions about the influence of variables, such as pH or ionic strength, on the mediated catalytic activity, one must first pay attention to the behaviour of the mediator, i.e. the protein that actually exchanges the electrons with the electrode. For this reason, the ionic strength effect was analysed using a promoter to render the cytochrome *c*–electrode–membrane interaction more hydrophobic in nature, so the variation observed for the catalytic activity could only be due to changes in the binding between BCCP and the redox partner. On the other hand, the use of promoters might mask the pH effect depending on their acid–base behaviour and a possible interference must be verified.

Acknowledgments This work was within the research project POCI/QUI/55743/2004, from Fundação para a Ciência e Tecnologia (FCT). D.R. thanks FCT for financial support.

References

1. Haladjian J, Bianco P, Nunzi F, Bruschi M (1994) Anal Chim Acta 289:15–20
2. Haladjian J, Thierry-Chef I, Bianco P (1996) Talanta 43:1125–1130
3. Armstrong FA (2002) In: Bard AJ, Stratmann M (eds) Encyclopedia of electrochemistry, vol 9. Wiley-VCH, Weinheim, pp 13–28
4. Laviron E (1979) J Electroanal Chem 101:19–28
5. Lojou E, Bianco P (2000) J Electroanal Chem 485:71–80
6. Correia dos Santos MM, Paes de Sousa PM, Simões Gonçalves ML, Krippahl L, Moura JJG, Lojou E, Bianco P (2003) J Electroanal Chem 541:153–162
7. Santos M, Correia dos Santos MM, Simões Gonçalves ML, Costa C, Romão JC, Moura JJG (2006) J Inorg Biochem 100:2009–2016
8. Lojou E, Cutruzzola F, Tegoni M, Bianco P (2003) Electrochim Acta 48:1055–1064
9. Ferapontova EE, Ruzgas T, Gorton L (2003) Anal Chem 75:4841–4850
10. Paes de Sousa PM, Pauleta SR, Simões Gonçalves ML, Pettigrew GW, Moura I, Correia dos Santos MM, Moura JJG (2007) J Biol Inorg Chem 12:691–698
11. Pauleta SR, Guerlesquin F, Goodhew CF, Devreese B, Van Beeumen J, Pereira AS, Moura I, Pettigrew GW (2004) Biochemistry 43:11214–11225
12. Gilmour R, Goodhew CF, Pettigrew GW, Prazeres S, Moura JJG, Moura I (1994) Biochem J 300:907–914
13. Pauleta SR, Cooper A, Nutley M, Errington N, Harding S, Guerlesquin F, Goodhew CF, Moura I, Moura JJG, Pettigrew GW (2004) Biochemistry 43:14566–14576
14. Pettigrew GW, Prazeres S, Costa C, Palma N, Krippahl L, Moura I, Moura JJG (1999) J Biol Chem 274:11383–11389
15. Pettigrew GW, Pauleta SR, Goodhew CF, Cooper A, Nutley M, Jumel K, Harding SE, Costa C, Krippahl L, Moura I, Moura J (2003) Biochemistry 42:11968–11981
16. Pettigrew GW, Goodhew CF, Cooper A, Nutley M, Jumel K, Harding SE (2003) Biochemistry 42:2046–2055
17. Goodhew CF, Wilson IB, Hunter DJ, Pettigrew GW (1990) Biochem J 271:707–712
18. Bowden EF, Hawkridge FM, Chlebowski JF, Bancroft EE, Thorpe C, Blount HN (1982) J Am Chem Soc 104:7641–7644
19. Kakihana M, Ikeuchi H, Satô GP, Tokuda K (1980) J Electroanal Chem 108:381–383
20. Eddowes MJ, Hill HAO (1977) J Chem Soc Chem Commun 21:771–772
21. Bard AJ, Faulkner LR (eds) (2001) Electrochemical methods, fundamentals and applications. Wiley, New York
22. Gilmour R, Goodhew CF, Pettigrew GW, Prazeres S, Moura I, Moura JJG (1993) Biochem J 294:745–752
23. Vandewalle PL, Petersen NO (1987) FEBS Lett 210:195–198
24. LoÈtzbeyer T, Schuhmann W, Schmidt HL (1996) Sens Actuators B 33:50–54
25. Lopes H, Besson S, Moura I, Moura JJG (2001) J Biol Inorg Chem 6:55–62
26. Nicholson RS, Shain I (1964) Anal Chem 36:706–723
27. Coury LA, Oliver BN, Egekeze JO, Sosnoff CS, Brumfield JC, Buck RP, Murray RW (1990) Anal Chem 62:452–458
28. Savéant JM, Vianello E (1965) Electrochim Acta 10:905–920
29. Kim KL, Kang DS, Vitello LV, Erman JE (1990) Biochemistry 29:9150–9159
30. Scott DL, Bowden EF (1994) Anal Chem 66:1217–1223
31. Dequaire M, Limoges B, Moiroux J, Savéant JM (2002) J Am Chem Soc 124:240–253
32. Pettigrew GW, Echalier A, Pauleta SR (2006) J Inorg Biochem 100:551–567
33. Moore GR, Pettigrew GW (eds) (1991) Cytochromes c: evolutionary, structural and physicochemical aspects. Springer, Berlin
34. Assfalg M, Bertini I, Dolfi A, Turano P, Mauk AG, Rosell FI, Gray HB (2003) J Am Chem Soc 125:2913–2922
35. Eddowes MJ, Hill HAO (1979) J Am Chem Soc 101:4461–4464
36. Cornish-Bowden A (ed) (2001) Fundamentals of enzyme kinetics. Portland, London
37. Harmer MA, Hill HAO (1984) J Electroanal Chem 170:369–375
38. Armstrong FA, Cox PA, Hill HAO, Lowe VJ, Oliver BN (1987) J Electroanal Chem 217:331–366
39. Sallez Y, Bianco P, Lojou E, (2000) J Electroanal Chem 493:37–49
40. Fedurco M, Augustynski J, Indiani C, Smulevich G, Antalik M, Bano M, Sedlak E, Glascock MC, Dawson JH (2005) J Am Chem Soc 127:7638–7646
41. Soininen R, Ellfolk N (1972) Acta Chem Scand 26:861–872
42. Koh M, Meyer TE, De Smet L, Van Beeumen JJ, Cusanovich MA (2003) Arch Biochem Biophys 410:230–237
43. Echalier A, Goodhew CF, Pettigrew GW, Fülöp V (2006) Structure 14:107–117
44. Koppenol WH, Rush JD, Mills JD, Margoliash E (1991) Mol Biol Evol 8:545–558

J Biol Inorg Chem (2011) 16:881–888
DOI 10.1007/s00775-011-0785-8

ORIGINAL PAPER

Analysis of the activation mechanism of *Pseudomonas stutzeri* cytochrome *c* peroxidase through an electron transfer chain

P. M. Paes de Sousa · D. Rodrigues · C. G. Timóteo · M. L. Simões Gonçalves · G. W. Pettigrew · I. Moura · J. J. G. Moura · M. M. Correia dos Santos

Received: 22 December 2010 / Accepted: 12 April 2011 / Published online: 6 May 2011

Abstract The activation mechanism of *Pseudomonas stutzeri* cytochrome *c* peroxidase (CCP) was probed through the mediated electrochemical catalysis by its physiological electron donor, *P. stutzeri* cytochrome *c*-551. A comparative study was carried out, by performing assays with the enzyme in the resting oxidized state as well as in the mixed-valence activated form, using cyclic voltammetry and a pyrolytic graphite membrane electrode. In the presence of both the enzyme and hydrogen peroxide, the peak-like signal of cytochrome *c*-551 is converted into a sigmoidal wave form characteristic of an E_rC_i' catalytic mechanism. An intermolecular electron transfer rate constant of $(4 \pm 1) \times 10^5$ M^{-1} s^{-1} was estimated for both forms of the enzyme, as well as a similar Michaelis–Menten constant. These results show that neither the intermolecular electron transfer nor the catalytic activity is kinetically controlled by the activation mechanism of CCP in the case of the *P. stutzeri* enzyme. Direct enzyme catalysis using protein film voltammetry was unsuccessful for the analysis of the activation mechanism, since *P. stutzeri* CCP undergoes an undesirable interaction with the pyrolytic graphite surface. This interaction, previously reported for the *Paracoccus pantotrophus* CCP, induces the formation of a non-native conformation state of the electron-transferring haem, which has a redox potential 200 mV lower than that of the native state and maintains peroxidatic activity.

Keywords Cytochrome *c* peroxidase · Cytochrome *c*-551 · *Pseudomonas stutzeri* · Mediated catalysis · Activation mechanism

P. M. Paes de Sousa (✉) · C. G. Timóteo · I. Moura · J. J. G. Moura
ReQuimte, Centro de Química Fina e Biotecnologia,
Departamento de Química,
Faculdade de Ciências e Tecnologia,
Universidade Nova de Lisboa,
2829-516 Caparica, Portugal
e-mail: patricia.sousa@dq.fct.unl.pt

D. Rodrigues · M. L. Simões Gonçalves · M. M. Correia dos Santos (✉)
Centro de Química Estrutural,
Instituto Superior Técnico,
Av. Rovisco Pais,
1049-001 Lisbon, Portugal
e-mail: mcsantos@ist.utl.pt

G. W. Pettigrew
Royal (Dick) School of Veterinary Studies,
University of Edinburgh,
Summerhall,
Edinburgh EH9 1QH, UK

Introduction

The incomplete reduction of molecular oxygen to water results in the formation of hydrogen peroxide, a species that can induce cell damage or death owing to its ability to form free radicals. In biological processes, catalases dismutate the hydrogen peroxide molecule or peroxidases reduce it to water [1].

Bacterial cytochrome *c* peroxidases (CCPs) are dimeric dihaem proteins that catalyse the reduction of hydrogen peroxide to water using small monohaem cytochromes as electron donors [1]. Well-characterized members of this group are the CCPs from *Pseudomonas aeruginosa* [2–5], *Paracoccus pantotrophus* [6–8], *Pseudomonas nautica* [9], *Nitrosomonas europaea* [10], *Methylococcus capsulatus* [11], *Rhodobacter capsulatus* [12] and *Pseudomonas stutzeri* [13]. In most of these enzymes, in the resting oxidized state

(Fig. 1, state A) one of the haems is in a low-spin/high-spin thermal equilibrium, has a high redox potential, reflecting a histidine–methionine coordination, and is believed to function as the electron-transferring haem (E haem). The second haem (P haem), with a low redox potential and a low-spin bishistidine coordination in the fully oxidized state, is thought to be the catalytic centre where hydrogen peroxide is reduced to water. Reduction of the E haem induces a series of complex spin state and coordination changes, producing a mixed-valence enzyme in which the P haem has become high-spin pentacoordinated, providing access to the substrate (Fig. 1, state B) [14]. Calcium ions are required for the conversion of the mixed-valence enzyme into the activated state, but members of the bacterial CCP family differ in their affinity for this cation. The enzymes from *P. nautica* [9] and *P. pantotrophus* [15–17] behave very similarly, with the activation mechanism hindered in the as-isolated conditions, whereas the enzymes from *R. capsulatus* [12] and *P. stutzeri* [13] do not require addition of further Ca^{2+} to the state in which they are isolated for full activity. With the enzyme in the active form, the catalytic cycle is completed in the presence of hydrogen peroxide (Fig. 1, states E and F).

In fact, *P. stutzeri* CCP seems to be purified in a form with tightly bound Ca^{2+}, in which the calcium binding site responsible for dimer formation and enzyme activation, i.e. change of the low-potential haem to a high-spin pentacoordinated state, is fully occupied. Spectroscopic studies suggested that this form is readily active upon reduction by sodium ascorbate [13]. The affinity for calcium ions in the mixed-valence state is so high that Ca^{2+} returns to it from the EGTA which was added to empty the site in the oxidized state of the enzyme (Fig. 1, states C and D). Steady-state kinetic studies of *P. stutzeri* CCP using either its physiological partner (*P. stutzeri* cytochrome *c*-551) or horse heart cytochrome *c* indicated that preincubation with Ca^{2+} has no effect on the activity of the enzyme [13].

The use of voltammetric techniques is well proved in unravelling important aspects of the chemistry of metalloproteins and metalloenzymes [18]. An especially attractive approach is protein film voltammetry (PFV), a strategy where the protein is adsorbed at (ideally) monolayer coverage on a suitable electrode [19]. In PFV, besides the extremely small sample amounts that can be used, diffusion limitations are avoided, direct electron transfer is achieved and important information about the intrinsic thermodynamic and kinetic properties of the protein can be obtained. In the particular case of direct electron transfer of redox enzymes, the replacement of the physiological redox partner by the electrode and the direct correlation between current and catalytic activity are powerful tools for the study of the catalytic mechanism and its redox-linked chemistry. However, the use of PFV may be hindered if adsorption at the electrode surface is not successfully achieved, affecting the enzyme's activity [20]. In the case of bacterial CCPs, we recently reported the formation of an altered form of the E haem when *P. pantotrophus* CCP is directly adsorbed on a pyrolytic graphite (PG) electrode [21], a preferential surface for PFV studies [18]. The altered form has a redox potential approximately 300 mV lower than that of the native state and the enzyme maintains peroxidatic activity.

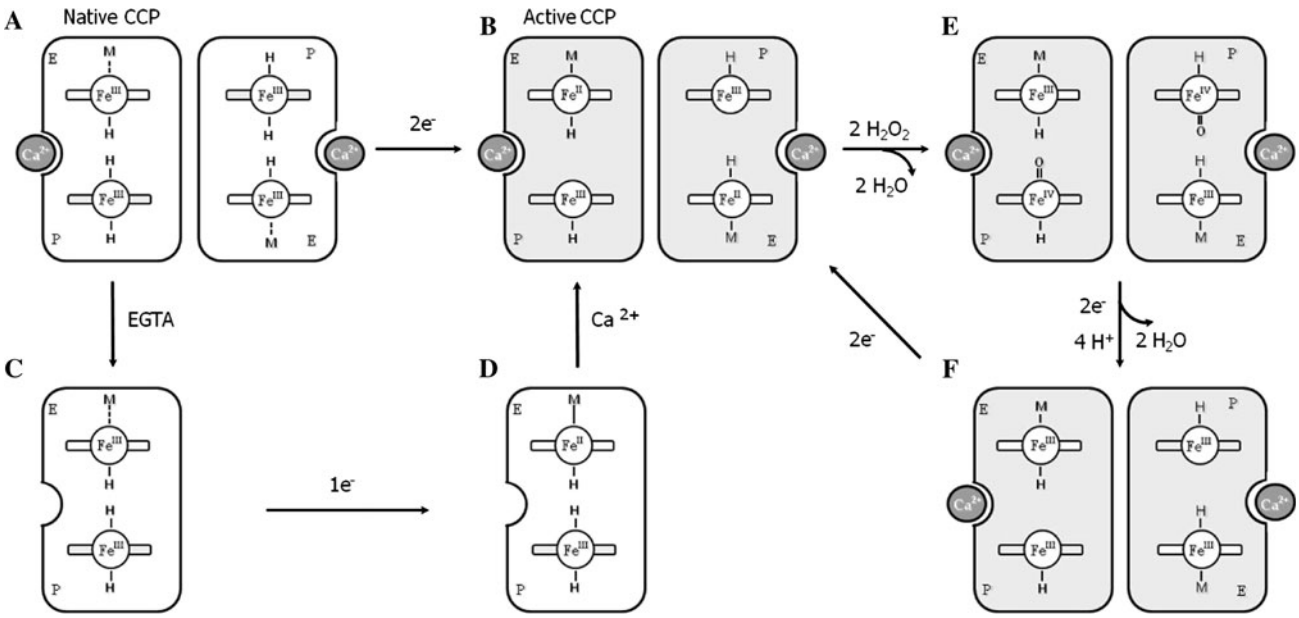

Fig. 1 Model for the mechanism of activation and turnover of *Pseudomonas stutzeri* cytochrome *c* peroxidase (*CCP*). *EGTA* ethylene glycol bis(2-aminoethyl ether)tetraacetic acid

An alternative approach is mediated enzyme electrochemistry, where, similarly to steady-state kinetics, the assays are performed with enzyme, cosubstrate (mediator) and substrate all present in solution. The mediator is the only species that interacts with the electrode and the electrochemical signal is directly related to the rate of its consumption during the catalytic reaction. In many cases, the mediators are stable molecules of low molecular weight that can easily exchange electrons with the electrode, and act as substituents of the redox metalloprotein natural partner [22]. When the physiological electron mediator is known, the natural electron transfer relay can be mimicked.

The use of membrane electrodes, a configuration where the proteins are entrapped between a dialysis membrane and the electrode surface, has been shown to be a very interesting strategy for this kind of study [23–25]. As happens in PFV, only small amounts of protein are necessary (3–4 μl) and, owing to instantaneous dialysis, various experimental parameters can be rapidly investigated [26, 27]. Moreover, the theoretical features have been analysed in detail and quantitative information about the redox processes can be easily obtained [28].

We have recently used cyclic voltammetry and a membrane electrode to analyse the mediated catalysis of *P. pantotrophus* CCP by one of its physiological donors, *P. pantotrophus* pseudoazurin [29]. We now report the mediated electrochemistry of *P. stutzeri* CCP, using its physiological partner, *P. stutzeri* cytochrome *c*-551, as an electron donor. To probe the activation mechanism of the enzyme, both the oxidized and the mixed-valence forms were analysed. Direct electrochemistry of the enzyme was also investigated.

Materials and methods

Reagents

Poly(L-lysine) hydrobromide was obtained from Sigma (M_W 15,000–30,000). All other chemicals were pro analysis grade and solutions were prepared with Milli-Q water.

Protein purification

P. stutzeri CCP and *P. stutzeri* cytochrome *c*-551 were isolated and purified as described before [13]. In this particular purification, a fraction of the enzyme was obtained in the mixed-valence, already active state, without addition of any chemical reductant at any point during the procedure. The concentration of the proteins was determined spectrophotometrically using the extinction coefficients at 408 nm ($\varepsilon = 252\ mM^{-1}\ cm^{-1}$) and 551 nm ($\varepsilon = 30.89\ mM^{-1}\ cm^{-1}$) for the oxidized enzyme and the reduced cytochrome, respectively [13].

Procedure

The cyclic voltammograms were collected with an EG&G PAR potentiostat/galvanostat (model 273A) controlled via the 270 software. The scan rate varied between 5 and 200 mV s^{-1}. Catalytic assays with the enzyme directly adsorbed on the electrode surface were performed with an electrode rotation rate of 3,000 rpm.

A conventional three-electrode configuration cell was used, with a carbon rod auxiliary electrode and an Ag/AgCl reference electrode (205 mV vs. the standard hydrogen electrode, SHE). Throughout this article, all potential values are referred to the SHE and are affected by an error of 5–10 mV. The working electrode was a basal plane PG electrode with a 0.2-cm nominal radius. The area of the electrode was determined from its response in a known concentration of the ferrocyanide/ferricyanide couple [30] and was found to be close to the nominal value.

Electrode preparation

Prior to each experiment, the PG electrode was polished by hand on a polishing cloth (Buehler 40-7212) with an aqueous alumina slurry (0.3 μm, Buehler 40-6363-006), sonicated for 1 min and rinsed very well with Milli-Q water.

For the direct electrochemistry of CCP, a 4-μl drop of working solution (containing the protein) was deposited on the electrode surface and left to dry at room temperature for 30 min.

The membrane configuration, prepared with a negatively charged Spectra/Por MWCO 3500 membrane, was used for the analysis of cytochrome *c*-551 and the mediated catalysis of CCP. Briefly, a small volume (4 μl) of the protein(s) solution was deposited on a square piece (about twice the diameter of the electrode's body) of the dialysis membrane, then the electrode was pressed against the membrane and a rubber ring was fitted around the electrode body so that the entrapped solution formed a uniform thin layer.

Electrolyte and working solution

In all experiments the supporting electrolyte was 10 mM *N*-(2-hydroxyethyl)piperazine-*N*′-ethanesulfonic acid (HEPES) buffer, pH 7.5 ± 0.1. In most cases 150 mM NaCl was used, which was replaced by 0.1 mg ml^{-1} poly(L-lysine) hydrobromide in the working solution in some assays. The working solution contained either 82 μM *P. stutzeri* CCP (direct electrochemistry) or 100 μM *P. stutzeri* cytochrome *c*-551

and 1 μM *P. stutzeri* CCP (mediated catalysis). The effect of substrate concentration was analysed for different hydrogen peroxide concentrations between 10 and 150 μM. In the experiments with a saturating substrate concentration, a concentration of 500 μM (direct electrochemistry) or 125 μM (mediated catalysis) was present in the electrolyte solution.

All solutions were deaerated for 30 min with high-purity nitrogen, and all measurements were performed at least in duplicate in a temperature-controlled room ($T = 20 \pm 1$ °C).

Results and discussion

Direct electrochemistry of *P. stutzeri* CCP

The direct electrochemistry of *P. stutzeri* CCP in non-turnover conditions was analysed at a PG electrode in 10 mM HEPES buffer, pH 7.5, without the addition of calcium ions. Although the enzyme has two *c*-type haems, cyclic voltammograms of *P. stutzeri* CCP adsorbed on the electrode surface revealed just one cathodic peak with an anodic counterpart, in the potential range +800 to −600 mV and for scan rates, v, between 5 and 200 mV s^{-1} (Fig. 2). The signal visible at potentials above +0.1 V is also present in the blanks and is therefore meaningless for the study presented. The analysis of the voltammograms showed that the electrochemical response arises from a diffusionless one-electron redox process where both the oxidized and the reduced forms are adsorbed. A formal potential $E^{0'} = -125$ mV was estimated at pH 7.5. Differential pulse voltammograms revealed two peaks with peak potentials $E_p = -107$ mV versus SHE and $E_p = -244$ mV versus SHE. Only the more positive one persisted upon successive scans, corresponding to the signal observed in cyclic voltammetry.

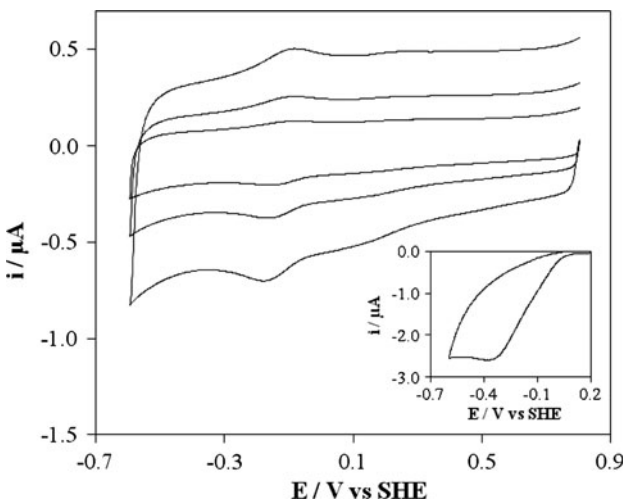

Fig. 2 Cyclic voltammograms ($v = 50$, 100 and 200 mV s^{-1}) of 110 μM *P. stutzeri* CCP adsorbed at a pyrolytic graphite (PG) electrode, in 10 mM *N*-(2-hydroxyethyl)piperazine-*N*′-ethanesulfonic acid (HEPES) buffer pH 7.5. *Inset*: Voltammetric signal ($v = 20$ mV s^{-1}, electrode rotation rate 3,000 rpm) in the presence of 500 μM H_2O_2. *SHE* standard hydrogen electrode

In the presence of hydrogen peroxide only one catalytic wave develops in the same potential range, with $E_{cat} = -136$ mV versus SHE and a current that increases with increasing substrate concentration. Experiments performed in the absence of enzyme demonstrated that the direct reduction of hydrogen peroxide does not occur within that potential window. It is clear from Fig. 2 that the shape of the cyclic voltammograms is not sigmoidal. Although the forward current tends to level off to a limiting value, in the reverse scan the current decreases considerably. Moreover, in successive scans the catalytic signal decreases until the initial non-turnover voltammogram is restored.

Similar behaviour was observed for the *P. pantotrophus* CCP at the same type of electrode surface [21]. Namely, just one non-turnover signal persists on successive scans at a potential that does not match the preliminary data from a potentiometric titration, where redox transitions at about +60 and −300 mV at pH 7.5 were estimated for the E and P haems of *P. stutzeri* CCP, respectively. Also, only a cathodic catalytic signal is detected in the presence of hydrogen peroxide, at a potential close to that of the signal without substrate, behaviour distinct from that observed for the *N. europaea* CCP, which displays catalytic activity at a high redox potential (more than 500 mV vs. SHE) [31].

At pH 7.5 the enzyme has an overall negative charge since its pI is 5.4 [32]. From examination of the electrostatic surface potential of *P. stutzeri* CCP, it is also clear that a negatively charged region surrounds the peroxidatic centre, whereas the surface of the protein around the E haem is much more hydrophobic (C. Timóteo, unpublished results). Therefore, the interaction of the enzyme with the negatively charged PG surface most likely occurs through hydrophobic interactions and/or hydrogen bonding between the electrode surface and neighbouring residues of the E haem. This is also supported by the fact that the electrochemical signal deteriorates in the presence of the positively charged coadsorbate poly(L-lysine), in spite of the acidic isoelectric point of the enzyme and the negative charge of the electrode at pH 7 [33].

Taking into account the electrochemical behaviour described and its resemblance to that verified for the *Paracoccus* enzyme [21], one can only attribute the signal observed for *P. stutzeri* CCP to a non-native conformation state of the E haem, induced by interaction with the PG

surface. This altered form of the E haem has a redox potential about 200 mV lower than that of the native state and also displays peroxidatic activity, as observed for *P. pantotrophus* CPP.

Direct enzyme voltammetry is not feasible but information regarding the activation mechanism can be obtained through the interaction with the natural partner, cytochrome *c*-551 from *P. stutzeri*. The electrochemical behaviour of the cytochrome was first analysed and then the mediated electrocatalysis of *P. stutzeri* CCP was investigated.

Direct electrochemistry of *P. stutzeri* cytochrome *c*-551

The direct electrochemistry of *P. stutzeri* cytochrome *c*-551 was obtained for the first time at a PG membrane electrode. Addition of NaCl to the electrolyte solution or of poly(L-lysine) to the working solution was necessary to obtain a well-defined electrochemical response. Direct electrochemistry of cytochrome *c*-551 from *P. aeruginosa* at a PG electrode has been reported [24], but in that case no modification of the electrode was necessary. Although both proteins have acidic isoelectric points [13, 24], from examination of the electrostatic surface potential, it is clear that the region around the haem is more positive in the *P. aeruginosa* cytochrome (Protein Daka Bank entry 451C) than in the *P. stutzeri* protein (Protein Data Bank entry 1COR). Therefore, the presence of positively charged species is an important condition for the reduction of *P. stutzeri* cytochrome *c*-551 at an electrode that bears a net negative charge at pH 7.5 [33], whereas in the case of cytochrome *c*-551 from *P. aeruginosa* no promoter was required. When the NaCl concentration was varied in the electrolyte (0–650 mM) the current increased by 60% up to 150 mM, staying constant for higher salt concentrations (data not shown). Similar results were obtained with poly(L-lysine). In all subsequent experiments 150 mM NaCl was present in the electrolyte solution.

A typical cyclic voltammogram of *P. stutzeri* cytochrome *c*-551 is shown in Fig. 3 (full line). The voltammograms are not affected by the presence of the enzyme in the entrapped solution. In all circumstances, a reversible one-electron transfer reaction occurs at least for $v < 50$ mV s^{-1} with i_p^c/i_p^a close to 1 and E_p^a and E_p^c being independent of the scan rate. A membrane configuration was used, but thin layer conditions were only verified for $v < 10$ mV s^{-1}. Above this value, i_p varies linearly with $v^{1/2}$ with a null intercept, and the diffusion coefficient $D = (1.0 \pm 0.1) \times 10^{-6}$ cm^2 s^{-1} was determined using the Randles–Ševčik equation [28], in perfect agreement with known values for other cytochromes of similar molecular mass [34]. As to the peak-to-peak separation, $\Delta E_p = E_p^a - E_p^c$, it is close to the theoretical value for a one-electron Nernstian reaction controlled by diffusion. Departure from reversibility is clearly observed for the highest scan rates through the increase of this parameter. However, for all scan rates the average $(E_p^a + E_p^c)/2$ is constant within the experimental error, and a formal reduction potential $E^{0'} = 219$ mV could be estimated at pH 7.5. This value is in accordance with the formal potential reported in [35] for this cytochrome, showing that the native state of the protein is preserved in the solution entrapped in the membrane electrode.

Catalytic activity of *P. stutzeri* CCP with *P. stutzeri* cytochrome *c*-551 as an electron donor

The catalytic activity of *P. stutzeri* CCP towards *P. stutzeri* cytochrome *c*-551 was investigated in the same experimental conditions using the oxidized and the mixed-valence (half-reduced) forms of the enzyme.

Voltammograms from solutions containing only *P. stutzeri* CCP either in the presence or in the absence of hydrogen peroxide were indistinguishable from the background current (data not shown) in the potential range used (+0.5 to −0.1 V). However, when both 100 μM *P. stutzeri* cytochrome *c*-551 and 1 μM *P. stutzeri* CCP are present, it is clear from Fig. 3 that, for assays with the oxidized form, the peak current of cytochrome *c*-551 increases with successive additions of hydrogen peroxide, until the peak-shaped signal is converted into a sigmoidal wave form. This change in shape is the result of the electrocatalytic reaction with the enzyme, i.e. in the entrapped solution

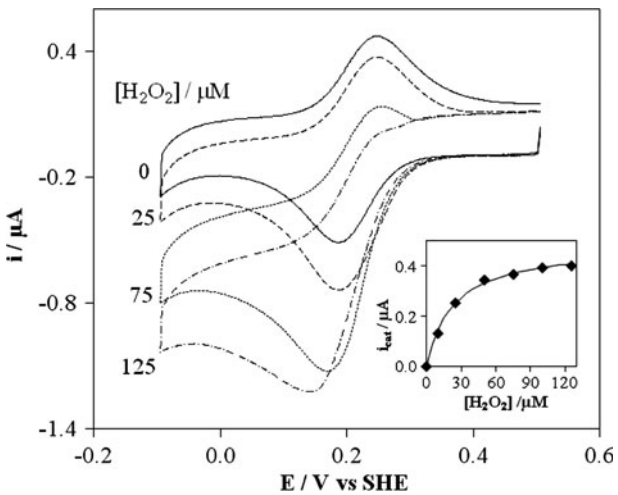

Fig. 3 Cyclic voltammograms ($v = 20$ mV s^{-1}) of 100 μM *P. stutzeri* cytochrome *c*-551 and 1 μM oxidized *P. stutzeri* CCP at a PG membrane electrode in the presence of increasing H_2O_2 concentrations, in 10 mM HEPES buffer pH 7.5 and 150 mM NaCl. *Inset*: Variation of the catalytic current with substrate concentration and fitting to the Michaelis–Menten equation

both *P. stutzeri* CCP and its physiologic donor were able to orient themselves in a way that the formation of the transient complex occurred and the intermolecular electron transfer took place.

For hydrogen peroxide concentrations higher than 125 μM the current decreases. Similar behaviour was observed in the mediated catalysis of *P. pantotrophus* CCP by *P. pantotrophus* pseudoazurin or horse heart cytochrome *c* [25, 29], most probably due to the inactivation of the enzyme in the presence of high substrate concentrations.

The catalytic current of the sigmoidal wave, developed when a saturating hydrogen peroxide concentration (125 μM) is added to the electrolyte, is independent of the scan rate up to 50 mV s^{-1}. The half-wave potential of this wave, $E_{1/2} = 218$ mV $= E^{0'}$ [28], confirms that the actual transfer process is the catalysed reduction of cytochrome *c*-551. As previously described [36], this behaviour is consistent with a reaction mechanism involving an initial heterogeneous electron transfer reaction at the electrode (Fig. 4, step 1), followed by homogeneous chemical reactions: the oxidized form of cytochrome *c*-551 is regenerated by CCP (Fig. 4, step 2), which, in turn, is recycled by hydrogen peroxide (Fig. 4, step 3), i.e. a E_rC_i' catalytic reaction scheme [28].

For each hydrogen peroxide concentration, the catalytic current i_{cat} was calculated as the difference between the experimental current in the presence and absence of substrate (both measured at the same potential) and plotted as a function of hydrogen peroxide concentration. The results, shown in the inset in Fig. 3, were non-linearly fitted to the Michaelis–Menten equation for concentrations up to 125 μM:

$$i_{cat} = \frac{i_{catmax}\, C_{H_2O_2}}{C_{H_2O_2} + K_M}, \quad (1)$$

where i_{catmax} is the catalytic current observed at the maximum rate and K_M is the Michaelis–Menten constant. As can be seen in Fig. 3, the fit shows that the experimental data are in good agreement with Eq. 1 and lead to a K_M of (25 ± 2) μM. It must be pointed out that for low concentrations the catalytic currents are affected by the substrate diffusion since a stationary electrode was used, leading to an overestimation of the Michaelis–Menten constant [37]. In fact, a K_M of 2 μM was estimated from steady-state kinetics, although horse heart cytochrome *c* was used as the electron donor [13]. However, when the differences between the two types of assays are taken into account, the results can be considered to be in reasonable agreement.

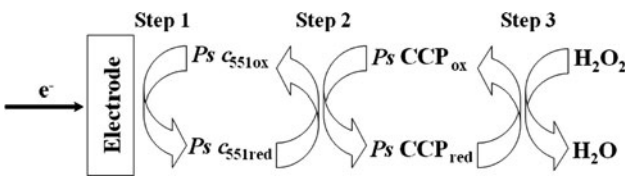

Fig. 4 Mediation scheme for CCP: the electrode reduces cytochrome *c*-551, which is immediately reoxidized by CCP; the level of oxidized CCP is then restored by conversion of H_2O_2 to water. *Ps* c_{551ox} oxidized *P. stutzeri* cytochrome *c*-551 , *Ps* c_{551red} reduced *P. stutzeri* cytochrome *c*-551, *Ps* CCP_{ox} oxidized *P. stutzeri* CCP, *Ps* CCP_{red} reduced *P. stutzeri* CCP

Since diffusion control was verified, i_{catmax} is given by the equation

$$i_{catmax} = nFAD^{1/2}C_{c_{551}}k'^{1/2}, \quad (2)$$

where $C_{c_{551}}$ is the concentration of the cytochrome *c*-551 (mediator) and k' is the pseudo-first-order rate constant for the intermolecular electron transfer, i.e. $k' = kC_{CCP}$, where C_{CCP} is the concentration of the enzyme. As long as the electron transfer between *P. stutzeri* cytochrome *c*-551 and *P. stutzeri* CCP is the rate-limiting step in the overall process, the second-order rate constant *k* can be determined by Eq. 2. Competition between the intermolecular and the enzyme–substrate electron transfer reactions can be evaluated through the kinetic parameter σ given by Limoges et al. [38]:

$$\sigma = \frac{kC_{c_{552}}}{\frac{k_{cat}C_{H_2O_2}}{C_{H_2O_2}+K_M}}. \quad (3)$$

An estimation of σ can be obtained with $K_M = 2$ μM and $k_{cat} = 88$ s^{-1} reported for *P. stutzeri* CCP at pH 7.5 with horse heart cytochrome *c* as the electron donor [13], and taking as an approximation for *k* the value reported for the electron transfer between *P. pantotrophus* pseudoazurin and *P. pantotrophus* CCP, 1×10^5 M^{-1} s^{-1}. For 125 μM hydrogen peroxide $\sigma \approx 0.1$, indicating that in principle Eq. 2 can be used. A rate constant $k = k'/C_{CCP} = (4 \pm 1) \times 10^5$ M^{-1} s^{-1} was determined with Eq. 2 for the intermolecular electron transfer reaction between fully oxidized *P. stutzeri* CCP and its physiological donor *P. stutzeri* cytochrome *c*-551.

Alternatively, *k* can be estimated from the slope of a plot of (i_{cat}/i_p) versus $(1/v)^{1/2}$, which should obey a linear relationship with a null intercept if the intermolecular electron transfer between *P. stutzeri* cytochrome *c*-551 and the enzyme limits the overall reaction rate. Cyclic voltammograms were recorded for scan rates in the range 5–100 mV s^{-1} in the absence of substrate, and at 20 mV s^{-1} in the presence of saturating hydrogen peroxide (125 μM). In the absence of substrate, the peak current is given by the equation

$$i_p = 2.69 \times 10^5 n^{3/2}AD^{1/2}C_{cyt}v^{1/2}, \quad (4)$$

whereas the catalytic current is given by Eq. 2. From the slope (0.20 ± 0.01) of the (i_{cat}/i_p) versus $(1/v)^{1/2}$ plot, a pseudo-first-order rate constant $k' = (0.31 \pm 0.03)$ s^{-1} was

determined, which corresponds to an intermolecular electron transfer rate constant $k = (3.1 \pm 0.3) \times 10^5$ M^{-1} s^{-1} for the mediated catalysis of oxidized *P. stutzeri* CCP by *P. stutzeri* cytochrome *c*-551.

The good agreement between the *k* values using different approaches is an indication that the conditions required to analyse the data according to the model depicted in Fig. 4 were met.

A similar set of experiments was performed with the mixed-valence enzyme. As mentioned (see "Materials and methods"), a fraction of the enzyme was purified in the mixed-valence state, but to guarantee that the high-potential haem of *P. stutzeri* CCP was reduced, experiments in the presence of sodium ascorbate were also performed [16]. As observed for the oxidized form, when both *P. stutzeri* cytochrome *c*-551 and mixed-valence *P. stutzeri* CCP are present in solution, the peak-shaped voltammograms transform, in the presence of increasing amounts of hydrogen peroxide, into a sigmoidal wave characteristic of a catalytic E_rC_i' mechanism. Fitting the variation of the catalytic current with hydrogen peroxide concentration to the Michaelis–Menten equation (Eq. 1), we estimated values of $K_M = (32 \pm 4)$ μM and $k = (5.7 \pm 0.5) \times 10^5$ M^{-1} s^{-1} for the Michaelis–Menten and intermolecular electron transfer rate constants, respectively.

Figure 5 shows the fit of the experimental *i*–*E* curve obtained for the mixed-valence enzyme in the presence of 125 μM hydrogen peroxide to the theoretical wave for a catalytic E_rC_i' mechanism [28, 38]:

$$i = \frac{nFAC_{c_{552}}(Dk'C_{CCP})^{1/2}}{1 + \exp\left[\frac{nF}{RT}(E - E_{1/2})\right]}. \quad (5)$$

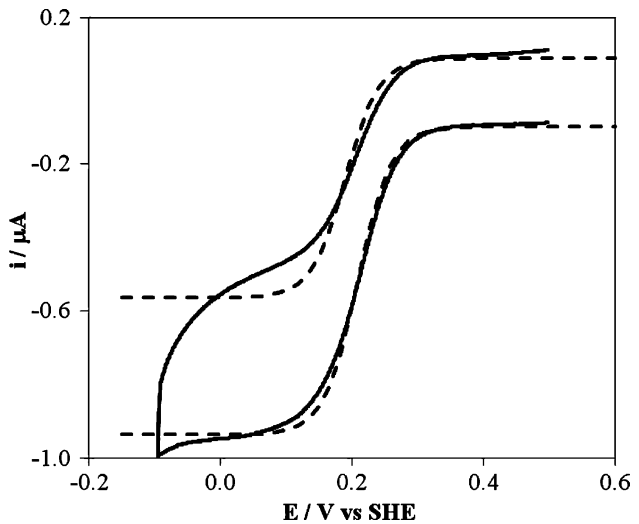

Fig. 5 Catalytic curve obtained for 1 μM mixed-valence enzyme and 100 μM *P. stutzeri* cytochrome *c*-551 in the presence of 125 μM H_2O_2 (*continuous line*) and theoretical wave for a catalytic E_rC_i' mechanism according to Eq. 5 (*dashed line*)

Fitting of the forward branch of the wave to Eq. 5 leads to the half-wave potential $E_{1/2} = 208$ mV ($=E^{0'}$) and $k' = 0.45$ s^{-1}, which corresponds to $k = 4.5 \times 10^5$ M^{-1} s^{-1}.

The similarity of the results obtained for K_M and *k*, using either the fully oxidized or the mixed-valence CCP, shows that the oxidation state of the high-potential haem of the enzyme has no effect on the mediated catalysis by *P. stutzeri* cytochrome *c*-551. These results support the proposal that the enzyme is readily active upon reduction, since the (tightly) Ca^{2+} binding site is already filled in the resting oxidized state.

Conclusions

The activation mechanism of *P. stutzeri* CCP was investigated using the physiological partner *P. stutzeri* cytochrome *c*-551 as an electron relay for mediated catalysis. A PG membrane electrode was used and this configuration was demonstrated once more to be a useful option for the electrochemical analysis of biological systems. The catalysis was analysed by cyclic voltammetry for both the oxidized enzyme and the mixed-valence enzyme. All experiments were done in the absence of added calcium. Similar intermolecular rate constants were estimated for the two forms of *P. stutzeri* CCP.

Previous spectroscopic studies had suggested that *P. stutzeri* CCP needs calcium ions to be active but, unlike other CCPs, is isolated in a dimeric form with one tightly bound Ca^{+2} and is active as soon as the mixed-valence state is attained. Further characterization of *P. stutzeri* CCP and cytochrome *c*-551 to elucidate the nature of the intermolecular electron transfer and the catalytic mechanism has now been reported. The electrochemical results presented for the mediated catalysis of oxidized and mixed-valence *P. stutzeri* CCP confirm that the activation mechanism of the enzyme is fast, since no differences were detected between the results obtained for each form.

Analysis of the activation mechanism through direct electron transfer of *P. stutzeri* CCP was not possible, since an altered form of the enzyme is induced by interaction with the PG surface, as observed for the *P. pantotrophus* CCP.

Acknowledgments This work was performed within the research project PPCDT/QUI/55743/2004. D.R. thanks Fundação para a Ciência e Tecnologia for financial support (POCI/QUI/55743/2004). P.M.P.S. and C.G.T. would like to thank the Ciência 2007 (FCT-MCTES) programme.

References

1. Halliwell B, Gutteridge JMC (eds) (1989) Free radicals in biology and medicine. Oxford Science Publications, Oxford

2. Ellfolk N, Soininen R (1970) Acta Chem Scand 24:2126–2136
3. Foote N, Thompson AC, Barber D, Greenwood C (1983) Biochem J 209:701–707
4. Foote N, Turner R, Brittain T, Greenwood C (1992) Biochem J 283:839–843
5. Ellfolk N (1983) Biochim Biophys Acta 743:23–30
6. Goodhew CF, Wilson IBH, Hunter DJB, Pettigrew GW (1990) Biochem J 271:707–712
7. Pettigrew GW (1991) Biochim Biophys Acta 1058:25–27
8. Hu W, Van Driessche G, Devreese B, Goodhew CF, McGinnity DF, Saunders N, Fülöp V, Pettigrew GW, Van Beeumen J (1997) Biochemistry 36:7958–7966
9. Alves T, Besson S, Duarte L, Pettigrew GW, Girio FMF, Devreese B, Vanderberghe I, Van Beeumen J, Fauque G, Moura I (1999) Biochim Biophys Acta 1434:248–259
10. Arciero DM, Hooper AB (1994) J Biol Chem 269:11878–11886
11. Zahn JA, Arciero DM, Hooper AB, Coats JR, DiSpirito AA (1997) Arch Microbiol 168:363–372
12. De Smet L, Pettigrew GW, Van Beeumen JJ (2001) Eur J Biochem 268:6559–6568
13. Timóteo CG, Tavares P, Goodhew CF, Duarte LC, Jumel K, Gírio FMF, Harding S, Pettigrew GW, Moura I (2003) J Biol Inorg Chem 8:29–37
14. Pettigrew GW, Echalier A, Pauleta SR (2006) J Inorg Biochem 100:551–567
15. Gilmour R, Goodhew CF, Pettigrew GW, Prazeres S, Moura I, Moura JJG (1993) Biochem J 294:745–752
16. Gilmour R, Goodhew CF, Pettigrew GW, Prazeres S, Moura I, Moura JJG (1994) Biochem J 300:907–914
17. Gilmour R, Prazeres S, McGinnity DF, Goodhew CF, Moura JJG, Moura I, Pettigrew GW (1995) Eur J Biochem 234:878–886
18. Léger C, Bertrand P (2008) Chem Rev 108:2379–2438
19. Butt JN, Armstrong FA (2008) In: Hammerich O, Ulstrup J (eds) Bioinorganic electrochemistry. Springer, Dordrecht, pp 91–128
20. Chen KI, McEwan AG, Bernhardt PV (2009) J Biol Inorg Chem 14:409–419
21. Paes de Sousa PM, Pauleta SR, Simões Gonçalves ML, Pettigrew GW, Moura I, Moura JJG, Correia dos Santos MM (2011) J Biol Inorg Chem 16:209–215
22. Savéant JM (2006) Elements of molecular and biomolecular electrochemistry. Willey, Hoboken
23. Ferapontova EE, Ruzgas T, Gorton L (2003) Anal Chem 75:4841–4850
24. Lojou E, Cutruzzolà F, Tegoni M, Bianco P (2003) Electrochim Acta 48:1055–1064
25. Paes de Sousa PM, Pauleta SR, Rodrigues D, Simões Gonçalves ML, Pettigrew GW, Moura I, Moura JJG, Correia dos Santos MM (2008) J Biol Inorg Chem 13:779–787
26. Haladjian J, Bianco P, Nunzi F, Bruschi M (1994) Anal Chim Acta 289:15–20
27. Correia dos Santos MM, Paes de Sousa PM, Simões Gonçalves ML, Krippahl L, Moura JJG, Lojou E, Bianco P (2003) J Electroanal Chem 541:153–162
28. Bard AJ, Faulkner LR (2001) Electrochemical methods, fundamentals and applications. Wiley, New York
29. Paes de Sousa PM, Pauleta SR, Simões Gonçalves ML, Pettigrew GW, Moura I, Correia dos Santos MM, Moura JJG (2007) J Biol Inorg Chem 12:691–698
30. Kakihana M, Ikeuchi H, Satô GP, Tokuda K (1980) J Electroanal Chem 108:381–383
31. Bradley AL, Chobot SE, Arciero DM, Hooper AB, Elliott SJ (2004) J Biol Chem 279:13297–13300
32. Villalain J, Moura I, Liu MC, Payne WJ, LeGall J, Xavier AV, Moura JJG (1984) Eur J Biochem 141:305–312
33. Armstrong FA, Cox PA, Hill HAO, Lowe VJ, Oliver BN (1987) J Electroanal Chem 217:331–366
34. Correia dos Santos MM, Paes de Sousa PM, Simões Gonçalves ML, Lopes H, Moura I, Moura JJG (1999) J Electroanal Chem 464:76–84
35. Leitch FA, Moore GR, Pettigrew GW (1984) Biochemistry 23:1831–1838
36. Lopes H, Besson S, Moura I, Moura JJG (2001) J Biol Inorg Chem 6:55–62
37. Chen CJ, Liu CC, Savinell RF (1993) J Electroanal Chem 348:317–338
38. Limoges B, Moiroux J, Savéant JM (2002) J Electroanal Chem 521:1–7

0090-9556/11/3910-1939–1945$25.00
Drug Metabolism and Disposition
Vol. 39, No. 10
40873/3713551
DMD 39:1939–1945, 2011
Printed in U.S.A.

Characterization and Crystallization of Mouse Aldehyde Oxidase 3: From Mouse Liver to *Escherichia coli* Heterologous Protein Expression

Martin Mahro, Catarina Coelho, José Trincão, David Rodrigues, Mineko Terao, Enrico Garattini, Miguel Saggu, Friedhelm Lendzian, Peter Hildebrandt, Maria João Romão, and Silke Leimkühler

Institut für Biochemie and Biologie, Universität Potsdam, Potsdam, Germany (M.M., S.L.); Requimte, Departamento de Química, Faculdade de Ciências e Tecnologia, Universidade Nova de Lisboa, Caparica, Portugal (C.C., J.T., D.R., M.J.R.); Laboratori Biologia Molecolare, Dipartimenti Biochimica e Farmacologia Molecolare*, Istituto di Ricerche Farmacologiche Mario Negri, Milano, Italy (M.T., E.G.); and Institut für Chemie, Technische Universität Berlin, Berlin, Germany (M.S., F.L., P.H.)*

Received May 25, 2011; accepted June 24, 2011

ABSTRACT:

Aldehyde oxidase (AOX) is characterized by a broad substrate specificity, oxidizing aromatic azaheterocycles, such as *N*^{1}-methylnicotinamide and *N*-methylphthalazinium, or aldehydes, such as benzaldehyde, retinal, and vanillin. In the past decade, AOX has been recognized increasingly to play an important role in the metabolism of drugs through its complex cofactor content, tissue distribution, and substrate recognition. In humans, only one AOX gene (*AOX1*) is present, but in mouse and other mammals different AOX homologs were identified. The multiple AOX isoforms are expressed tissue-specifically in different organisms, and it is believed that they recognize distinct substrates and carry out different physiological tasks. AOX is a dimer with a molecular mass of approximately 300 kDa, and each subunit of the homodimeric enzyme contains four different cofactors: the molybdenum cofactor, two distinct [2Fe-2S] clusters, and one FAD. We purified the AOX homolog from mouse liver (mAOX3) and established a system for the heterologous expression of mAOX3 in *Escherichia coli*. The purified enzymes were compared. Both proteins show the same characteristics and catalytic properties, with the difference that the recombinant protein was expressed and purified in a 30% active form, whereas the native protein is 100% active. Spectroscopic characterization showed that FeSII is not assembled completely in mAOX3. In addition, both proteins were crystallized. The best crystals were from native mAOX3 and diffracted beyond 2.9 Å. The crystals belong to space group P1, and two dimers are present in the unit cell.

Introduction

Aldehyde oxidase (AOX) is a complex molybdoflavoprotein that belongs to a family of structurally related molybdoenzymes that bind the molybdenum cofactor (Moco) (Hille, 1996). AOX is homologous to xanthine oxidoreductase (XOR), another mammalian molybdoflavoenzyme, and both AOX and XOR show a remarkable degree of sequence similarity (Krenitsky, 1978; Garattini et al., 2003). AOX is active as a homodimer, and each 150-kDa monomer consists of three separate domains that bind different cofactors: the 20-kDa N-terminal domain binds two distinct [2Fe-2S] clusters, the 40-kDa central domain binds the FAD cofactor, and the 80-kDa C-terminal domain binds Moco (Garattini et al., 2008). Moco-containing enzymes are divided further into three different families, the xanthine oxidase (XO) family, the sulfite oxidase family, and the dimethyl sulfoxide reductase family, which are classified in accordance to the ligands at the molybdenum active site (Hille, 1996).

Members of the XOR family are characterized by an equatorial sulfur ligand at the Moco that is essential for enzyme activity (Wahl and Rajagopalan, 1982). Given the similarities in the overall structures and subunit composition of AOX and XOR, the properties of the two enzymes are related closely. Both enzymes are present in the cytosol and are found in all vertebrates (Garattini et al., 2003). However, the primary difference is that XOR can exist in two interconvertible forms, XO and xanthine dehydrogenase (XDH) (Nishino et al., 2008), whereas AOX solely exists in the oxidase form. AOX uses only molecular oxygen as the electron acceptor, in contrast to

This work was supported by the Cluster of Excellence "Unifying Concepts in Catalysis" coordinated by the Technische Universität Berlin; and Fundação para a Ciência e Tecnologia, Portugal [Grant SFRH/BD/37948/2007] (to C.C.) and Project [PTDC/QUI/64733/2006]. The exchange of researchers among laboratories involved in the work was funded by the Deutscher Akademischer Austauschdienst Programm-GRICES program.

M.M. and C.C. contributed equally to this work.

Article, publication date, and citation information can be found at http://dmd.aspetjournals.org.

doi:10.1124/dmd.111.040873.

ABBREVIATIONS: AOX, aldehyde oxidase; Moco, molybdenum cofactor; XOR, xanthine oxidoreductase; XO, xanthine oxidase; XDH, xanthine dehydrogenase; MCSF, Moco sulfurase; mAOX, mouse aldehyde oxidase; mMCSF, mouse Moco sulfurase; Ni-NTA, nickel-nitrilotriacetic acid; PAGE, polyacrylamide gel electrophoresis; DCPIP, 2,6-dichlorophenolindophenol; ICP-MS, inductively coupled plasma mass spectrometry; CD, circular dichroism; ESRF, European Synchrotron Radiation Facility.

XOR, which transfers electrons to NAD^+ and oxygen in the XDH and XO forms, respectively. It is notable that the substrate and inhibitor specificities of XOR and AOX are different, and, in general, AOX has the ability to oxidize a broader range of substrates than XOR (Krenitsky et al., 1972). Typical substrates for AOX are compounds containing an aldehyde function, nitro/nitroso compounds, or *N*-heterocycles (Pryde et al., 2010). The biochemical and physiological functions of AOX in humans are still largely obscure. Single monogenic deficits for any AOX have not been described so far in mammalia; however, AOX is not essential for humans because genetic deficiencies in the Moco sulfurase (MCSF) gene are not associated with pathophysiological consequences. The ability of AOX to oxidize *N*-heterocycles makes it an important enzyme in the metabolism of drugs and xenobiotics (Pryde et al., 2010). In animals, AOX is likely to detoxify exogenously derived nonphysiological compounds of wide structural diversity, and it is believed that the absence of AOX leads to symptoms under unusual circumstances of high intake of such xenobiotics. In humans, only one gene for AOX exists, whereas in mice and other mammals different homologs of AOX were identified (Garattini et al., 2003). Because the identified proteins are highly homologous with the originally known AOX (named AOX1, the first vertebrate AOX identified and characterized), the three related proteins are known currently as AOX3, AOX4, and AOX3L1 (formerly AOH1, AOH2, and AOH3, respectively) (Garattini et al., 2003; Terao et al., 2006; Garattini and Terao, 2011). These multiple AOX isoforms are expressed tissue-specifically in different organisms, but their existence and expression pattern vary in different animal species (Garattini et al., 2003; Terao et al., 2006). It is believed that the various AOX isoforms recognize distinct substrates and carry out different physiological tasks.

The best studied AOX homologs are the ones identified in mouse. The tissue distribution of mouse AOX3 (mAOX3) is superimposable to that of mAOX1, and the two enzymes are synthesized predominantly in hepatic, lung, and testicular tissues (Vila et al., 2004). Therefore, comparison of the enzymatic properties of mAOX3 and mAOX1 is particularly relevant but so far has been very difficult (Terao et al., 2001).

In this study, we established a reproducible system for the expression of mAOX3 in *Escherichia coli* in a 30% functional form. The recombinant protein was compared in detail with the native protein purified from mouse liver as to its kinetic and spectroscopic properties. It was shown that both proteins had similar properties, although in comparison to mAOX1 the FeSII saturation was lower. The heterologous expression system for mAOX3 provided us with enough material to perform broad crystallization screenings. The vast majority of the crystallization trials were performed using the recombinant protein, and the crystallization conditions obtained were used to reproduce crystals using the native mAOX3 protein purified from mouse livers. We were able to obtain a usable dataset to a resolution of 2.9 Å with native mAOX3 crystals.

Materials and Methods

Bacterial Strains, Plasmids, and Growth Conditions. *E. coli* TP1000 (Δ*mobAB*) (Palmer et al., 1996) cells were used for the coexpression of wild-type mAOX3 with mouse MCSF (mMCSF) (pSS110) (Schumann et al., 2009). *E. coli* expression cultures were grown in Luria-Bertani medium under aerobic conditions at 30°C for 24 h.

Cloning and Expression. The cDNA of mAOX3 was cloned from mouse CD1 liver (Vila et al., 2004) using primers designed to permit cloning into the NdeI and SalI sites of the expression vector pTrcHis (Temple et al., 2000). The resulting plasmid was designated pMMA1 and expresses mAOX3 as an N-terminal fusion protein with a His_6 tag. For heterologous expression in *E. coli*, pMMA1 and pSS110 (Schumann et al., 2009) were transformed into TP1000 cells. To express the recombinant proteins, cells were grown at 30°C in 14 liters of Luria-Bertani medium supplemented with 150 μg/ml ampicillin, 50 μg/ml chloramphenicol, 1 mM molybdate, and 10 M isopropyl β-D-thiogalactoside.

Purification of Recombinant mAOX3. After 24 h of expression at 30°C and low aeration, the cells were harvested by centrifugation and resuspended in 50 mM sodium phosphate buffer (pH 8.0) and 300 mM NaCl. To disrupt the cells, a cell disruptor (TS Benchtop Series; Constant Systems, Northamptonshire, UK) was used at 12°C and 1.35 kbar in the presence of DNase I and lysozyme (1 mg/l). The cleared lysate was loaded onto a nickel-nitrilotriacetic acid (Ni-NTA) (QIAGEN, Valencia, CA) column using 0.2 ml of resin per liter of culture. Two washing steps were performed with 35 and 50 mM imidazole, and mAOX3 was eluted with 250 mM imidazole. Buffer was exchanged to 50 mM potassium phosphate (pH 7.8) and 0.1 mM EDTA, using PD10 columns (GE Healthcare, Chalfont St. Giles, Buckinghamshire, UK). To increase the activity of the enzyme, chemical sulfuration was performed under conditions similar to those reported previously (Massey and Edmondson, 1970; Wahl et al., 1982). The purified enzyme was incubated for 1 h with 500 μM sodium dithionite, 25 μM methyl viologen, and 2 mM sodium sulfide in an anaerobic chamber (Coy Lab Systems, Grass Lake, MI). After buffer exchange to 50 mM sodium phosphate (pH 8.0) and 300 mM NaCl, the protein sample was loaded onto a Superose 6 column (GE Healthcare), and fractions containing dimeric mAOX3 were combined and stored in 100 mM potassium phosphate (pH 7.4) at −80°C.

To cleave the N-terminal His_6 tag, the enzyme was incubated in 50 mM Tris-HCl (pH 8.0) and 1 mM EDTA at 4°C for 12 h. The thrombin cleavage site introduced by pTrcHis was used, and the 17 amino acid sequence containing the His_6 tag was cleaved after Arg17 (Temple et al., 2000). The protein was purified afterward by size exclusion chromatography using a HiLoad 26/60 Superdex 200 column (GE Healthcare) equilibrated with 50 mM sodium phosphate (pH 8.0) and 300 mM NaCl. The fractions containing the dimeric His_6-mAOX3 were combined and concentrated by ultrafiltration (Amicon 50-kDa molecular weight cut-off; Millipore Corporation, Billerica, MA) to a final concentration of 17.8 mg/ml. Protein aliquots were frozen in liquid nitrogen and stored at −80°C until usage, without loss of activity.

Purification of Native mAOX3. Native mAOX3 was purified following the protocol described by Terao et al. (2001). One hundred CD1 mouse livers were homogenized in three volumes of sodium phosphate buffer (pH 7.5) with an Ultra-Turrax (Omni 2000; Omni International, Kennesaw, GA), and the cleared lysate was heated to 55°C for 10 min. After ammonium sulfate precipitation overnight (50% saturation), the pellet was resuspended and subjected to benzamidine Sepharose chromatography (GE Healthcare, Munich, Germany). The protein was purified further using a linear NaCl gradient on a 5/5 FPLC Mono Q column (GE Healthcare).

SDS-Polyacrylamide Gel Electrophoresis. SDS-polyacrylamide gel electrophoresis (PAGE) was performed as described by Laemmli (Laemmli UK, 1970) using 10% polyacrylamide gels. The gels were stained with Coomassie Brilliant Blue R (Sigma, Munich, Germany). The mAOX3 activity was visualized on native polyacrylamide gels by staining with 25 mM benzaldehyde and 1 mM 3-(4,5-dimethylthiazol-2-yl)-2,5-diphenyltetrazolium in 50 mM Tris (pH 8.0) (Pérez-Vicente et al., 1992).

Enzyme Assays. Enzyme assays were performed at 37°C in 50 mM Tris-HCl (pH 8.0) and 1 mM EDTA with variable substrate (0–250 μM benzaldehyde, 0–10 mM butyraldehyde, and 0–500 μM 2-OH-pyrimidine) and purified mAOX3 (50–200 nM) concentrations. As electron acceptors, 100 μM 2,6-dichlorophenolindophenol (DCPIP) or 1 mM potassium ferricyanide were used in a final reaction volume of 500 μl. Enzyme activity was monitored at 600 nm for DCPIP and 420 nm for ferricyanide. Specific activity was calculated using the molecular extinction coefficient of 21,400 M^{-1} cm^{-1} for mAOX3. Kinetic parameters were obtained by nonlinear fitting of the Michaelis-Menten equation or the substrate inhibition equation using R, build 2.12.00 (R Development Core Team, 2010).

Metal Analysis by Inductively Coupled Plasma Mass Spectrometry. The molybdenum and iron contents were determined using inductively coupled plasma mass spectrometry (ICP-MS) (PE SCIEX ELAN6000; PerkinElmer Life and Analytical Sciences, Waltham, MA). Samples of 500 μl containing 5 μM protein were wet-ashed with 32.5% nitric acid at 100°C overnight. Three hundred microliters of the wet-ashed sample was diluted with water into 5 ml,

and metal presence was quantified by ICP-MS using a multielement standard solution (XVI; Merck, Darmstadt, Germany) and an internal yttrium standard.

FAD Analysis by High-Performance Liquid Chromatography. FAD was determined by the AMP content after the hydrolysis of 20 μM mAOX3 in 5% sulfuric acid for 10 min at 95°C. Released AMP was detected on a C18 reversed-phase column as reported previously (Schmitz et al., 2008) and quantified against a FAD standard.

Circular Dichroism Spectroscopy. UV/visible circular dichroism (CD) spectra of 8 M enzyme samples were recorded in 50 mM potassium phosphate (pH 7.8) and 0.1 mM EDTA, using a CD spectrophotometer (J-715; Jasco, Tokyo, Japan). The scanning mode was set stepwise, for each nanometer a data pitch was recorded with a response time of 2 s, and each measurement was repeated four times.

EPR Spectroscopy. The 9.5-GHz X-band EPR spectra were recorded on an ESP300E spectrometer (Bruker, Newark, DE) equipped with a TE_{102} microwave cavity (Bruker, Madison, WI). For temperature control between 5 and 300 K, a helium flow cryostat (ESR 900; Oxford Instruments, Oxfordshire, UK) with a temperature controller (ITC4; Oxford Instruments) was used. The microwave frequency was detected with a frequency counter (EIP Microwave Inc., San Jose, CA). The magnetic field was calibrated using a Li/LiF standard with a known g value of 2.002293 ± 0.000002 (Stesmans and Van Gorp, 1989). Samples (typically 0.1 mM enzyme) were prepared in quartz tubes with an outer diameter of 4 mm. Chemical reduction to generate the reduced Fe(II)/Fe(III) form of the FeS clusters was performed by adding a small volume of anaerobic sodium dithionite solution to the protein solution under a weak stream of argon gas (20-fold excess dithionite with respect to the protein). The sample tubes were frozen in liquid nitrogen after a color change was observed (typically a reaction time of 30 s). Baseline corrections, if required, were performed by subtracting a background spectrum, obtained under the same experimental conditions, from the spectrum of a sample containing only a buffer solution. Simulations of the experimental EPR spectra, based on a spin Hamilton operator approach, were performed with the program *EasySpin* (Stoll and Schweiger, 2006).

Crystallization. Initial crystallization studies were pursued with the purified recombinant mAOX3. Several additives as well as some known mAOX3 inhibitors (e.g., menadione) were tested to optimize the crystals. Ionic liquids (butylmethylimidazolium chloride and 1-butyl-3-methylimidazolium diethyleneglycolmonomethylethersulfate) also were tested as additives, because, in a similar case of crystal optimization, this proved to be a very attractive alternative (Coelho et al., 2010). The best protein needles of recombinant mAOX3 were obtained in the following conditions: 12 to 16% polyethylene glycol 8000, 0.1 M potassium phosphate (pH 7.0), equal amounts of protein (17.8 mg/ml, incubated with fresh dithiothreitol at 4°C for 1 h), and precipitant solutions at 20°C (Fig. 1a). Because His tags usually have little effect on the protein native structure but can have an impact in crystallization (Carson et al., 2007), the recombinant protein His_6 tag (with 17 residues) was cleaved. With this protein preparation, crystals also were formed under similar conditions but without significant improvement.

Similar crystallization conditions were tested for mouse liver mAOX3: buffer pH was adjusted to 6.5, protein concentration was decreased to 10 mg/ml, and 2 mM EDTA was added to the crystallization solution. Larger, rectangular crystals (0.40 × 0.15 × 0.05 mm; Fig. 1b) of the native mAOX3 were formed reproducibly. These were the only crystals that allowed collection of a usable diffraction data set.

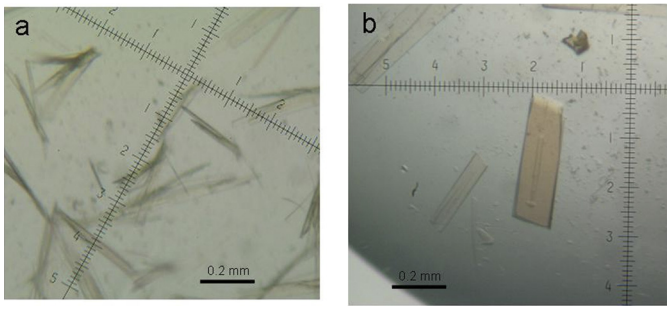

FIG. 1. Crystals of mAOX3 protein: needles from the recombinant protein (a) and crystals from native mouse liver protein (b).

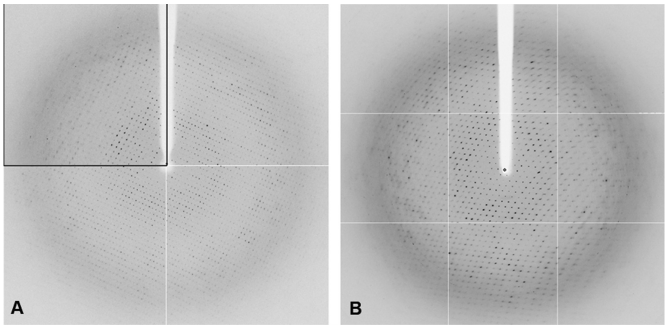

FIG. 2. Diffraction pattern of the native mAOX3 protein obtained at ID14-1 (A) before (top left quadrant) and after reannealing and at ID23-1 (ESRF) (B). The resolution at the edge is 3.0 Å in both images.

Data Collection, Processing, and Structure Solution. All of the tested crystals were flash-cooled directly in liquid nitrogen, using Paratone oil (Hampton Research, Aliso Viejo, CA) as cryoprotectant. Some of the native mAOX3 crystals diffracted to 6 Å, but after being annealed, diffraction improved dramatically to a resolution beyond 3 Å (Fig. 2). A first data set (mNAT-I) consisting of 180° of data were collected at ID14-1 at the European Synchrotron Radiation Facility (ESRF) (Grenoble, France) (Table 1). The crystal belonged to space group P1, with unit cell dimensions a = 91.07 Å, b = 135.02 Å, c = 147.48 Å, α = 78.27°, β = 77.77°, and γ = 89.96°. The calculated Matthews coefficient was 2.89 $Å^3$ Da^{-1}, corresponding to two dimers in the unit cell with a solvent content of 57.4% (Matthews, 1968). Because the data were very anisotropic and the mosaicity was high, the initial data processing using iMosflm 1.0.4 was incomplete (~89% complete to 2.9 Å) (Leslie, 1992). The same crystal was measured later at ID23-1 at the ESRF. Although a full 360° of data were collected, only approximately 220° were useable (mNAT-II), because the crystal was very anisotropic. The two data sets were merged to increase the completeness and improve the multiplicity. The resulting data set presents very high precision-indicating merging R factor (as expected) and is only ~80% complete to 2.9 Å (mNAT), but the overall redundancy improved to ~3.0. The structure of the mAOX3 will be solved by molecular replacement using BALBES on the mNAT-I data set (Long et al., 2008) in the future. The bovine milk XDH structure (Protein Data Bank code 3BDJ) can be used as a search model (Okamoto et al., 2008), and four monomers were found in the unit cell.

Results and Discussion

Comparison of Recombinant mAOX3 Expressed in *E. coli* with the Native Protein Purified from Mouse Livers. Several heterologous expression systems for mammalian AOX have been described. So far, a main drawback of these systems is the low catalytic activity of the purified enzymes due to the low Moco content or reduced content of the terminal Mo=S ligand at the Mo site (Huang et al., 1999; Adachi et al., 2007). In a previous report, we described successful purification of mAOX1 in an active form, after simultaneous expression of mAOX1 and mMCSF in *E. coli* TP1000 cells (Schumann et al., 2009). This approach ensured a higher level of sulfurated Moco insertion into the enzyme and resulted in a 20% active enzyme that could be purified in a reproducible manner. We adapted this system for the expression of mAOX3. Comparison of the activity of mAOX3 after expression in the presence or absence of mMCSF showed that the content of the terminal sulfur ligand was increased by 19% in the presence of mMCSF (M. Mahro and S. Leimkühler, unpublished observations). Thus, we have used this system for the expression of catalytically active recombinant mAOX3.

Recombinant mAOX3 was purified from 14 liters of *E. coli* culture using sequential Ni-NTA chromatography and size exclusion chromatography. In addition, a chemical sulfuration step was performed to

TABLE 1

X-ray crystallography data collection statistics

Values in parentheses correspond to the highest resolution shell.

	Crystal Sample		
	mNAT-I	mNAT-II	mNAT (Merged)
X-ray source	ID 14-1	ID 23-2	
Crystal system	Triclinic	Triclinic	Triclinic
Unit-cell parameters (Å, °)			
a, *b*, *c*, Å	91.07, 135.02, 147.48	91.54, 135.83, 147.84,	
α, β, γ, °	78.27, 77.77, 89.96	78.22, 77.89, 89.97	
Maximum resolution, Å	2.9	3.2	3.0
Mosaicity, °	1.0	1.0	1.0
Molecules per asymmetric unit	4	4	4
Matthews coefficient, Å^3/Da	2.89	2.93	
Space group	P1	P1	P1
Wavelength, Å	0.934	0.975	
No. of observed reflections	219,268 (20,892)	223,954 (24,999)	338,761 (41,810)
No. of unique reflections	133,319 (16,784)	78,529 (10,857)	112,209 (16,428)
Resolution limits, Å	51.1–2.9	50.0–3.2	50 0.0–3.20
Redundancy	1.6 (1.2)	2.8 (2.2)	3.0 (2.5)
Completeness, %	89.8 (77.3)	69.5 (65.1)	81.8 (81.7)
R_{pim}, %	5.6 (14.0)	14.3 (68.9)	17.5 (63.4)
I/σ	9.6 (3.6)	6.3 (1.4)	7.0 (4.2)

further increase the activity of the enzyme 1.4-fold (Table 2). The purification protocol used for mAOX3 is summarized in Table 2. The overall purification of recombinant mAOX3 from the soluble fraction was more than 35.7-fold with a yield of 2.3%. The total yield was 0.8 mg of pure enzyme per liter of *E. coli* culture. For comparison, we also purified native mAOX3 from CD1 livers according to the protocol described by Terao et al. (2001).

SDS-PAGE performed under reducing conditions demonstrated the presence of one major band with a size of 150 kDa for both proteins after purification (Fig. 3). Under these experimental conditions, additional bands of minor intensity with sizes of 130, 80, 70, and 55 kDa that were not present in native mAOX3 were observed for the recombinant protein (Fig. 3). Electrospray mass spectrometry analysis revealed that these bands were degradation products of mAOX3 (data not shown). These degradation products were only detected after the incubation of the protein with β-mercaptoethanol. Both proteins were detectable as a single band in native PAGE visualized by activity staining or Coomassie Blue staining (Fig. 4). The recombinant protein has a slightly different migration behavior on polyacrylamide gels due to the presence of the N-terminal His_6 tag (2 kDa). Both native and recombinant mAOX3 eluted from size exclusion chromatography columns mainly at a size of 300 kDa, indicating a functional dimer as the main product of expression and purification (data not shown). The UV/visible spectra of both proteins are identical and display typical features of molybdoflavoenzymes (Fig. 5). The A_{280}/A_{444} ratio of 5.2 for the recombinant protein indicates the high purity of the enzyme. The proportion for the native enzyme was similar. The A_{444}/A_{550} absorbance ratio in the UV/visible spectrum was calculated to be 3.1 for the recombinant enzyme and 3.1 for the native enzyme, demonstrating that both proteins were saturated fully with FAD. In addition, the FAD content of both proteins was determined to be 100% by quantifying the AMP content of the protein. The molybdenum and iron contents were quantified by inductively coupled plasma optical emission spectroscopy (Table 3) and revealed levels for the recombinant mAOX3 of 58.0 ± 0.2% saturation for molybdenum and 57.6 ± 0.3% saturation for iron (with respect to the 2×[2Fe-2S] clusters). For the native mAOX3, the molybdenum saturation was determined to be 103.8 ± 0.2% and the iron saturation was determined to be 53.0 ± 0.6%. Thus, the overall metal content for both proteins is comparable but displays an incomplete saturation for both metals. The cyanolyzable sulfur was determined to be present to 33 ± 0.5% for recombinant mAOX3, whereas the native protein is expected to be fully sulfurated when the activities of the two enzymes are compared (see below).

Steady-State Kinetics of mAOX3 with Different Substrates. Apparent k_{cat} and K_M values were determined by the rate of $K_3[Fe(CN)_6]$ reduction at 420 nm and 25°C in 100 mM potassium phosphate buffer (pH 7.4) (Table 4). Initial rates were plotted against substrate concentrations and fitted nonlinearly to the Michaelis-Menten equation. As substrates, benzaldehyde, butyraldehyde, and 2-OH-pyrimidine were used, and the results were found to be similar to literature data (Vila et al., 2004). Kinetic parameters of native and

TABLE 2

Purification of recombinant mAOX3 after expression in E. coli TP1000 cells

Total protein was quantified with the Bradford assay (Bradford, 1976). The activity was measured by monitoring the decrease in absorption at 600 nm in the presence of 250 μM benzaldehyde and 100 μM DCPIP. Specific enzyme activity is defined as the oxidation of 1 μM benzaldehyde per minute and milligram of enzyme under the assay conditions.

Step	Volume	Total Protein	Benzaldehyde/DCPIP Activity			
			Total Activity	Specific Enzyme Activity	Yield	Fold Purification
	ml	*mg*	*IU*	*IU/mg*	*%*	
Crude extract	280	17,513	163.3	0.009	77	0.8
Cleared lysate	280	18,354	212.9	0.012	100	1.0
Flow-through	280	18,597	170.8	0.009	80	0.8
Ni-NTA	30.4	35	3.6	0.104	1.71	9.0
Chemical sulfuration	49.4	32	5.0	0.158	2.34	13.6
Superose 6	15.2	12	4.9	0.414	2.30	35.7

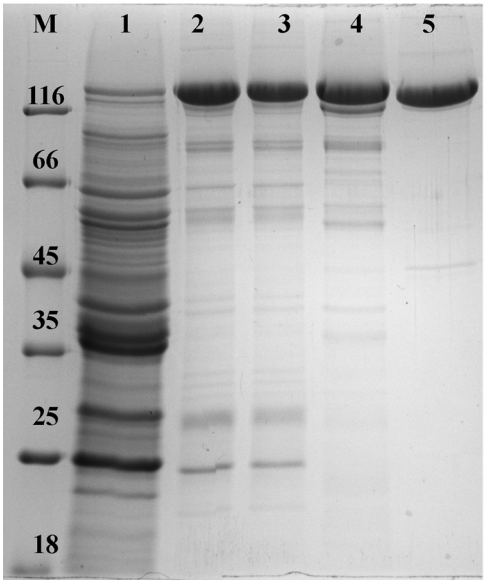

FIG. 3. A 12% SDS-PAGE analysis of mAOX3 purification after heterologous expression in *E. coli*. The protein was purified after Ni-NTA chromatography, a chemical sulfuration step, and Superose 6 chromatography. Purified mAOX1 displays a molecular mass of 150 kDa on SDS-PAGE, and the bands with molecular masses of 130, 80, 70, and 50 kDa correspond to degradation products of recombinant mAOX3, as determined by mass spectrometry. Lane 1, recombinant mAOX3 *E. coli* crude extract; lane 2, recombinant mAOX3 after Ni-NTA chromatography; lane 3, recombinant mAOX3 after chemical sulfuration; lane 4, recombinant mAOX3 after Superose 6 chromatography; lane 5, native mAOX3.

recombinant mAOX3 are in agreement considering that the activity of the recombinant enzyme is only 30% due to the limited saturation of the cyanolyzable sulfur ligand. The values reported in the literature are slightly different, probably due to different experimental conditions.

CD Spectroscopy. CD spectra of the air-oxidized forms were measured in the region from 250 to 850 nm. The spectra of the recombinant and native mAOX3 were found to be identical (Fig. 6). The spectra of the oxidized enzymes exhibited strong negative CD bands at approximately 350 to 400 nm and 520 to 580 nm and intensive

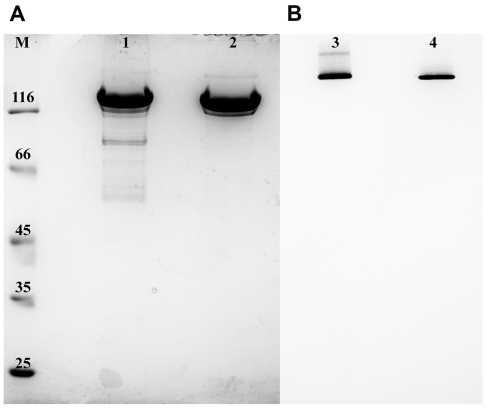

FIG. 4. Comparison of recombinant and native mAOX3 by SDS-PAGE and native PAGE. A, purified mAOX3 (2 μg per lane) was analyzed by 10% SDS-PAGE and stained by Coomassie Blue. Bands at molecular masses of 130, 80, 70, and 50 kDa were identified as degradation products by electrospray ionization mass spectrometry analysis. Lane 1, recombinant mAOX3; lane 2, native mAOX3. B, native PAGE of purified mAOX3 (2 μg per lane) was stained by activity staining with 25 mM benzaldehyde and 1 mM 3-(4,5-dimethylthiazol-2-yl)-2,5-diphenyltetrazolium as substrates. Lane 3, recombinant mAOX3; lane 4, native mAOX3. Recombinant mAOX3 has reduced gel mobility due to the N-terminal His_6 tag, which increases the molecular mass by approximately 2 kDa.

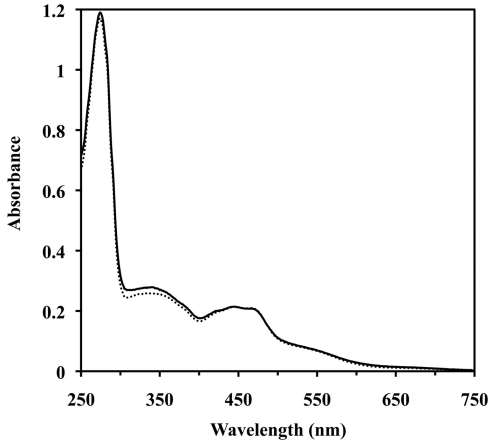

FIG. 5. Characterization of native and recombinant mAOX3 by UV/visible absorption spectroscopy. Spectra of air-oxidized recombinant mAOX3 (solid line) and native mAOX3 (dotted line) were recorded in 50 mM potassium phosphate (pH 7.4) under aerobic conditions. Recorded spectra were normalized to a concentration of 10 μM.

positive bands between 400 and 500 nm (Fig. 6). From the various maxima and inflections, transitions can be identified at 380 (−), 432 (+), 474 (+), and 552 (−) nm. The visible CD spectra of oxidized mAOX3 for the recombinant and the native protein are similar. There are differences in comparison to the CD spectrum obtained for mAOX1 (Schumann et al., 2009), especially in the region around 372 and 434 nm, indicating differences in the structure of FeSII.

EPR Spectroscopy of the mAOX3 [2Fe-2S] Clusters. Because the purified mAOX3 proteins showed a reduced level of iron, the [2Fe-2S] clusters were characterized by EPR spectroscopy. Figure 7 shows the EPR spectra of native and recombinant dithionite-reduced wild-type mAOX3 with the corresponding simulations. The spectra display signals from several superimposed paramagnetic species, which are usually observed for enzymes of the XO family. However, the most prominent signals are the characteristic EPR signals assigned to the two iron sulfur centers FeSI and FeSII, which are similar for all of the members of the XO family that have been described to date (Hille, 1996; Parschat et al., 2001). FeSI has EPR properties showing a rhombic g tensor similar to those of many other [2Fe-2S] proteins, being fully developed at relatively high temperatures (up to $T = 80$ K), whereas FeSII has unusual EPR properties for [2Fe-2S] species with a strongly rhombic g tensor, showing broad lines that can only be observed clearly at much lower temperatures ($T < 40$ K). The g values and line widths were evaluated by simulating the spectra using the program *EasySpin* (Stoll and Schweiger, 2006). In both proteins, FeSI has similar EPR properties, including the typical, rhombic g tensor as observed for the other [2Fe-2S] of the ferredoxin type (Table 5). The spectra indicate heterogeneities of FeSI, which can be seen especially for the g_x components. FeSII shows only weak signals in both mAOX3 preparations at lower temperatures, indicating incomplete saturation of FeSII for both recombinant and native mAOX3. How-

TABLE 3

Determination of the molybdenum and iron content for native and recombinant mAOX3

Molybdenum was quantified by ICP-MS, as described under *Materials and Methods*. Iron was determined by ICP-MS, as described under *Materials and Methods*.

mAOX3	Mo Content	Fe Content
	%	
Native	103 ± 0.2	53 ± 0.6
Recombinant	58 ± 0.2	57 ± 0.3

TABLE 4

Steady-state kinetic parameters of recombinant and native mAOX3, with different aldehyde and purine substrates

Apparent kinetic parameters were recorded in 100 mM potassium phosphate (pH 7.4) by varying the concentration of substrate in the presence of 1 mM ferricyanide as an electron acceptor.

	Native mAOX3		Recombinant mAOX3	
	k_{cat}	K_M	k_{cat}	K_M
	l/min	*μM*	*l/min*	*μM*
Benzaldehyde	130 ± 8	13 ± 6	44 ± 2	20 ± 6
Butyraldehyde	384 ± 40	29 ± 8	140 ± 10	26 ± 5
2-OH-pyrimidine	1279 ± 55	173 ± 18	413 ± 16	97 ± 11

ever, native mAOX3 displays a slightly higher amount of FeSII. Under the experimental conditions to reduce the proteins, no clear signals of the reduced flavin semiquinone (FAD) or Moco (Mo^V) were observed. The line widths and positions of the FeS signals at lower temperatures were affected by magnetic interactions. Due to the additional heterogeneities present in the samples, a reliable simulation of FeSII to determine the exact level of FeSII saturation in the enzymes was not possible. Therefore, we report only the *g* values for FeSI. The obtained *g* tensor and line width for FeSI of mAOX3 are almost identical to the values previously published for mAOX1 (Schumann et al., 2009), indicating the high structural similarity of the proteins as expected from the amino acid sequence identity of 61%.

Protein Crystallization, Data Collection, and Structure Solution. Expression and purification of recombinant mAOX3 was crucial for the crystallization and structure determination of the native protein. The vast majority of the crystallization trials were performed using the recombinant protein (Fig. 1A), overcoming the restrictions imposed by the limited amount of the native mouse protein available. Thus, it was possible to identify suitable crystallization conditions, which were applied successfully to the native protein purified from the mouse liver (Fig. 1B). In spite of the very difficult handling of the crystals and the fact that most of the crystals tested for diffraction did not yield measurable data, we were able to obtain a usable data set with a resolution of 2.9 Å at ID14-1 and ID23-1 at the ESRF (Fig. 2). With these data, the structure of mAOX3 can be solved by molecular replacement methods in the future using homologous XOR as a search model. The present work constitutes a major achievement because it will help to obtain the first crystal structure of AOX, an enzyme of well known importance in drug metabolism and therefore of increasing importance in recent drug design programs (Pryde et al., 2010). Furthermore, the crystal structure of mAOX3 will allow us to explain and understand the mechanistic and substrate specificity differences observed between AOX and XOR despite their remarkable similarity.

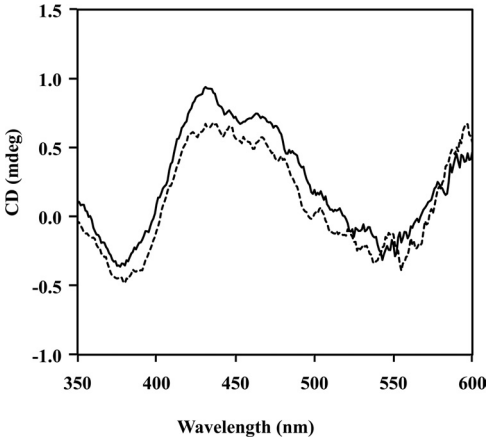

FIG. 6. CD spectra of native and recombinant mAOX3. Spectra recombinant mAOX3 (solid line) and native mAOX3 (dotted line) were recorded in 50 mM potassium phosphate (pH 7.8) and 0.1 mM EDTA at 10°C using a CD spectrometer. The protein concentration was 8 μM.

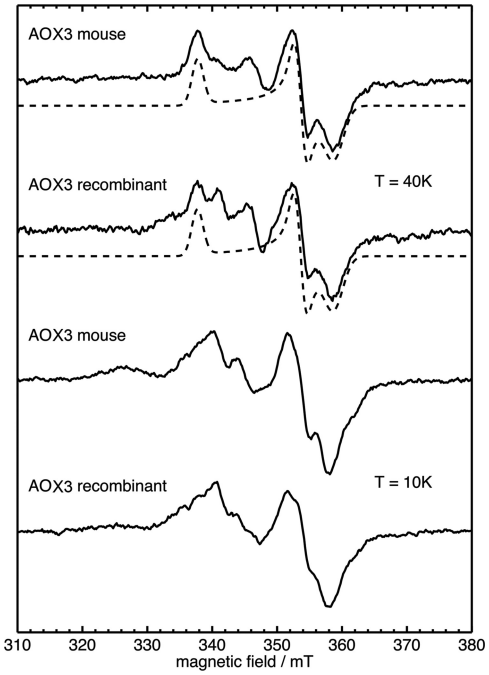

FIG. 7. EPR spectra of native and recombinant mAOX3. The figure shows the dithionite-reduced native mAOX3 (top spectrum) and recombinant mAOX3 (bottom spectrum) at temperatures of 40 and 10 K with the corresponding simulations (dashed traces). In both proteins, FeSI has similar EPR properties, showing a rhombic *g* tensor as observed for other [2Fe-2S] ferredoxins. FeSII shows only weak signals in mAOX3 at 10 K, whereas a slightly higher amount of FeSII is observed in native mAOX3.

Conclusions

We have reported a system for heterologous expression of mAOX3 in *E. coli*. To ensure a higher sulfuration level of mAOX3, we engineered *E. coli* for simultaneous expression of the mMCSF and mAOX3 proteins, as reported previously for mAOX1 (Schumann et al., 2009). After coexpression with mMCSF and chemical sulfuration, 30% of mAOX3 exists in the catalytically active form. The recombinant mAOX3 displays similar catalytic properties in comparison to those of the enzyme purified from mouse livers. This finding demonstrates that the protein was folded correctly in mMCSF-engineered *E. coli* cells and could be used for more detailed analyses. The recombinant enzyme displayed only 30% of the activity with benzaldehyde, butyraldehyde, or 2-OH-pyrimidine as substrates in comparison to that of the native enzyme, values that are consistent with its sulfuration level. Both recombinant and native mAOX3 were compared in detail on the basis of their spectroscopic properties. The EPR spectra of mAOX3 were found to be very similar to those from the mAOX1 protein, showing a rhombic signal for FeSI (Schumann et al., 2008). There are essentially no differences in the *g* values and line widths for the native and the recombinant enzymes. However, in particular, the FeSII center was not saturated fully in both enzymes, a finding that is consistent with the iron saturation of both enzymes. Because FeSII is the more surface exposed FeS cluster of the two, as revealed by the crystal structure of bovine XO/XDH, it might be possible that the cluster is partially lost during the purification of the enzymes. At least, the lower saturation of FeSII is not based on the inability of the *E. coli* system to insert the cluster correctly,

TABLE 5

EPR line widths and g values of FeSI and FeSII from mAOX3

The *g* strain was included in the simulation with 0.04 for g_x. *The g* strain was included in the simulation with 0.01 for g_z. Numbers in parentheses are estimated error of *g* values.

Sample	Cluster	*g* Value				Line Width
		g_x	g_y	g_z	g_{av}	
						mT
Native mAOX3	FeSI (40 K)	2.023 (0.005)	1.932	1.904 (0.015)	1.95	1.9
Recombinant mAOX3	FeSI (40 K)	2.023 (0.005)	1.932	1.904 (0.015)	1.95	1.9

because both enzymes display almost identical EPR spectra. Overall, the close similarity of the EPR parameters indicated the presence of the same ligands and similar geometries of the two redox centers in comparison to those of mAOX1. The recombinant enzyme was used to optimize the crystallization conditions for the native enzyme. We were able to obtain a usable data set at a resolution of 2.9 Å with crystals of native mAOX3. This is a major achievement for the characterization of AOX, an enzyme of well known importance in drug metabolism, and therefore of increasing importance in recent drug design programs.

In addition, the established expression system for mAOX3 in *E. coli* can be used further for detailed site-directed mutagenesis and structure-function studies of this enzyme.

Acknowledgments

We thank Manfred Nimtz (Helmholtz Center for Infection Research, Braunschweig, Germany) for matrix-assisted laser desorption ionization peptide mapping and the ID 14-1 ID23-2 staff at the ESRF for assistance during data collection.

Authorship Contributions

Participated in research design: Mahro, Coelho, Trincão, Rodriguez, Garattini, Lendzian, Romão, and Leimkühler.

Conducted experiments: Mahro, Coelho, Trincão, Rodriguez, Terao, and Saggu.

Contributed new reagents or analytic tools: Coelho.

Performed data analysis: Mahro, Coelho, Trincão, Saggu, Lendzian, and Leimkühler.

Wrote or contributed to the writing of the manuscript: Mahro, Coelho, Trincão, Garattini, Saggu, Lendzian, Hildebrandt, Romão, and Leimkühler.

References

Adachi M, Itoh K, Masubuchi A, Watanabe N, and Tanaka Y (2007) Construction and expression of mutant cDNAs responsible for genetic polymorphism in aldehyde oxidase in Donryu strain rats. *J Biochem Mol Biol* **40:**1021–1027.

Bradford MM (1976) A rapid and sensitive method for the quantitation of microgram quantities of protein utilizing the principle of protein-dye binding. *Anal Biochem* **72:**248–254.

Carson M, Johnson DH, McDonald H, Brouillette C, and Delucas LJ (2007) His-tag impact on structure. *Acta Crystallogr D Biol Crystallogr* **63:**295–301.

Coelho C, Trincão J, and Romão MJ (2010) The use of ionic liquids as crystallization additives allowed to overcome nanodrop scaling up problems: a success case for producing diffraction-quality crystals of nitrate reductase. *J Cryst Growth* **312:**714–719.

Garattini E and Terao M (2011) Increasing recognition of the importance of aldehyde oxidase in drug development and discovery. *Drug Metab Rev* doi:10.3109/03602532.2011.560606.

Garattini E, Fratelli M, and Terao M (2008) Mammalian aldehyde oxidases: genetics, evolution and biochemistry. *Cell Mol Life Sci* **65:**1019–1048.

Garattini E, Mendel R, Romão MJ, Wright R, and Terao M (2003) Mammalian molybdo-flavoenzymes, an expanding family of proteins: structure, genetics, regulation, function and pathophysiology. *Biochem J* **372:**15–32.

Hille R (1996) The Mononuclear Molybdenum Enzymes. *Chem Rev* **96:**2757–2816.

Huang DY, Furukawa A, and Ichikawa Y (1999) Molecular cloning of retinal oxidase/aldehyde oxidase cDNAs from rabbit and mouse livers and functional expression of recombinant mouse retinal oxidase cDNA in Escherichia coli. *Arch Biochem Biophys* **364:**264–272.

Krenitsky TA (1978) Aldehyde oxidase and xanthine oxidase–functional and evolutionary relationships. *Biochem Pharmacol* **27:**2763–2764.

Krenitsky TA, Neil SM, Elion GB, and Hitchings GH (1972) A comparison of the specificities of xanthine oxidase and aldehyde oxidase. *Arch Biochem Biophys* **150:**585–599.

Laemmli UK (1970) Cleavage of structural proteins during the assembly of the head of phage T4. *Nature* **227:**680–685.

Leslie AGW (1992) Recent changes to the MOSFLM package for processing film and image plate data. *Joint CCP4*ESF-EAMCB Newsletter on Protein Crystallography* **26**.

Long F, Vagin AA, Young P, and Murshudov GN (2008) BALBES: a molecular-replacement pipeline. *Acta Crystallogr D Biol Crystallogr* **64:**125–132.

Massey V and Edmondson D (1970) On the mechanism of inactivation of xanthine oxidase by cyanide. *J Biol Chem* **245:**6595–6598.

Matthews BW (1968) Solvent content of protein crystals. *J Mol Biol* **33:**491–497.

Nishino T, Okamoto K, Eger BT, Pai EF, and Nishino T (2008) Mammalian xanthine oxidoreductase - mechanism of transition from xanthine dehydrogenase to xanthine oxidase. *FEBS J* **275:**3278–3289.

Okamoto K, Eger BT, Nishino T, Pai EF, and Nishino T (2008) Mechanism of inhibition of xanthine oxidoreductase by allopurinol: crystal structure of reduced bovine milk xanthine oxidoreductase bound with oxipurinol. *Nucleosides Nucleotides Nucleic Acids* **27:**888–893.

Palmer T, Santini CL, Iobbi-Nivol C, Eaves DJ, Boxer DH, and Giordano G (1996) Involvement of the narJ and mob gene products in distinct steps in the biosynthesis of the molybdoenzyme nitrate reductase in Escherichia coli. *Mol Microbiol* **20:**875–884.

Parschat K, Canne C, Hüttermann J, Kappl R, and Fetzner S (2001) Xanthine dehydrogenase from Pseudomonas putida 86: specificity, oxidation-reduction potentials of its redox-active centers, and first EPR characterization. *Biochim Biophys Acta* **1544:**151–165.

Pérez-Vicente R, Alamillo JM, Cárdenas J, and Pineda M (1992) Purification and substrate inactivation of xanthine dehydrogenase from Chlamydomonas reinhardtii. *Biochim Biophys Acta* **1117:**159–166.

Pryde DC, Dalvie D, Hu Q, Jones P, Obach RS, and Tran TD (2010) Aldehyde oxidase: an enzyme of emerging importance in drug discovery. *J Med Chem* **53:**8441–8460.

R Development Core Team (2010) *R: A Language and Environment for Statistical Computing*, R Foundation for Statistical Computing, Vienna, Austria.

Schmitz J, Chowdhury MM, Hänzelmann P, Nimtz M, Lee EY, Schindelin H, and Leimkühler S (2008) The sulfurtransferase activity of Uba4 presents a link between ubiquitin-like protein conjugation and activation of sulfur carrier proteins. *Biochemistry* **47:**6479–6489.

Schumann S, Saggu M, Möller N, Anker SD, Lendzian F, Hildebrandt P, and Leimkühler S (2008) The mechanism of assembly and cofactor insertion into Rhodobacter capsulatus xanthine dehydrogenase. *J Biol Chem* **283:**16602–16611.

Schumann S, Terao M, Garattini E, Saggu M, Lendzian F, Hildebrandt P, and Leimkühler S (2009) Site directed mutagenesis of amino acid residues at the active site of mouse aldehyde oxidase AOX1. *PLoS One* **4:**e5348.

Stesmans A and Van Gorp G (1989) Novel method for accurate g measurements in electron-spin resonance. *Rev Sci Instrum* **60:**2949–2952.

Stoll S and Schweiger A (2006) EasySpin, a comprehensive software package for spectral simulation and analysis in EPR. *J Magn Reson* **178:**42–55.

Temple CA, Graf TN, and Rajagopalan KV (2000) Optimization of expression of human sulfite oxidase and its molybdenum domain. *Arch Biochem Biophys* **383:**281–287.

Terao M, Kurosaki M, Barzago MM, Varasano E, Boldetti A, Bastone A, Fratelli M, and Garattini E (2006) Avian and canine aldehyde oxidases. Novel insights into the biology and evolution of molybdo-flavoenzymes. *J Biol Chem* **281:**19748–19761.

Terao M, Kurosaki M, Marini M, Vanoni MA, Saltini G, Bonetto V, Bastone A, Federico C, Saccone S, Fanelli R, et al. (2001) Purification of the aldehyde oxidase homolog 1 (AOH1) protein and cloning of the AOH1 and aldehyde oxidase homolog 2 (AOH2) genes. Identification of a novel molybdo-flavoprotein gene cluster on mouse chromosome 1. *J Biol Chem* **276:**46347–46363.

Vila R, Kurosaki M, Barzago MM, Kolek M, Bastone A, Colombo L, Salmona M, Terao M, and Garattini E (2004) Regulation and biochemistry of mouse molybdo-flavoenzymes. The DBA/2 mouse is selectively deficient in the expression of aldehyde oxidase homologues 1 and 2 and represents a unique source for the purification and characterization of aldehyde oxidase. *J Biol Chem* **279:**8668–8683.

Wahl RC and Rajagopalan KV (1982) Evidence for the inorganic nature of the cyanolyzable sulfur of molybdenum hydroxylases. *J Biol Chem* **257:**1354–1359.

Wahl RC, Warner CK, Finnerty V, and Rajagopalan KV (1982) Drosophila melanogaster ma-l mutants are defective in the sulfuration of desulfo Mo hydroxylases. *J Biol Chem* **257:**3958–3962.

Address correspondence to: Prof. Dr. Silke Leimkühler, University of Potsdam, Institute of Biochemistry and Biology, Department of Molekular Enzymology, Karl-Liebknecht Str. 24-25, 14476 Potsdam, Germany. E-mail: sleim@uni-potsdam.de

Journal of Electroanalytical Chemistry 693 (2013) 105–113

Contents lists available at SciVerse ScienceDirect

Journal of Electroanalytical Chemistry

journal homepage: www.elsevier.com/locate/jelechem

Induced peroxidase activity of haem containing nitrate reductases revealed by protein film electrochemistry

Catarina Coelho [a], Jacopo Marangon [a], David Rodrigues [a], José J.G. Moura [a], Maria João Romão [a], Patrícia M. Paes de Sousa [a,*], Margarida M. Correia dos Santos [b,*]

[a] REQUIMTE/CQFB, Departamento de Química, Faculdade de Ciências e Tecnologia, Universidade Nova de Lisboa, 2829-516 Caparica, Portugal
[b] Centro de Química Estrutural, Instituto Superior Técnico, Av. Rovisco Pais, 1049-001 Lisboa, Portugal

ARTICLE INFO

Article history:
Received 2 September 2012
Received in revised form 17 January 2013
Accepted 24 January 2013
Available online 9 February 2013

Keywords:
Periplasmic nitrate reductase
Respiratory nitrate reductase
Direct voltammetry
Peroxidase activity

ABSTRACT

Direct voltammetry of adsorbed redox enzymes at pyrolytic graphite electrodes has shown to be very useful to probe the catalytic activity of several nitrate reductases in the presence of nitrate. In this work we demonstrated that in some cases an electrode-induced haem alteration leads to a loss of nitrate reductase activity.

Nitrate reductases are key enzymes in the biological nitrogen cycle. In particular, NapAB from *Cupriavidus necator* has an important role in the scavenging of nitrate and NarGHI from *Marinobacter hydrocarbonoclasticus* 617 is essential for the anaerobic respiration. These enzymes present haem groups among their redox centres, which are essential for the electron transfer from the reducing to the oxidising substrate. When adsorbed at graphite electrodes, both enzymes displayed a non-turnover signal corresponding to a one-electron redox process, with formal reduction potentials at pH 7.6 of −159 mV and −139 mV vs. SHE for Nap and Nar, respectively. Both enzymes displayed peroxidase activity at a potential close to that of the non-turnover response. Experiments with the whole enzymes and the haem free NapA from *Desulfovibrio desulfuricans* and NarGH from *M. hydrocarbonoclasticus* 617 were a valuable tool to get information about the cofactor undergoing electron transfer. We confirmed that this behaviour is related with the haems present in subunit B and subunit I of NapAB and NarGHI, respectively.

1. Introduction

Nitrate reductases (NRs) are key enzymes in the biological nitrogen cycle. They are responsible for reducing nitrate to nitrite in a two-electron (two-proton) redox process, with release of one water molecule, according to the reaction:

$$NO_3^- + 2H^+ + 2e^- \rightarrow NO_2^- + H_2O \qquad E^0 = +420\,mV\ vs.\ SHE$$

Prokaryotic nitrate reductases constitute a broad group of enzymes, belonging to the dimethyl sulfoxide (DMSO) reductase family of molybdenum-containing enzymes [1,2]. NRs can be classified according to their localization in the cell, function and molecular properties of the active site as periplasmic (Nap), respiratory (Nar) and assimilatory (Nas) nitrate reductases (Fig. 1).

In the case of Nap several functions have been proposed, such as dissipation of excess cellular reductant during growth on reduced carbon substrates and scavenging of nitrate [3]. Several crystal structures of periplasmic nitrate reductases have been reported in the past decade: the monomeric NapA from the sulphate reducing bacteria *Desulfovibrio desulfuricans* (*Dd*) ATCC 27774 [4]; the individual NapA subunit from *Escherichia coli* (*Ec*) [5]; and the heterodimeric NapAB complexes from *Rhodobacter sphaeroides* (*Rs*) [6] and *Cupriavidus necator* (*Cn*) [7]. With the exception of *Dd* NapA, the majority of periplasmic nitrate reductases consist of two different subunits (NapA and NapB), tightly bound in the case of *Cn* NapAB. The large catalytic subunit (NapA) contains the molybdenum active site cofactor, a molybdopterin guanine dinucleotide (MoCo), plus one [4Fe–4S] cluster. The MoCo is accessible through a funnel-like cavity coated with a few charged residues that favour the binding and orientation of charged substrate molecules. The small subunit (NapB) contains two *c*-type haems involved in electron transfer. The NapB haems are almost parallel to each other, with a Fe–Fe distance of approximately 10 Å. The nearest iron atom from the [4Fe–4S] center is 14 Å away from haem I.

The respiratory nitrate reductases (NarGHI) are membrane bound proteins with a central role in the anaerobic respiration, where the nitrate reduction is coupled with the generation of the proton motive force by protons translocation to the periplasm [8]. All Nars isolated so far are heterotrimeric enzymes constituted

* Corresponding authors. Tel.: +351 212948300x10957; fax: +351 212948550 (P.M. Paes de Sousa), tel.: +351 218419272; fax: +351 218464455 (M.M. Correia dos Santos).

E-mail addresses: patricia.sousa@fct.unl.pt (P.M. Paes de Sousa), mcsantos@ist.utl.pt (M.M. Correia dos Santos).

1572-6657/$ - see front matter © 2013 Elsevier B.V. All rights reserved.
http://dx.doi.org/10.1016/j.jelechem.2013.01.030

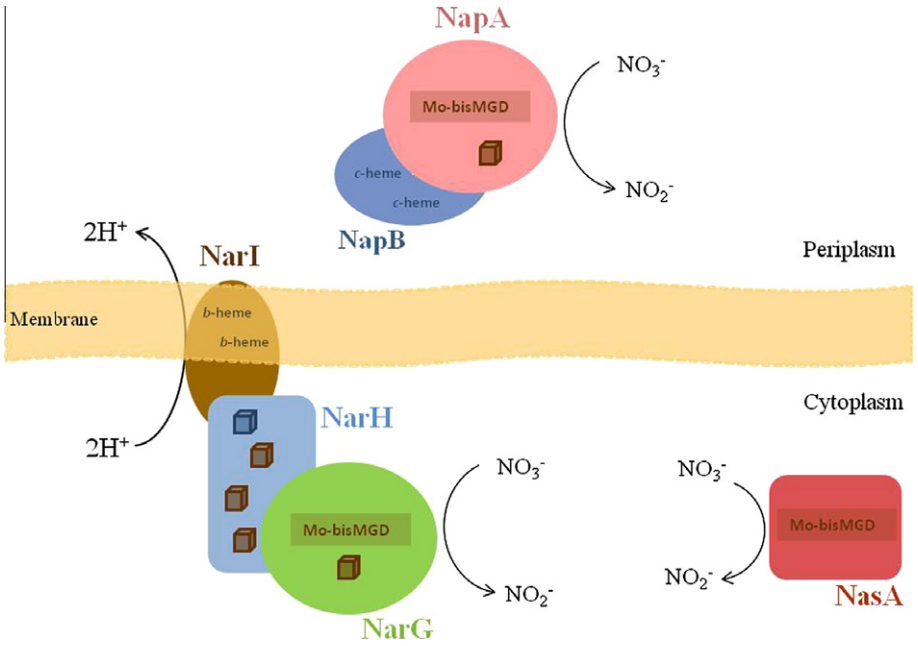

Fig. 1. Schematic representation of the localization of nitrate reductases in prokaryotic cells: NarGHI anchored to the membrane, NapAB in the periplasm, and Nas in the cytoplasm. The brown cubes represent the [4Fe–4S] centres and the blue cube the NarH [3Fe–4S] cluster. Nas is very diverse in terms of number and type of electron transfer centres for different organisms, and only NasA is represented. (For interpretation of the references to colour in this figure legend, the reader is referred to the web version of this article.)

by the subunits NarG (112–140 KDa), NarH (52–64 KDa) and NarI (19–25 KDa). The subunits NarG and NarH are located in the cytoplasm and are anchored to the membrane through the subunit NarI. The crystal structures available are for the oxidized form of the *Ec* NarGH [9] and *Ec* NarGHI [10]. The main subunit NarG hosts the MoCo and a [4Fe–4S] cluster designated as FeS0, and the NarH subunit contains one [3Fe–4S] (FeS4) and three [4Fe–4S] clusters (FeS1-3). The membrane subunit NarI contains two *b*-type haems termed b_P (proximal) and b_D (distal), which are involved in the quinolinic pool (MQH_2) oxidation and proton translocation across the membrane. A distance of 12–14 Å divides each redox cofactor allowing the electron transfer through the system.

Unlike spectroscopic techniques, dynamic electrochemical methods are not able to provide structural information. Yet, the use of voltammetric techniques is well proved nowadays in unravelling important aspects of the chemistry of metalloenzymes, allowing *in situ* measurements of the reduction potentials, together with the acquisition of information about relevant parameters of coupled reactions, including catalysis [11]. Most studies of direct electrochemistry of these molecules use the concept of protein film voltammetry (PFV) [12]. PFV involves a biocompatible adsorption of the protein onto the electrode surface, in such a way that a direct electrochemical communication between the enzyme and the electrode is established.

To date, several membrane-bounded (Nar) and periplasmic nitrate (Nap) reductases have been studied by direct electrochemistry, with the protein adsorbed onto an electrode: NarGH from *Paracoccus pantotrophus* (*Pp*) [13], NarGH from *Marinobacter hydrocarbonoclasticus* 617 (*Mh*) [14] and NarGHI *from E. coli* [15]; NapAB from *Pp* [16] and NapAB from *R. sphaeroides* [17]. The cytoplasmic assimilatory nitrate reductase NarB from *Synechococcus* sp. PCC 7942 was also studied using the same approach [18]. It was shown that these enzymes share a similar behaviour: non-turnover signals are never observed but in the presence of nitrate a cathodic catalytic current is always developed indicative of the electrocatalytic reduction of nitrate by the enzyme. As the electrode potential is taken more negative, catalytic activity for nitrate goes through a maximum at a given potential and then decreases and eventually levels off or, as is the case of *Mh* NarGH, a boost in activity (second sigmoidal component) is verified. The reason for these behaviours is still unclear and how unambiguous this is observed on the voltammetric waves may depend on nitrate concentration. Maximums are more clearly seen for low nitrate concentrations and they exist both in the forward and the reverse potential sweeps. For the homologous NapAB proteins from *P. pantotrophus* and *R. sphaeroides*, depending on the experimental conditions (pH and T) maximum catalytic activity occurs in the range of −100 to −200 mV [16,17,19–21]. It is difficult or not possible to relate the potential at the onset of catalysis with the redox potentials of the Mo cofactor. In the case of *Pp* NapAB these values are not known. For *Rs* NapAB the reduction potentials of the Mo cover a large potential range, −225 mV for Mo(IV)/Mo(V) and +550 mV for Mo(V)/Mo(VI) [6,22]. However, the observance of catalytic currents in the presence of nitrate indicates that electrons are flowing between the substrate and the electrode via the active site and so the electrocatalytic behaviour observed must be related with the redox chemistry of the MoCo. A similar behaviour was observed for *Ec* NarGHI, with the maximum of catalytic activity occurring at −25 mV while the reduction potentials of the couples Mo(V)/Mo(VI) and Mo(IV)/Mo(V) are +200 mV and +100 mV [15,23].

In this work we report a voltammetric study of two nitrate reductases, NapAB from *C. necator* and NarGHI from *M. hydrocarbonoclasticus* 617, formerly known as *Pseudomonas nautica* 617. The redox potentials of some of the metal cofactors of *Cn* NapAB were determined by spectrophotometric redox titrations, namely +50 mV for haem II (the more exposed haem), +160 mV for haem I and −15 mV for the [4Fe–4S] cluster [7]. The respiratory nitrate reductase (NarGHI) receives electrons from the oxidation of MQH_2 or UQH_2 [24]. The electrons are then transferred through the redox cofactors (b_D, b_P, FeS4, FeS3, FeS2, FeS1, FeS0, Mo-bis-MGD). The redox potentials of the cofactors are not known for *Mh* NarGHI, but they have been determined by UV–Vis- and EPR-mediated potentiometry in the case of the *E. coli* enzyme [23,25,26], which presents a high homology with *Mh* 617. The

Mo-bisMGD from *Ec* NarGHI presents midpoint potentials of +100 mV for the transition Mo(IV)/Mo(V) and +200 mV for the transition Mo(V)/Mo(VI). The midpoint potentials reported for the [4Fe–4S] clusters are −55 mV, +130 mV, −420 mV and −55 mV for centres FeS0, FeS1, FeS2, and FeS3, respectively. A value of +180 mV was estimated for the [3Fe–4S] cluster (FeS4) [23]. The haems b_P and b_D have midpoint potentials of +120 mV and +20 mV, respectively [26].

The electrochemical studies were done in non-turnover and turnover conditions and different strategies were used for promoting direct electron transfer. Electrocatalytic activity was never observed in the presence of nitrate. Unexpectedly, the enzymes displayed peroxidase activity. To probe the nature of this activity some direct electrochemical studies were performed using the haem free *Mh* NarGH and NapA from *D. desulfuricans*. The catalytic reduction of nitrate was only observed in the mediated voltammetry with methyl viologen as electron donor.

2. Materials and methods

2.1. Reagents

Poly-L-lysine hydrobromide (M_r 19 200) (PLL), neomycin, 4,4′-dipyridyl, and methyl viologen (MV) were obtained from Sigma, didodecyldimethylammonium bromide (DDAB) was from Aldrich and the ionic liquid 1-butyl-3-methylimidazolium chloride ([C_4mim] Cl^-) was from Fluka. *n*-Dodecyl β-D-maltoside (DDM) was purchased from Sigma–Aldrich (purity > 98%). All other chemicals were pro-analysis grade and solutions were prepared with Milli-Q water.

2.2. Protein purification

The periplasmic nitrate reductase NapAB from *C. necator* was expressed and purified as previously described [7]. The protein stock solutions were concentrated to 93 μM (determined by the BCA procedure from Sigma) in 10 mM Tris–HCl, pH 7.6, and stored in aliquots at −80 °C. Qualitative detection of NAP activity was performed after protein purification to ensure the presence of nitrate reductase activity, as previously described [27].

M. hydrocarbonoclasticus 617 was grown under denitrifying conditions in artificial seawater at 303 K with 10 mM nitrate as electron acceptor [28,29]. NarGHI was purified using DDM as detergent in order to release the heterotrimer from the membrane fraction as reported by Correia et al. [30]. The protein was dialyzed against 10 mM Tris–HCl pH 7.6 and the activity was monitored following the oxidation of the artificial donor methyl viologen at 604 nm (ε_{604} = 13.6 mM^{-1} cm^{-1}, Sigma) as reported by Craske and Ferguson [31]. Solutions of 72 μM of fully active *Mh* NarGHI were stored at −80 °C.

2.3. Procedure

Voltammetric measurements were performed using an Autolab PSGTAT10 potentiostat/galvanostat from ECO Chemie (Utrecht, The Netherlands). The system was controlled and data analyzed with the GPES software package from ECO Chemie. Scan rate (v) varied between 5 and 200 mV s^{-1}. Unless otherwise stated, catalytic assays were performed using the Methrom Stand VA 663 with an electrode rotation rate of 3000 rpm.

A three electrodes configuration cell was used, with a platinum auxiliary electrode, and an Ag/AgCl reference electrode (205 mV vs. standard hydrogen electrode, SHE). Throughout the paper, all potential values are referred to SHE. As working electrodes, graphite and gold disks were used. The latter (AuE) was from Metrohm (6.1204.020) with a nominal radius of 0.1 cm. The graphite electrodes were self-made basal plane pyrolytic graphite (PGE) with nominal radius of 0.2 cm or 0.15 cm (graphite from GE Quartz Europe, ref. ACSF01315), and a commercial ultra-trace graphite (UTGE) with nominal radius of 0.1 cm (Metrohm, ref. 6.1204.100).

The effective surface area of the electrodes were determined from their responses in a known concentration of the ferrocyanide/ferricyanide couple ($D = 7.84 \times 10^{-6}$ cm^2 s^{-1} [32]) and were found to be within 5% of the nominal area.

2.4. Electrode preparation

Before each experiment the electrodes were polished by hand on polishing cloth (Buehler 40-7212) using a water/alumina slurry (0.3 μm, Buehler 40-6365-006), sonicated for 1 min and then well rinsed with Milli-Q water. In most experiments, a 2 μl drop of working solution containing the protein (12–93 μM) was deposited on the electrode surface and left to dry at room temperature for 30 min while in others the electrode was dipped in the protein solution for 30 min and then left to dry. In some experiments, a membrane electrode configuration was prepared (either with AuE or PGE) using a negatively charged Spectra/Por MWCO 3500 dialysis membrane. Briefly, a 2–4 μl drop of the protein solution was deposited on a square piece (about twice the diameter of the electrode body) of the membrane, the electrode was pressed against the membrane and a rubber ring was fitted around the electrode body so that the entrapped solution formed a uniform thin layer.

The mediated catalysis of NapAB by methyl viologen was analysed both at graphite and gold membrane electrodes, with 100 or 200 μM MV in the electrolyte and the enzyme entrapped in the membrane. In the case of NarGHI, a graphite electrode and 250 μM MV were used.

2.5. Electrolyte and working solution

In typical experiments the supporting electrolyte, as well as the working solution, contained 10 mM Tris–HCl pH 7.6 and 0.1 M NaCl.

The working solution contained the protein and in some experiments the following promoters were also present: 0.1 mg/ml PLL, 0.4 M [C_4mim] Cl^-, 0.5 mM DDAB, 2 mM neomycin or 0.5 mM 4,4′-dipyridyl.

The effect of substrate concentration was analyzed varying nitrate concentration between 0.010 and 10 mM. In the experiments with hydrogen peroxide the final concentration varied between 0.05 and 0.50 mM.

Oxygen was removed from the electrolyte solutions by bubbling a constant nitrogen or argon stream directly in the solution for 20 min. The gas continued to flow on the top of the solution during all experiments in order to maintain anaerobic conditions. Some experiments were performed in an anaerobic glove box filled with Argon (O_2 < 1 ppm).

All measurements were performed at least in duplicate in a temperature-controlled room at 20 ± 1 °C.

3. Results

3.1. Cn NapAB in non-turnover conditions

The direct electrochemistry of *C. necator* NapAB was investigated at different electrodes either by PFV or with the enzyme entrapped in a dialysis membrane. Cyclic voltammetry was used in the potential range +160 to −600 mV and scan rates (v) varied between 5 and 200 mV s^{-1}.

With the enzyme immobilized onto the graphite electrodes (PGE or UTGE), the cyclic voltammograms (CVs) revealed the presence of one cathodic peak with an anodic counterpart (Fig. 2). Peak currents, i_p, varied linearly with v though without a null intercept. The separation between the cathodic, E_p^c, and the anodic, E_p^a, peak potentials ($\Delta E_p = E_p^c - E_p^a$) was never zero and increased with v. The peak widths at half-height, $\Delta E_{p,1/2}$ varied between 97.5 and 125 mV. This behaviour is consistent with a diffusionless one-electron quasireversible reaction [33]. However, given that the average $(E_p^c + E_p^a)/2$ remained almost constant for all scan rates, a formal reduction potential $E^{0\prime} = (E_p^c + E_p^a)/2 = -159 \pm 11$ mV could be estimated at pH 7.6.

The effect of several promoters on the voltammetric signal was tested. Neomycin and PLL are positively charged promoters typically used with graphite electrodes, which are negatively charged at pH 7.6 [34]. The ionic liquid (IL) [C_4mim] Cl^- (at 0.4 M) was important in the crystallization of *Cn* NapAB and therefore was also tested [35]. DDAB is a common surfactant used to facilitate electron transfer between redox proteins and electrodes [36].

No significant changes were observed in the CVs in the presence of any promoter, in particular the cathodic peak potentials remained constant within the experimental error, and equal to E_p^c in the absence of promoter (average value $E_p^c = -157 \pm 11$ mV for $v = 20$ mV s^{-1}). In the presence of the surfactant DDAB, the cathodic peak was shifted to more positive values ($E_p^c = -74$ mV for $v = 20$ mV s^{-1}).

In all situations, identical surface coverage areas, Γ, were estimated from the amount of charge consumed in the reduction process ($Q = (1.4 \pm 0.6) \times 10^{-7}$ C, in the case of the UTGE electrode) and the geometric areas of the electrodes (A), $\Gamma = Q/(nFA) = (5 \pm 2) \times 10^{-11}$ mol/cm^2. For monolayer coverage, this Γ value corresponds to an area "occupied" by each NapAB molecule of ca. 3×10^{-14} cm^2, equivalent to a circle of 20 Å diameter. The importance of this value will be discussed below.

The use of a membrane electrode configuration is an interesting strategy for electrochemical studies of redox enzymes ([37] and references there in). This configuration also enables the use of very small protein volumes (2 μl) and avoids the problems concerning diffusion, given that the entrapment of the proteins between the membrane and the electrode surface enables the achievement of thin layer conditions. The voltammetric behaviour of *Cn* NapAB was analysed following this approach at a graphite membrane electrode, but the results were very similar to those with the protein casted on the electrode surface.

With the AuE electrode no voltammetric signal was observed either with the enzyme immobilized on the electrode surface, in the absence or presence of any of the promoters (neomycin, 4,4′-dipyridyl, PLL or IL), or entrapped in the membrane electrode configuration.

3.2. Cn NapAB in turnover conditions

The catalytic activity of the *Cn* NapAB was investigated in the potential range +160 to −600 mV in the presence of increasing concentrations of potassium nitrate in the electrolyte solution.

Most experiments were performed with the enzyme immobilized either on the UTGE or the AuE electrodes, using a rotation rate of 3000 rpm, or on the PGE electrode using a magnetic stirrer in order to hydro dynamically control the substrate supply. Some assays were performed with the enzyme entrapped in a dialysis membrane and analysed from homogenized quiescent solutions. The effect of adding to the ionic medium the promoters previously referred was also tested. A reductive activation step was also tested applying a potential of −400 mV for 60 s prior to the voltammetric run. Moreover, *Cn* NapAB samples from different purification batches were used to ensure that the results were not dependent on protein preparation.

The addition of nitrate to the electrolyte in the range of 10 μM–10 mM caused no consistent alteration in the cyclic voltammograms. In some experiments with the graphite electrodes upon nitrate additions a catalytic wave developed at a potential close to that of the non-turnover signal. Once the solutions were well deaerated, no changes could be detected on the CVs. It was also observed that upon air or water additions a similar wave developed at the same potential (Fig. 3, black lines). Therefore, the appearance of this wave can only be attributed to the presence of dissolved oxygen in the nitrate solution.

Given that dissolved oxygen is readily reduced in the working potential range according to $O_2(g) + 2H^+ + 2e^- \Leftrightarrow H_2O_2$ and also the reported catalytic activity for oxygen and hydrogen peroxide by several peroxidases/catalases [38], increasing amounts of a well deaerated solution of hydrogen peroxide were added to the voltammetric cell with the enzyme immobilized at the UTPGE.

An increase in the cathodic peak current was always observed with increasing H_2O_2 concentrations in the range of 50–500 μM (Fig. 3, grey lines), and a half-wave potential of $E_{1/2} = -155 \pm 13$ mV was measured for the forward current. Given that direct reduction of hydrogen peroxide at the UTPGE was not detected in the potential range used, these results can only be interpreted in terms of a catalytic process. For each H_2O_2 concentration the catalytic current was measured at a fixed potential in the plateau ($E = -500$ mV) and the data fitted to a Lineweaver–Burk plot.

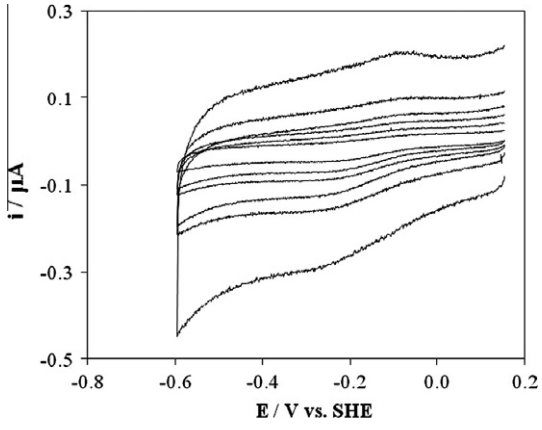

Fig. 2. Cyclic voltamogramms ($5 < v < 50$ mV s^{-1}) of 93 μM *Cupriavidus necator* NapAB adsorbed at a graphite electrode in 10 mM Tris–HCl pH 7.6 and 0.1 M NaCl.

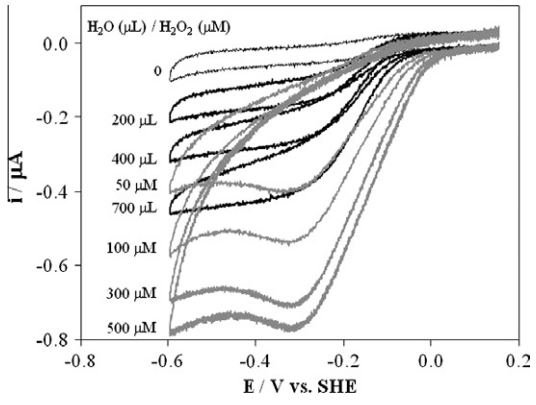

Fig. 3. Cyclic voltammograms ($v = 20$ mV s^{-1}, 3000 rpm) of 46.5 μM *Cupriavidus necator* NapAB adsorbed at a graphite electrode upon the addition of increasing aliquots of water (black lines) and in the presence of increasing concentrations of H_2O_2 (grey lines). Medium: 10 mM Tris–HCl pH 7.6 and 0.1 M NaCl.

A Michaelis–Menten constant K_M of (100 ± 20) μM and a maximum catalytic current i_{catmax} of $(7.4 \pm 0.5) \times 10^{-7}$ A were determined. Knowing the amount of enzyme adsorbed, the catalytic current was converted into the turnover number $k_{cat} = i_{catmax}/(nFA\Gamma) = (5 \pm 2)\ s^{-1}$.

Despite the absence of a non-turnover signal at the gold electrode, some experiments were performed in the presence of increasing amounts of nitrate, but the voltammograms remained featureless. No catalytic wave was developed in the presence of hydrogen peroxide. Only the direct reduction of H_2O_2 at the gold electrode was clearly observed, which occurs at a less negative potential than the one observed at the PG electrode in the same conditions.

3.3. Mh NarGHI in non-turnover and turnover conditions

The voltammetric behaviour of *Mh* NarGHI was analysed with the enzyme adsorbed at a rotating disk PG electrode for scan rates in the range $10 < v < 800$ mV/s. Neomycine was essential for the adsorption of the protein and the electrolyte was 10 mM Tris–HCl pH 7.6, 0.1 M NaCl, in all experiments. A single non-turnover signal, with a cathodic peak and the anodic counterpart, was observed in the range $+0.4\ V < E < -0.7$ V, corresponding to a quasi-reversible one-electron redox process (Fig. 4a). However, the average $(E_p^c + E_p^a)/2$ remained almost constant for all scan rates, allowing the determination of a formal reduction potential $E^{0'} = -139 \pm 10$ mV at pH 7.6. A surface coverage of 2×10^{-11} mol cm^{-2} was estimated from the amount of charge consumed.

This non-turnover signal could only be unequivocally identified for assays performed in strictly anaerobic conditions. Outside the glove box, with oxygen removed by purging the electrolyte with argon, the voltammograms presented only a cathodic peak that became sigmoidal in shape when the electrode was rotated (Fig. 4b). This behaviour can only be due to a catalytic response to traces of oxygen present in the electrolyte.

The addition of nitrate to the electrochemical cell (using a rotation rate of 2000 rpm) had no effect in the voltammograms, while a catalytic current developed when hydrogen peroxide was added (Fig. 4c), either inside or outside the glove box. A k_{cat} of 150 s^{-1} was estimated for the peroxidase activity of *Mh* NarGHI.

3.4. Mediated catalysis

The catalytic activity of Cn NapAB towards nitrate was tested by mediated enzyme electrochemistry, in the potential range of 0 to −700 mV, using methyl viologen in solution as cosubstrate. The UTGE was used with the enzyme entrapped in a membrane. Assays were performed maintaining the concentration of methyl viologen constant (100 or 200 μM) while varying the enzyme's concentration in the range 12–93 μM. In Fig. 5 the voltammograms in the absence and presence of nitrate are shown. MV showed a reversible electrochemical behaviour at the UTGE electrode with a formal reduction potential of $E^{0'} = -433$ mV. Upon nitrate addition, the change in shape and the half-wave potential of the sigmoidal wave, $E_{1/2} = -420$ mV confirms that the actual transfer process is the catalyzed reduction of methyl viologen by *Cn* NapAB. As can also be seen in Fig. 5, no catalytic wave was observed for potentials above −350 mV.

The variation of the catalytic current with the nitrate concentration could be well fitted to the Michaelis–Menten kinetics and an

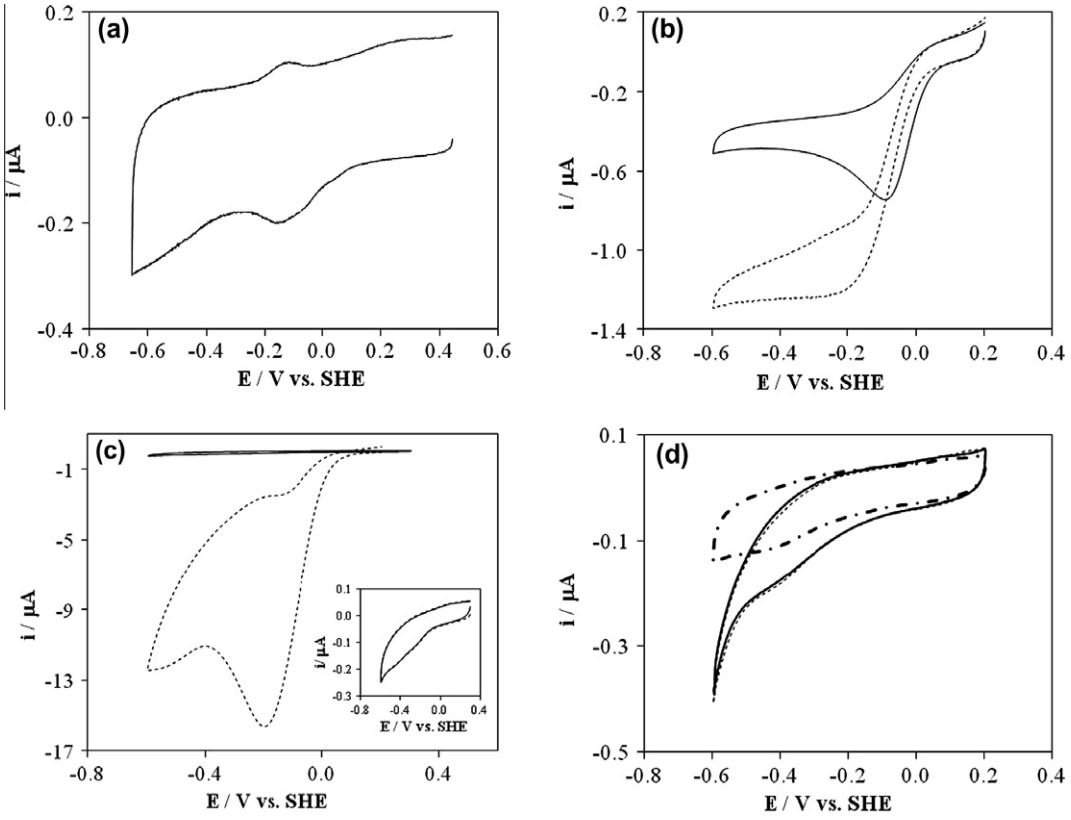

Fig. 4. Cyclic voltammograms (20 mV s^{-1}) of 65 μM *Mh* NarGHI adsorbed at a graphite electrode in 10 mM Tris–HCl pH 7.6 and 0.1 M NaCl, inside (a) and outside (b and c) a glove box. In (c) 500 μM H_2O_2 were present in the electrolyte (----); the response of NarGH in these conditions is also shown (—); a zoom of the response of NarGH in the absence (—) and presence (----) of 500 μM H_2O_2 is presented in the inset. In (d) the CVs are for 60 μM *Dd* NapA in the absence (-·-·-) and presence (—) of 500 μM H_2O_2; the voltammogram obtained in the presence of 500 μM H_2O_2 with no protein at the electrode is also shown (----).

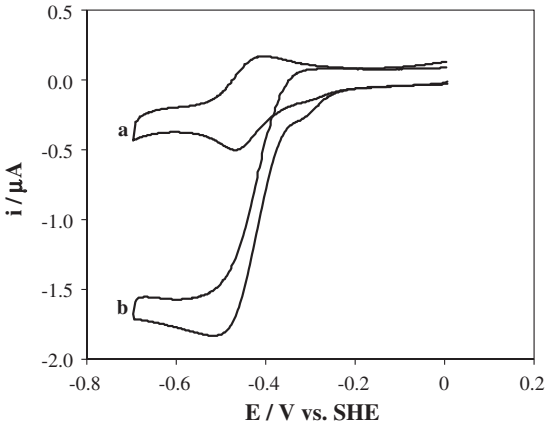

Fig. 5. Cyclic voltammograms ($v = 20\ mV\ s^{-1}$) of 200 μM methyl viologen (in 10 mM Tris–HCl pH 7.6 and 0.1 M NaCl) and 40 μM *Cupriavidus necator* NapAB at the UTGE membrane electrode in the absence (a) and presence (b) of 5 mM NO^{3-}.

apparent Michaelis constant $K_M = (88 \pm 15)$ μM was estimated. The second order rate constant for the intermolecular electron transfer between methyl viologen and *Cn* NapAB, *k*, was determined from the maximum catalytic current according to $i_{catmax} = nFAD^{1/2}C_{MV}C^{NapAB\,1/2}k^{1/2}$ [39,40]. The values obtained from the dependence of i_{catmax} on the concentration of enzyme or mediator were $2.6 \pm 0.3 \times 10^7\ M^{-1}\ s^{-1}$ and $2.1 \pm 0.2 \times 10^7\ M^{-1}\ s^{-1}$, respectively, therefore equivalent within the experimental error. A similar behaviour was observed for NarGHI. Just one set of conditions were tested (250 μM MV and 65 μm of enzyme), but a catalytic current unequivocally developed when nitrate was added (data not shown).

With the enzymes immobilized onto the graphite electrodes no catalytic current was observed in the presence of MV and nitrate.

The electrocatalytic reduction of *Cn* NapAB by MV was also observed at the AuE electrode in a membrane configuration but given that MV showed a quasireversible behaviour the data were not further analyzed.

4. Discussion

In this work the direct electrochemistry of *Cn* NapAB and *Mh* NarGHI in non-turnover and catalytic conditions was analysed at different electrode interfaces, using different configurations, in the absence and presence of several promoters and a mediator. The catalytic activity towards hydrogen peroxide was also investigated.

No voltammetric signals were observed either in non-turnover conditions or in the presence of nitrate, or hydrogen peroxide when a gold electrode was used. This was not the case with the graphite electrodes.

For *Cn* NapAB a clear voltammetric signal corresponding to a one-electron quasireversible reaction was observed at the PGE or UTGE. This signal was not affected by the presence of several promoters (neomycine, PLL, DDAB, IL). Similar redox potentials were observed and indistinguishable surface coverages, Γ, were obtained when the enzyme was incubated with the promoter and then immobilized onto the electrode surface. Additionally, the electric environment built up by the charge of the membrane, when the membrane electrode configuration was used, had no effect on the voltammetric behaviour of *Cn* NapAB. The redox potential of the process observed, $E^{0'} = -159$ mV at pH 7.6, does not correspond to any of the redox potentials of the metal cofactors determined for *Cn* NapAB, +50 mV for haem II, +160 mV for haem I and −15 mV for the [4Fe–4S] cluster [7]. In all conditions the voltammetric signal is insensitive to the presence of nitrate. However, in the presence of oxygen or hydrogen peroxide a negative catalytic current develops at a potential close to that of the non-turnover response, and therefore the two signals must correspond to the same redox process.

In the case of *Mh* NarGHI, a non-turnover signal with $E^{0'} = -139$ mV at pH 7.6 was observed. A catalytic wave develops both in the presence of oxygen and hydrogen peroxide at a potential that correlates with the non-turnover signal, with similar characteristics (potential and shape) to those observed for *Cn* NapAB. However, the electrocatalytic activities of *Mh* NarGHI were significantly higher than those observed for the *Cn* enzyme (for H_2O_2, k_{cat} was 150 s^{-1} and 5 s^{-1}, respectively).

There is no doubt that the nitrate reductases are responsible for the observed behaviour. Protein samples from different purification batches were used to ensure that the results were not dependent on protein purification. In the case of *Cn* NapAB the protein batch used for the voltammeric experiments was also used to obtain protein crystals that successfully allowed solving the crystal structure of the protein with bound substrates and inhibitors at 1.7 Å resolution (unpublished data), ruling out the influence of other proteins or impurities on the observed peroxidase activity.

Cn NapAB and *Mh* NarGHI proved to be active and thus competent to catalyze the reduction of nitrate when probed through the mediated catalysis by methyl viologen at the UTGE with the enzyme entrapped in a membrane. The K_M value for *Cn* NapAB value determined with UTGE electrode (88 μM) compares well with those reported for *P. pantotrophus* NapAB, measured by PFV ($K_M = 45$ μM) and spectrophotometric assays with methyl viologen ($K_M = 112$ μM) [16], as well as the one determined by PFV for *R. sphaeroides* NapAB ($K_M = 97$ μM) [41]. Equivalent second order rate constants were determined from the dependence of i_{catmax} with either the enzyme or MV concentration, thus showing that the catalytic response is limited by the reaction of the enzyme with the co-substrate [39,40].

The results here reported are rather different from those observed in the independent investigations by direct PFV of bacterial nitrate reductases reported so far for *Pp* NarGH [13], *Ec* NarGHI [15], *Mh* NarGH [14] *Se* NarB [18], *Pp* NapAB [16] and *Rs* NapAB [17].

The interaction between such complex molecules and the electrode surface can be tuned by many factors. Direct electron transfer between an electrode and an enzyme is often interpreted based on the proposal that the electrode is replacing the physiological redox partner, at the putative docking site, with the electrons flowing till the active site through the intramolecular electron transfer pathway [42]. So, for the homologous *Rs* and *Cn* NapAB (whose X-ray structures are both known) the site of entry of the electrons should be the exposed haem in subunit NapB, through a favourable interaction with the pyrolytic graphite electrode. The electron transfer subunits (NapB) share 52% sequence identity, and the electrostatic surface potential around the exposed haem is positive for both enzymes as shown in Fig. 6a and b [6,7]. Accordingly, similar discrete charge point interactions with the negatively charged PG electrode would be expected.

The catalytic subunits NapA share 71% sequence identity but in *Cn* NapAB the electrostatic surface potential around the solvent exposed-funnel is slightly more positive (Fig. 6c) than in the case of *Rs* NapAB (Fig. 6d). According to this, the interaction between the electrode and the region around the active site should be more favourable for *Cn* NapAB. However, the results reported for *Rs* NapAB point towards that the enzyme is interacting with the electrode through NapA subunit. Indeed, neomycin showed to improve the stability of the electrocatalytical signal of *Rs* NapAB at the negatively charged PG electrode [19]. Interactions between

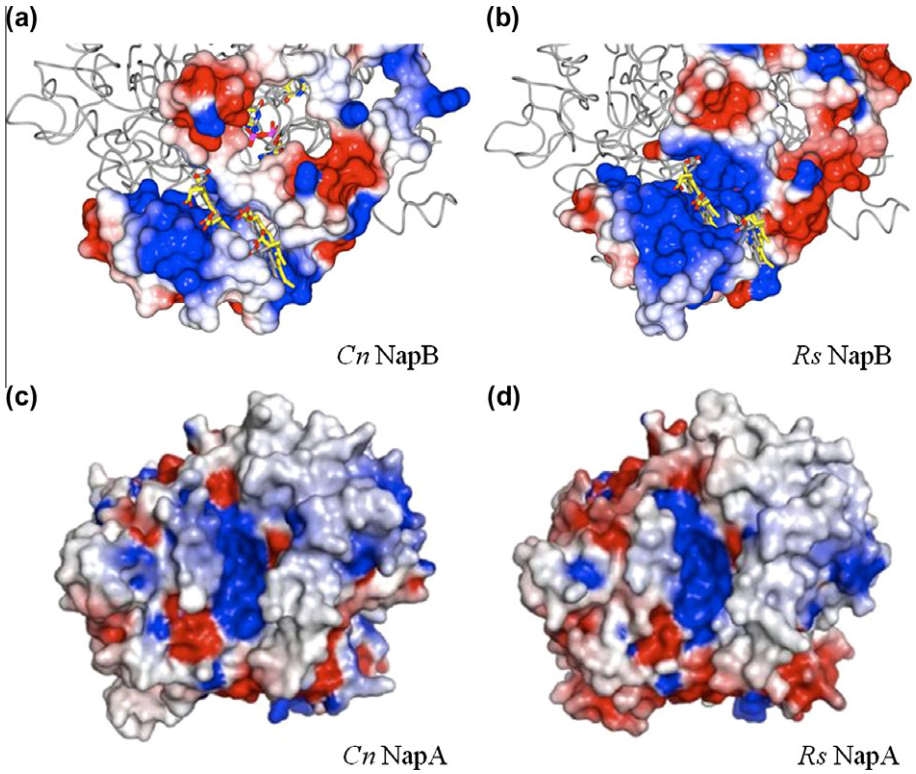

Fig. 6. Electrostatic surface potential for NapB from *Cn* (a) and from *Rs* (b) and for NapA from *Cn* (c) and from *Rs* (d). In (a) and (b) NapA polypeptides are represented in grey; for a better comparison the haems from the two proteins are overlapped (*Cn* haems in yellow). In (c) and (d) the view towards the substrate tunnel leading to the active site is represented. Electrostatic surface potentials were calculated and represented using the ccp4 mg program [43] with the colour of the surface potentials ranging from −0.08 (red) to +0.08 (blue). (For interpretation of the references to colour in this figure legend, the reader is referred to the web version of this article.)

the NH_3^+ groups of neomycin and the C–O functionalities on the electrode surface showed to be determinant in the orientation of the enzyme in such a way that electrons are exchanged between the electrode and the substrate, through the catalytic subunit. This is also supported by the observance of electrocatalytic activity for *Rs* NapA, where the haems are absent, as reported by Fourmond and co-workers [19].

In the case of *Cn* NapAB, electrons are not flowing between the electrode and nitrate, given that no electrocatalysis is detected. Therefore, contrarily to what could be anticipated from simple electrostatic electrode/protein interactions, the active site seems not to communicate with the negatively charged electrode surface. Our voltammetric data suggest that in the case of *Cn* NapAB the communication with the electrode occurs through the small di-haem *c*-type subunit NapB, and electrons are transferred between the electrode and most probably the positive solvent exposed haem II. This would also explain why the presence of positive promoters had no effect on the voltammetric signal. Additionally, the surface coverage calculated ($\Gamma = (5 \pm 2) \times 10^{-11}$ mol/cm^2, see Section 3) and the corresponding area "occupied" by each *Cn* NapAB molecule (3×10^{-14} cm^2), is consistent with monolayer coverage of the protein with only one haem group in contact with the electrode. In fact, *Cn* NapA has an overall globular shape with approximate dimensions of 65 Å × 65 Å × 58 Å and *Cn* NapB presents a globular domain with approximate dimensions of 30 Å × 20 Å × 20 Å [7] and the estimated "contact area" between the protein and the electrode is equivalent to a circle of 20 Å diameter (see Section 3.1). Therefore, the catalytic activity observed can only be due to the haems. This assignment was corroborated by voltammetric experiments in the same experimental conditions performed with NapA from *D. desulfuricans*, for which no non-turnover signal or peroxidase activity was observed (Fig. 4d).

For *Mh* NarGHI no catalytic activity towards nitrate was detected as well, and only a peroxidase activity was observed. In the lack of the crystallographic structure for *Mh* NarGHI no comparison can be made with *Ec* NarGHI in order to understand the difference in electrochemical behaviour. Nevertheless, the attribution of the peroxidase activity to the haem b_P and/or b_D present in subunit NarI could be confirmed through voltammetric experiments performed with *Mh* NarGH in the same experimental conditions. In the absence of the membrane subunit, no non-turnover signal or peroxidase activity was observed (Fig. 4c and inset).

In summary, for both *Cn* NapAB and *Mh* NarGHI we observed a consistent non-catalytic signal at the PG electrodes that can be assigned to the haems. The two enzymes possess several cofactors and experiments with the whole enzyme and parts of it were a valuable tool to get information about the cofactor undergoing electron transfer. Catalytic activity towards nitrate was never detected in our direct electron transfer conditions. In some experiments a reductive activation step was also imposed for *Cn* NapAB but, unlike what was observed for other nitrate reductases [19,44], the enzyme remained insensitive to the presence of nitrate. However, nitrate reductase activity was established using methyl viologen as mediator with all other conditions being the same. The peroxidase catalytic activity observed when *Cn* NapAB and *Mh* NarGHI were probed by direct electrochemistry occurred at a potential close to that of the non-turnover response. Therefore, it has to be related with the haems present in subunit B or subunit I.

Some works have reported the formation of altered forms of *c*-type cytochromes, associated to the loss of the methionine axial ligand, which present redox potentials more negative than those of the native state when interrogated at graphite surfaces [45,46]. The same phenomenon has been observed by us for a bacterial cyto-

chrome *c* peroxidase [47]. In that work we also showed that the displacement of an axial ligand of the haem, of *c*-type cytochromes either Met-His or bis-His coordinated, confers peroxidase activity to the protein. Indeed, this was detected for Met-His monohaem cytochromes (mitochondrial cytochrome *c* and *Desulfovibrio vulgaris* cytochrome c_{553}), as well as for the bis-His multihaem cytochrome c_3 from *Desulfovibrio gigas*.

The electrochemical behaviour here reported for *Cn* NapAB and *Mh* NarGHI can only be interpreted on the basis of the interaction of the haems present in both enzymes with the graphite surface, most probably haem II in the case of *Cn* NapAB and the distal haem of *Mh* NarGHI, the more exposed haems. The non-catalytic signals for *Cn* NapAB and *Mh* NarGHI observed at the PG electrodes were very similar, corresponding to a near reversible one electron redox reaction, and therefore their peroxidase activity can be compared. In the case of *Cn* NapAB, the haems are both *c*-type with bis-His coordination and the turnover number ($k_{cat} \sim 5\ s^{-1}$) compares well with the values reported for *c*-type cytochromes in [47]. The haems present in *Mh* NarGHI are *b*-type and interestingly the peroxidase activity observed for this enzyme is significantly higher ($k_{cat} \sim 150\ s^{-1}$). This surely is a consequence of the more labile nature of this type of haems.

Attribution of the peroxidase activity to the interaction of the haems with the graphite surface is compatible with the observation of nitrate activity when the enzymes are probed through the mediated catalysis with methyl viologen because this artificial mediator can supply its electrons directly to the molybdenum cofactor, as shown for the cytochrome-free derivatives of *E. coli* and *Paracoccus denitrificans* nitrate reductase [48,49]. Therefore, the absence of electrocatalytic activity towards nitrate when the enzymes are investigated by direct voltammetry indicates that in our experimental conditions the natural electron transfer pathway has been disrupted.

In the case of the mitochondrial cytochrome *c* the peroxidase activity observed has biological relevance in the apoptotic cycle [50]. The same cannot be said for the peroxidase activity of the nitrate reductases here reported.

5. Conclusions

Immobilization of enzymes on graphite electrode surfaces has been one of the most used procedures in direct voltammetry of enzymes. However, the interpretation of electrochemical signals should be carefully done when haems are among the metal cofactors. Both *Cn* NapAB and *Mh* NarGHI when immobilized (or entrapped) at graphite electrodes, even in the presence of several promoters, were incapable of undergoing electrochemically driven catalysis in the presence of nitrate. In fact, a non-native state of the haem is induced by interaction with the graphite electrode, which displays peroxidase activity. The phenomenon was observed for nitrate reductases containing *c*-type as well as *b*-type haems, demonstrating that this effect is not dependent on the nature of the haem. Previously we had demonstrated that for *c*-type haems was not dependent on the nature of the axial ligands [47].

In all previous voltammetric studies of nitrate reductases, protein film voltammetry together with pyrolytic graphite electrodes successfully probed the catalytic activity in the presence of nitrate. The reason for the differences found between the voltammetric behaviour here described and that reported so far for other nitrate reductases remains unclear. It is true that despite their homology, different enzymes do not necessarily behave similarly and this also applies to how they succeed to interact with the graphite electrodes. Our results show that for both *Cn* NapAB and *Mh* NarGHI more elaborate strategies of immobilization need to be explored to probe their electrocatalytic activity in the presence of nitrate.

Acknowledgments

CC and JM thank Fundação para a Ciência e a Tecnologia (FCT) for fellowships SFRH/BD/37948/2007 and SFRH/BD/60725/2009, respectively. PMPS thanks program Ciência 2007 from FCT for funding. This work has been supported by FCT through Grant No. PEst-C/EQB/LA0006/2011 and project PTDC/QUI/64733/2006.

References

[1] R. Hille, Chemical Reviews 96 (1996) 2757–2816.
[2] M.J. Romão, Dalton Transactions (2009) 4053–4068.
[3] H.J. Sears, P.J. Little, D.J. Richardson, B.C. Berks, S. Spiro, S.J. Ferguson, Archives of Microbiology 167 (1997) 61–66.
[4] J.M. Dias, M.E. Than, A. Humm, R. Huber, G.P. Bourenkov, H.D. Bartunik, S. Bursakov, J. Calvete, J. Caldeira, C. Carneiro, J.J. Moura, I. Moura, M.J. Romão, Structure 7 (1999) 65–79.
[5] B.J. Jepson, S. Mohan, T.A. Clarke, A.J. Gates, J.A. Cole, C.S. Butler, J.N. Butt, A.M. Hemmings, D.J. Richardson, The Journal of Biological Chemistry 282 (2007) 6425–6437.
[6] P. Arnoux, M. Sabaty, J. Alric, B. Frangioni, B. Guigliarelli, J.M. Adriano, D. Pignol, Nature Structural Biology 10 (2003) 928–934.
[7] C. Coelho, P.J. González, J.G. Moura, I. Moura, J. Trincão, M.J. Romão, Journal of Molecular Biology 408 (2011) 932–948.
[8] D.J. Richardson, Microbiology 146 (2000) 551–571.
[9] M. Jormakka, D. Richardson, B. Byrne, S. Iwata, Structure 12 (2004) 95–104.
[10] M.G. Bertero, R.A. Rothery, M. Palak, C. Hou, D. Lim, F. Blasco, J.H. Weiner, N.C. Strynadka, Nature Structural Biology 10 (2003) 681–687.
[11] C. Léger, P. Bertrand, Chemical Reviews 108 (2008) 2379–2438.
[12] F.A. Armstrong, H.A. Heering, J. Hirst, Chemical Society Reviews 26 (1997) 169–179.
[13] L.J. Anderson, D.J. Richardson, J.N. Butt, Biochemistry 40 (2001) 11294–11307.
[14] J. Marangon, P.M. Paes de Sousa, I. Moura, C.D. Brondino, J.J. Moura, P.J. González, Biochimica et Biophysica Acta 1817 (2012) 1072–1082.
[15] S.J. Elliott, K.R. Hoke, K. Heffron, M. Palak, R.A. Rothery, J.H. Weiner, F.A. Armstrong, Biochemistry 43 (2004) 799–807.
[16] A.J. Gates, D.J. Richardson, J.N. Butt, The Biochemical Journal 409 (2008) 159–168.
[17] B. Frangioni, P. Arnoux, M. Sabaty, D. Pignol, P. Bertrand, B. Guigliarelli, C. Léger, Journal of the American Chemical Society 126 (2004) 1328–1329.
[18] B.J. Jepson, L.J. Anderson, L.M. Rubio, C.J. Taylor, C.S. Butler, E. Flores, A. Herrero, J.N. Butt, D.J. Richardson, The Journal of Biological Chemistry 279 (2004) 32212–32218.
[19] V. Fourmond, B. Burlat, S. Dementin, P. Arnoux, M. Sabaty, S. Boiry, B. Guigliarelli, P. Bertrand, D. Pignol, C. Léger, The Journal of Physical Chemistry. B 112 (2008) 15478–15486.
[20] V. Fourmond, B. Burlat, S. Dementin, M. Sabaty, P. Arnoux, E. Etienne, B. Guigliarelli, P. Bertrand, D. Pignol, C. Léger, Biochemistry 49 (2010) 2424–2432.
[21] V. Fourmond, M. Sabaty, P. Arnoux, P. Bertrand, D. Pignol, C. Léger, The Journal of Physical Chemistry. B 114 (2010) 3341–3347.
[22] S. Dementin, P. Arnoux, B. Frangioni, S. Grosse, C. Leger, B. Burlat, B. Guigliarelli, M. Sabaty, D. Pignol, Biochemistry 46 (2007) 9713–9721.
[23] R.A. Rothery, A. Magalon, G. Giordano, B. Guigliarelli, F. Blasco, J.H. Weiner, The Journal of Biological Chemistry 273 (1998) 7462–7469.
[24] R.A. Rothery, F. Blasco, J.H. Weiner, Biochemistry 40 (2001) 5260–5268.
[25] R.A. Rothery, M.G. Bertero, R. Cammack, M. Palak, F. Blasco, N.C. Strynadka, J.H. Weiner, Biochemistry 43 (2004) 5324–5333.
[26] R.A. Rothery, F. Blasco, A. Magalon, M. Asso, J.H. Weiner, Biochemistry 38 (1999) 12747–12757.
[27] R.A. Siddiqui, U. Warnecke-Eberz, A. Hengsberger, B. Schneider, S. Kostka, B. Friedrich, Journal of Bacteriology 175 (1993) 5867–5876.
[28] P. Baumann, L. Baumann, The Prokaryotes. A Handbook on Habitats, Isolation, and Identification of Bacteria, Springer Verlag, New York, 1981.
[29] R.L. Starkey, Archives of Microbiology 9 (1938) 268–304.
[30] C. Correia, S. Besson, C.D. Brondino, P.J. González, G. Fauque, J. Lampreia, I. Moura, J.J. Moura, Journal of Biological Inorganic Chemistry 13 (2008) 1321–1333.
[31] A. Craske, S.J. Ferguson, European Journal of Biochemistry/FEBS 158 (1986) 429–436.
[32] M. Kakihana, H. Ikeuchi, G.P. Satô, K.J. Tokuda, Journal of Electroanalytical Chemistry 108 (1980) 381–383.
[33] A. Bard, L. Faulkner, Electrochemical Methods: Fundamentals and Applications, John Wiley & Sons, New York, 2001.
[34] F.A. Armstrong, P.A. Cox, H.A.O. Hill, V.J. Lowe, B.N. Oliver, Journal of Electroanalytical Chemistry 217 (1987) 331–366.
[35] C. Coelho, J. Trincão, M.J. Romão, Journal of Crystal Growth 312 (2010) 714–719.
[36] J.F. Rusling, Accounts of Chemical Research 31 (1998) 363–369.
[37] M.M. Correia dos Santos, P.M. Sousa, M.L. Gonçalves, M.J. Romão, I. Moura, J.J. Moura, European Journal of Biochemistry 271 (2004) 1329–1338.
[38] Z. Zhang, S. Chouchane, R.S. Magliozzo, J.F. Rusling, Analytical Chemistry 74 (2002) 163–170.

[39] B. Limoges, J. Moiroux, J.M. Savéant, Journal of Electroanalytical Chemistry 609521 (2002) 1–7.
[40] J.M. Saveánt, E. Vianello, Electrochimica Acta 10 (1965) 905–920.
[41] V. Fourmond, T. Lautier, C. Baffert, F. Leroux, P.P. Liebgott, S. Dementin, M. Rousset, P. Arnoux, D. Pignol, I. Meynial-Salles, P. Soucaille, P. Bertrand, C. Léger, Analytical Chemistry 81 (2009) 2962–2968.
[42] J. Butt, F. Armstrong, In: Bioinorganic Electrochemistry Springer, 2008.
[43] S. McNicholas, E. Potterton, K.S. Wilson, M.E.M. Noble, Acta Crystallographica Section D 67 (2011) 386–394.
[44] S.J. Field, N.P. Thornton, L.J. Anderson, A.J. Gates, A. Reilly, B.J. Jepson, D.J. Richardson, S.J. George, M.R. Cheesman, J.N. Butt, Dalton Transactions (2005) 3580–3586.
[45] B.D. Levin, M. Can, S.E.J. Bowman, K.L. Bren, S.J. Elliott, Journal of Physical Chemistry B 115 (2011) 11718–11726.
[46] T. Ye, R. Kaur, F.T. Senguen, L.V. Michel, K.L. Bren, S.J. Elliott, Journal of the American Chemical Society 130 (2008) 6682–6683.
[47] P.M. Paes de Sousa, S.R. Pauleta, M.L. Simões Goncalves, G.W. Pettigrew, I. Moura, J.J. Moura, M.M. Correia dos Santos, Journal of Biological Inorganic Chemistry 16 (2011) 209–215.
[48] A. Craske, S.J. Ferguson, European Journal of Biochemistry 158 (1986) 429–436.
[49] F.F. Morpeth, D.H. Boxer, Biochemistry 24 (1985) 40–46.
[50] N.A. Belikova, Y.A. Vladimirov, A.N. Osipov, A.A. Kapralov, V.A. Tyurin, M.V. Potapovich, L.V. Basova, J. Peterson, I.V. Kurnikov, V.E. Kagan, Biochemistry 45 (2006) 4998–5009.